GEOLOGIC MAP OF THE

ARROYO CUERVO 7.5-MINUTE QUADRANGLE,

DOÑA ANA AND SIERRA COUNTIES, NEW MEXICO

By
Andrew P. Jochems

June 2017
[Revised August 2018]

New Mexico Bureau of Geology and Mineral Resources
Open-file Digital Geologic Map OF-GM 261

Scale 1:24,000

This work was supported by the U.S. Geological Survey, National Cooperative Geologic Mapping Program (STATEMAP) under USGS Cooperative Agreement G15AC00243 and the New Mexico Bureau of Geology and Mineral Resources.

New Mexico Bureau of Geology and Mineral Resources, New Mexico Institute of Mining and Technology, 801 Leroy Place, Socorro, New Mexico, 87801-4796

CONTENTS

EXECUTIVE SUMMARY

The Arroyo Cuervo 7.5-minute quadrangle is located in the western part of the Hatch-Rincon basin, a west- to northwest-trending, structurally symmetrical basin in the southern Rio Grande rift. The map area features mostly low-lying topography, from the gently sloping La Mesa geomorphic surface on its south to the Rio Grande floodplain and Rincon Valley on its northeast. Several east-flowing tributaries to the Rio Grande cross the quadrangle, including Arroyo Cuervo and Arroyo Yeso. The oldest unit exposed in the quadrangle is the Miocene Rincon Valley Formation. The Plio-Pleistocene Camp Rice Formation unconformably overlies the Rincon Valley Formation. Younger units deposited after initial entrenchment of the Rio Grande include middle to late Pleistocene terraces in the major drainages and Holocene valley-floor deposits. One prominent valley floor alluvial unit returned radiocarbon ages of ~4400-4200 cal yr BP. Aquifers are hosted in the Camp Rice Formation and late Quaternary valley-fill units.

Gypsiferous mud and gently cross-stratified siltstone and very fine sandstone of the Rincon Valley Formation (Trv) were deposited in a playa lake or lake-margin environment that extended as far north as Garfield and possibly to Truth or Consequences. In the southwest corner of the quadrangle, strongly clay-cemented fanglomerate of the Rincon Valley Formation (Trvc) was deposited in a proximal alluvial fan setting. The upper contact of the Rincon Valley Formation with lowermost Camp Rice Formation facies is disconformable or a slight angular unconformity.

The Camp Rice Formation can be subdivided into 10 mostly conformable sub-units. Lowermost Camp Rice Formation beds are either fluvial sands of the lower axial-fluvial facies (Tcf) or mixed extra-channel, fluvial, and debris-flow deposits of the lower transitional and lower piedmont facies (QTcplt and QTcpl). Unit Tcf is 4-15 m thick and units QTcplt and QTcpl are 7-60 m thick in tandem. Gravelly beds in these units have transmitted groundwater in the past, as indicated by pervasive cementation above their contact with Trv. Above QTcpl lies the middle piedmont facies (QTcpm), consisting of 9-31 m of clay, silt, and gravel representing both extra-channel and fluvial deposition. Toward the south, unit QTcpm is laterally gradational with the transitional facies of the Camp Rice Formation (QTct), which includes up to 65 m of mud, silt, and sand deposited in the ancestral Rio Grande floodplain and surrounding alluvial flats. It includes a 3- to 6-m-thick upper unit (QTctu) that locally overlies a laterally extensive tongue of the upper axial-fluvial facies (QTcf). The latter consists of tongues and lentils of pebbly sand deposited by the ancestral Rio Grande. The upper piedmont facies (QTcpu) overlies units QTcpm and QTct in the southern part of the map area and consists of up to 27 m of pebbly to cobbly gravel deposited on alluvial fans. La Mesa geomorphic surface caps the upper piedmont facies and is typically marked by a 1-2 m thick petrocalcic horizon. Thin beds of sandy clay (Qcl) and gravelly piedmont deposits (Qcp) are locally associated with La Mesa surface.

The most notable structure of the Arroyo Cuervo quadrangle is the Arroyo Cuervo fault, a southwest-down fault crossing the middle part of the map area. Stratigraphic displacement along this fault is generally meter-scale as observed at the surface. It locally juxtaposes clayey Rincon Valley Formation sediment with gravelly axial-fluvial or piedmont deposits of the lower Camp Rice Formation, and thus forms an important hydrogeologic barrier in this part of the Hatch-Rincon basin.

INTRODUCTION

This report accompanies the *Geologic Map of the Arroyo Cuervo 7.5-Minute Quadrangle, Doña Ana and Sierra Counties, New Mexico* (NMBGMR OF-GM 261). Its purpose is to discuss the geologic setting and history of this area, and to identify and explain significant stratigraphic and structural relationships uncovered during the course of mapping.

The Arroyo Cuervo quadrangle is located in the western part of the Hatch-Rincon basin in the southern Rio Grande rift (Fig. 1). The quadrangle is characterized by valleys of modest relief carved by tributaries to the Rio Grande and their small side drainages. These valleys include Arroyo Cuervo, Arroyo Jaralosa, and Arroyo Yeso in the north. The Rio Grande flows through the northeastern corner of the quadrangle, forming the western border of Rincon Valley. The southern end of the quadrangle is dominated by La Mesa geomorphic surface, with surface slopes of typically 2° or less. The highest location in the quadrangle is 1416 m (~4650 ft) above sea level (asl) in the easternmost foothills of the Good Sight Mountains in section 17, T19S, R5W. The lowest point is 1241 m (~4070 ft) asl where the Rio Grande exits the quadrangle in section 33, T18S, R4W.

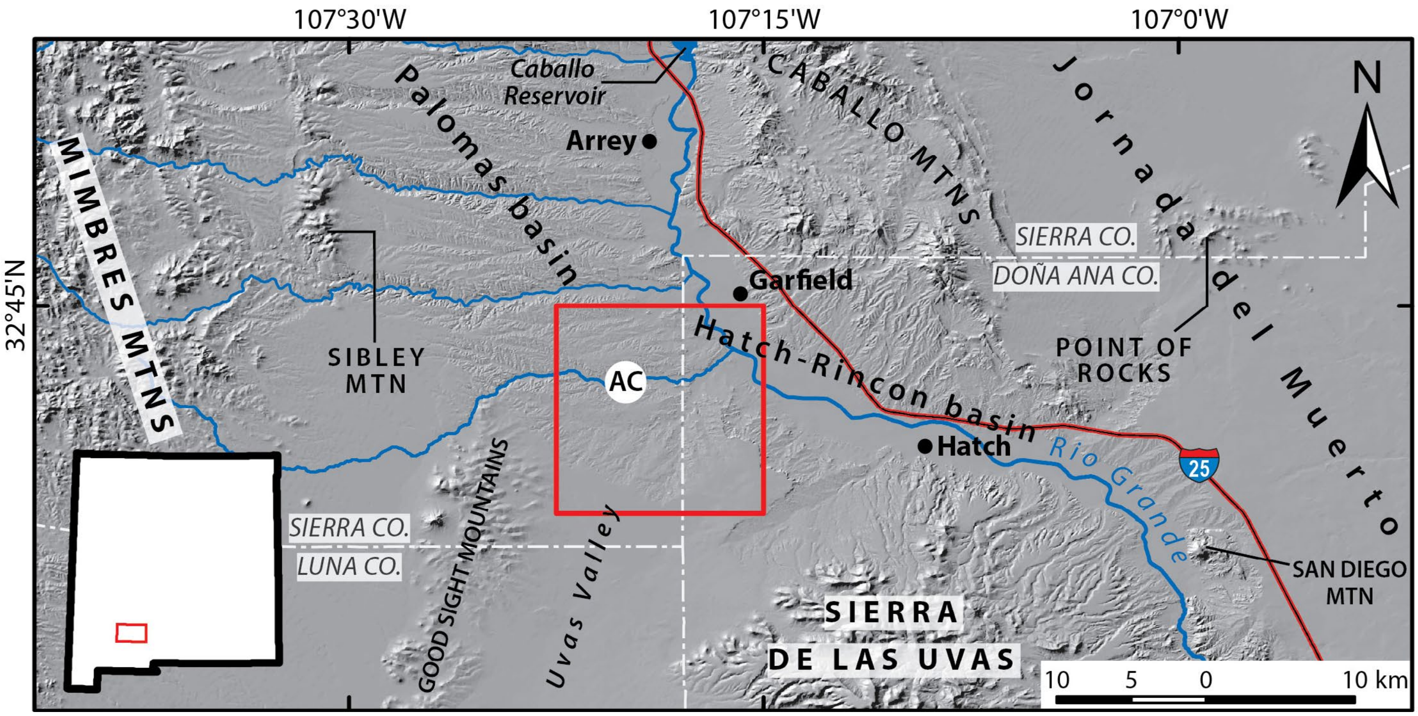

Figure 1. Shaded-relief map showing major physiographic features of the southern Palomas basin, Hatch-Rincon basin, and surrounding areas. The Hatch-Rincon basin is bordered on the north by the Caballo Mountains and on the south by the Sierra de las Uvas. The Arroyo Cuervo quadrangle is outlined in red. Inset map shows location in southern New Mexico. AC = Arroyo Cuervo.

Most of the Hatch-Rincon basin, including the Arroyo Cuervo quadrangle, has an arid climate. The summer months (June through August) experience mean temperatures of 24.6-26.1° C (76.2-79.0° F). The winter months (December through February) experience mean temperatures of 5.4-8.0° C (41.7-46.4° F). Mean annual precipitation is 26.24 cm (10.33 in), nearly half of which (12.62 cm) falls during the North American monsoon in the months of July through September. All climate data listed above are from the Hatch station (ID# 293855) in the NWS Cooperative network and averaged over the years 1981-2010 (Western Regional Climate Center, 2016).

The geology of the Arroyo Cuervo quadrangle was previously mapped as part of the 1:125,000-scale northwest Las Cruces 1° x 2° sheet by Seager and others (1982). Nearby 1:48,000-scale mapping by Clemons (1979) covers the Hockett, Jug Canyon, and Nutt quadrangles. Surrounding quadrangles mapped at a scale of 1:24,000 include Garfield (Seager and Mack, 1991), Hatch (Seager, 1995), McLeod Tank (Seager and Mack, 1998), and Souse Springs (Clemons and Seager, 1973). Preliminary 1:24,000-scale mapping of parts of the Arroyo Cuervo quadrangle was carried out by Rick Kelley and John Hawley in the 1970s. Their unpublished work helped inform the author's mapping efforts in select locations.

This report includes a summary of the geologic setting before describing mapped units and their depositional settings by age, oldest to youngest. The structural geology of the area is discussed, as are hydrogeologic implications for mapped basin-fill units and, briefly, non-metallic resource potential in the map area. Clast counts, imbrication measurements, maximum clast size, radiocarbon data, and detailed unit descriptions are provided as appendices.

GEOLOGIC SETTING

The Arroyo Cuervo quadrangle is located in the southern Rio Grande rift, a series of en echelon basins stretching from northern Colorado to northern Mexico (Hawley, 1978; Chapin and Cather, 1994). The quadrangle includes the western part of the Hatch-Rincon basin, a structurally symmetrical, northwest-trending graben containing Miocene through early Pleistocene basin-fill (Figs. 1, 2). The Hatch-Rincon basin is bordered on the north by a structurally complex array of fault blocks of the southern Caballo Mountains, and on the south by the Uvas Valley. The Uvas Valley coincides with the Nutt-Hockett basin, a small synclinal basin ringed by the Good Sight Mountains and western Sierra de la Uvas. The Good Sight Mountains and Sierra de las Uvas are composed of Eocene-Oligocene volcanic and volcaniclastic strata (Clemons, 1979; Seager

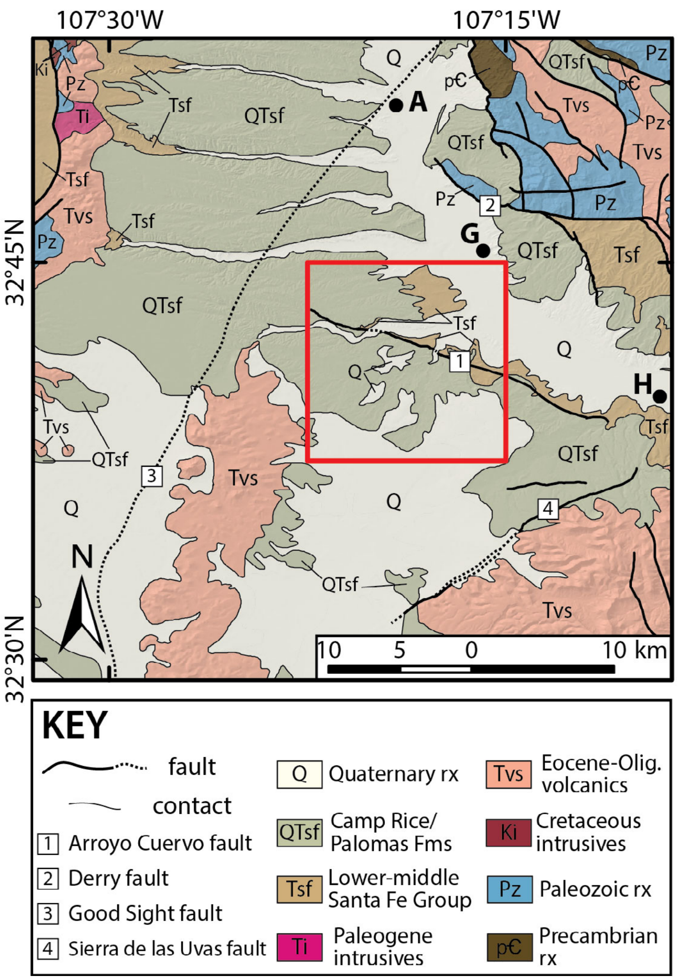

Figure 2. Simplified geologic map of the southern Palomas basin, western Hatch-Rincon basin, and vicinity (New Mexico Bureau of Geology and Mineral Resources, 2003). The Arroyo Cuervo quadrangle is outlined in red. Numbers correspond to faults discussed in text (see key). Towns abbreviated as follows: A = Arrey, G = Garfield, H = Hatch.

et al., 1982), whereas the southern Caballo Mountains are composed chiefly of faulted and folded Paleozoic rocks with some Tertiary strata in structurally low areas (Seager et al., 1982; Seager and Mack, 2003). The map area lies along the west side of the Good Sight-Cedar Hills depression, an east-tilted half graben inferred to represent the earliest phase of Rio Grande rift extension after ~35 Ma (Mack et al., 1994a, b).

The Rincon Valley Formation records a later phase of rift extension and subsidence in the Hatch-Rincon basin. Strata of the Rincon Valley and Hayner Ranch Formations (latter not exposed in map area) generally become finer and dip toward the northeast, implying that the western part of the basin was a half-graben with its master fault to the northeast during the Miocene (Mack et al., 1994a; Seager and Mack, 2003). This area is located in the Rincon transfer zone of Mack and Seager (1995) and coincides with a northwest-trending zone of buried Laramide structural elements as interpreted by Seager and others (1986). Prior to a late phase of extension in the Pliocene-Pleistocene, the transfer zone consisted of a northern and southern half graben, the former hosting a playa lake during the middle to late Miocene. This lake extended to at least Garfield and possibly as far north as Truth or Consequences.

Following the arrival of the ancestral Rio Grande ~5 Ma (Mack et al., 2006; Koning et al., 2016), axial-fluvial and piedmont strata of the Camp Rice Formation were deposited on the Rincon Valley Formation, forming a disconformity or slight to moderate angular unconformity (2-5°). These strata are more-or-less uniformly distributed on either side of the Hatch-Rincon basin, suggesting that symmetrical subsidence during the Pliocene-Pleistocene was superimposed on the earlier pair of half graben (Mack and Seager, 1990). This later round of extension resulted in segmentation and narrowing of older basins (Mack et al., 1994c)

Where preserved, the uppermost Camp Rice Formation is capped by a gently inclined (≤2°) surface known as the La Mesa surface that dates to ~0.8 Ma (Mack et al., 1993, 1998; Leeder et al., 1996). The Rio Grande and its tributaries began incising into the Camp Rice Formation in the middle Pleistocene, alternating with periods of backfilling that resulted in a series of inset terrace deposits distinguished by landscape position, texture, and soil development.

METHODS

Geologic mapping of the Arroyo Cuervo quadrangle consisted of traditional field techniques (Compton, 1985) coupled with newer digital approaches. Stereogrammetry software (Stereo Analyst for ArcGIS 10.1, an ERDAS extension, version 11.0.6) permitted accurate placement of geologic contacts using aerial photography obtained from the National Agricultural Imagery Program (NAIP). Planimetric and vertical accuracy of this dataset is approximately 5 m (USDA, 2008). Contacts plotted using stereogrammetry were then field-checked at a scale of 1:12,000.

Descriptions of individual units were made in the field utilizing both visual and quantitative estimates based on outcrop and hand lens inspection. For clastic sediments, grain sizes follow the Udden-Wentworth scale and the term “clast(s)” refers to the grain size fraction greater

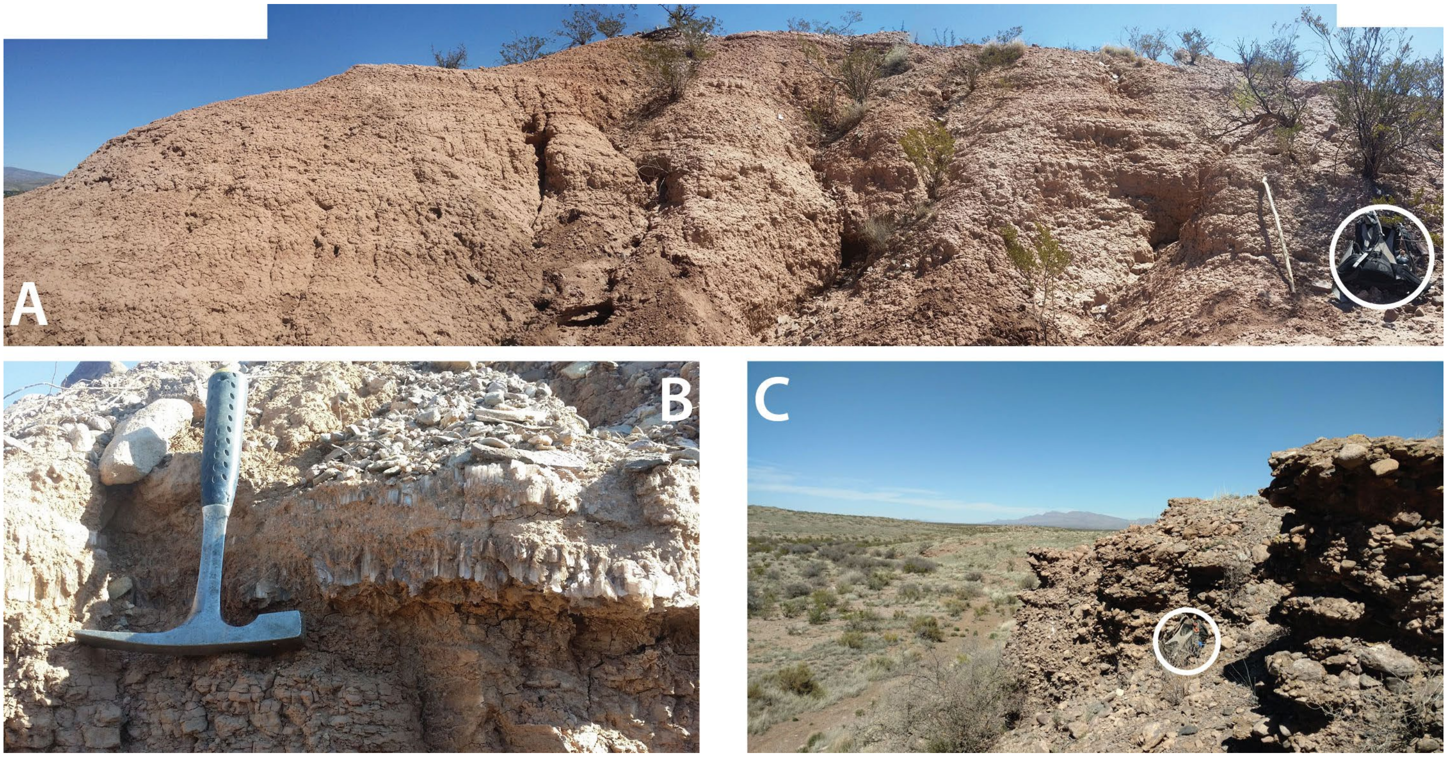

Figure 3. Rincon Valley Formation (Trv). (A) Typical vaguely bedded mudstone and rare siltstone-very fine sandstone ledges. Note backpack (white circle) for scale. Section 13, T18S, R5W. (B) Thin (~10 cm) selenite layer interbedded with mudstone and siltstone of unit Trv. Hammer for scale is ~25 cm long. Section 12, T18S, R5W (southernmost Garfield 7.5-minute quadrangle). (C) Fanglomerate facies (Trvc) consisting of andesite-rich pebble-cobble conglomerate. Note backpack (white circle) for scale. Section 16, T19S, R5W.

than 2 mm in diameter (Udden, 1914; Wentworth, 1922). Descriptions of bedding thickness follow Ingram (1954). Colors of sediment are based on visual comparison of dry (and occasional moist) samples to Munsell soil color charts (Munsell Color, 2009).

Surface characteristics and relative landscape position were used in mapping middle Pleistocene to Holocene units, i.e. stream terrace, alluvial fan, and valley-floor deposits. Surface characteristics dependent on age include desert pavement development, clast varnish, soil development, and preservation of original bar-and-swale topography. Soil horizon designations and descriptive terms follow those of Birkeland and others (1991), Birkeland (1999), and Soil Survey Staff (1999). Stages of pedogenic calcium carbonate morphology follow those of Gile and others (1966) and Birkeland (1999).

STRATIGRAPHY

QUATERNARY-TERTIARY BASIN-FILL

Rincon Valley Formation

The Rincon Valley Formation was named by Hawley and others (1969) and Seager and others (1971) for reddish alluvial-flat, playa-lake, and alluvial-fan lithofacies in the San Diego Mountain area. Alluvial-flat and playa deposits are fine-grained and may contain abundant gypsum, whereas fanglomerate and minor siltstone and sandstone represent deposition in proximal to distal alluvial fan environments. Mack and others (1994a) showed that the Rincon Valley Formation was deposited in two half graben, northern and southern basins bordered by the Caballo Mountains and Sierra de las Uvas, respectively. Rincon Valley deposits in the map area were deposited in the northern half graben based on northeastward dips and paleocurrent data and provenance in fanglomerate facies.

In the Arroyo Cuervo quadrangle, the Rincon Valley Formation (Trv) is primarily composed of fine-grained sediment deposited in a playa lake. The unit is typified by dark reddish brown to red (2.5-5YR) mudstone and clayey silt with common gypsum in the form of prismatic crystals, shards, amalgamated masses, and selenite beds up to 10 cm thick (Fig. 3a, b). Minor silty sandstone is massive to ripple cross-laminated, indicating low-flow regime deposition in small streams draining into the northern Rincon Valley half graben. The Rincon Valley Formation is at least 600 m thick based on lithologic data from a test well near Hatch (King et al., 1971; Seager, 1995).

In the southwest corner of the map area, reddish brown to reddish yellow (2.5-5YR) conglomerate and sandstone cemented by clay belongs to the fanglomerate facies of the Rincon Valley Formation (Trvc; Fig. 3c). Imbrication and cross-stratification suggest fluvial deposition although rare matrix-supported beds could be debris flows. Clasts consist almost entirely of andesites recycled from the Uvas basaltic andesite and Rubio Peak Formation exposed in the Good Sight Mountains to the west. Thus, the unit represents a proximal alluvial fan setting. Its total thickness is unknown but exceeds 9 m.

Age of the Rincon Valley Formation

The age of the Rincon Valley Formation is only partly constrained. In Selden Canyon (between Hatch and Las Cruces), the Rincon Valley Formation interbeds with basalts with K/Ar ages of ~9.6 Ma (Seager et al., 1984). The age of its base is not known but its upper boundary is slightly older than ~5.0-4.5 Ma, a general age range for tholeiitic basalt flows interbedded with the basal Palomas Formation to the north (Seager et al., 1984; Jochems, 2015; Koning et al., 2015).

Camp Rice Formation

The Camp Rice Formation and correlative deposits of the Palomas Formation to the north of the map area consist of gravel, sand, silt, and clay deposited by coalesced fan complexes and the ancestral Rio Grande in the Palomas and Hatch-Rincon basins. The Camp Rice Formation was named by Strain (1966) for basin-fill in the Hueco basin of west Texas and was carried into southern New Mexico by Hawley and others (1969), Hawley and Kottlowski (1969), and Seager and others (1971, 1982, 1987). Camp Rice basin-fill can be subdivided into 10 units in the Arroyo Cuervo quadrangle.

Basal beds of the Camp Rice Formation belong to one of three units distinguished by depositional setting. In the eastern part of the quadrangle, the lower axial-fluvial facies (Tcf) lies disconformably or with slight angular unconformity on the Rincon Valley Formation. This unit represents the earliest exposed deposits of the ancestral Rio Grande and is characterized by pale brown (10YR) sand and pebble gravel with common planar cross-stratification (Fig. 4). Sand grains are dominantly quartz (70-80%) and vertebrate fossils and petrified wood are common. Unit Tcf occurs in tongues that are 4-15 m thick.

Figure 4. Contact (white line) between lower axial-fluvial facies of the Camp Rice Formation (Tcf) and Rincon Valley Formation (Trv). Here, contact is a slight (~1-2°) angular unconformity. Tcf consists of grayish sand and pebble gravel that is typically calcite-cemented just above its contact with Trv. Note backpack (white circle) for scale. Section 25, T18S, R5W.

The lithology of piedmont and axial-fluvial Camp Rice Formation units above unit Tcf is shown in Figure 5. West of approximately 107°18'30" W, the Rincon Valley Formation may be overlain by either the lower transitional (QTcplt) or lower piedmont facies (QTcpl) of the Camp Rice Formation. Unit QTcplt is found in an approximately 9 km^2 area in the northern part of the quadrangle where it consists of silt, sand, and pebble gravel/conglomerate with occasional stage II calcic paleosols. Unit QTcpl features similar lithology (Fig. 5, 6), except for 3 distinguishing criteria: (1) calcic horizons with stage I to II carbonate accumulation are more common; (2) gravels/conglomerates contain larger clasts, including 10-15% boulders; and (3) massive carbonate beds inferred to be groundwater calcretes are found in the lower part of the unit. Thinner sand and pebbly gravel/conglomerate beds in these units were likely deposited as sheetfloods whereas thicker and coarser gravel beds may have been deposited fluvially or as debris flows. Silt beds were probably deposited as extra-channel sediment although some may be eolian. Unit QTcplt is relatively thin (0-15 m), whereas QTcpl attains a thickness of up to 45 m.

The lower piedmont facies is conformably overlain by the middle piedmont facies (QTcpm). This unit contains 9-31 m of brownish (10YR) clay, silt, and gravel (Fig. 5, 7). Silt and clay beds constitute 55-70% of the unit. Finer beds are inferred to consist of extra-channel sediments whereas gravels were deposited fluvially or by sheetfloods, as indicated by imbrication and occasional to common lamination.

South of Arroyo Cuervo, the middle piedmont facies

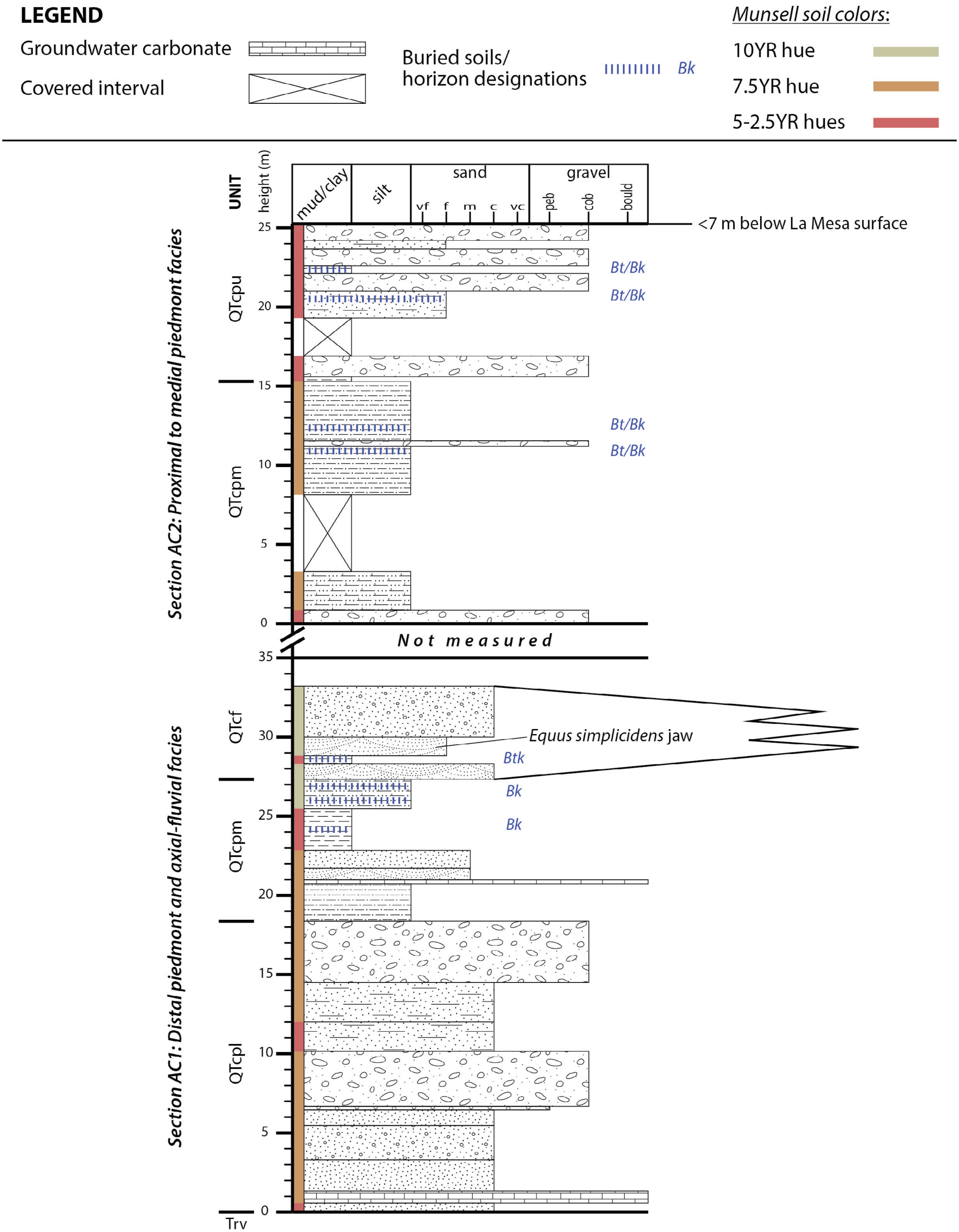

Figure 5. Stratigraphic sections measured in axial-fluvial and piedmont facies of the Camp Rice Formation. Section AC1 was measured in section 36, T18S, R 5W. Section AC2 was measured in sections 32-33, T18S, R5W.

Figure 6. Lower piedmont facies of the Camp Rice Formation (QTcpl). Unit consists of interbedded pebble-cobble gravel, light colored silt, and groundwater calcrete formed in medial to distal alluvial fan settings. Walking stick for scale (white oval) is 1.5 m tall. Section 35, T18S, R5W.

interfingers with the transitional facies (QTct), consisting of reddish to brownish (5-7.5YR) mud, silt, and sand (Fig. 8a). Vertebrate fossils may be found throughout this unit but are particularly concentrated in a lens of distinctive yellowish brown to olive (2.5-5Y) sand that is probably axial-fluvial in origin but included in QTct due to limited areal extent. Fossils recovered from this deposit include camel (*Camelops*), peccary (*Platygonus*), desert tortoise (*Gopherus*), and mud turtle (*Kinosternon*) (G. Morgan, pers. comm., 2017). Other rare but distinctive beds in unit QTct include mottled shale with small clusters of organic material in the upper 15 m of the unit (Fig. 8b). The fine-grained facies of QTct are interpreted as having been deposited in alluvial-flat, floodplain, or lacustrine settings; fluvial facies are rare except for intertonguing axial-fluvial deposits. Unit QTct is as much as 65 m thick excluding a 3-6 m bed of similar lithology (QTctu) found above a tongue of axial-fluvial facies traceable over 2-3 km in section 7, T19S, R4W. This bed contains a higher percentage (up to 35-40%) of sandy and sandy pebble beds than does QTct.

At least four tongues of the upper axial-fluvial facies (QTcf) are observed to interfinger with units QTcpm and QTct in the central and southern portions of the map area. These tongues feature light colored (10YR) sand and pebbly sand that is commonly cross-stratified with minor yellowish red (5YR) mud (Fig. 9a). South of La Capilla de Don Silverio, QTcf beds feature possible seismite features such as ball-and-flame structures (Fig. 9b). Vertebrate fossils are common in this unit and include the Blancan horses *Equus simplicidens* and *E. scotti*(?) as well as the small camel *Hemiauchenia* (Fig. 9c) (G. Morgan, pers. comm., 2017). The overall gray color and presence of granite and exotic quartzite pebbles indicate that this unit was deposited by the ancestral Rio Grande. Unit QTcf forms scoured contacts on units QTcpm and QTct, although it is laterally gradational with the latter in the south-central part of the quadrangle. Individual tongues are up to 18 m thick.

The upper piedmont facies (QTcpu) is found in the western and southern parts of the map area and includes reddish brown to light reddish brown (5YR), sandy pebble-cobble gravel and subordinate sand and mud (Figs. 5, 10). Well imbricated gravels of mostly volcanic clasts and common

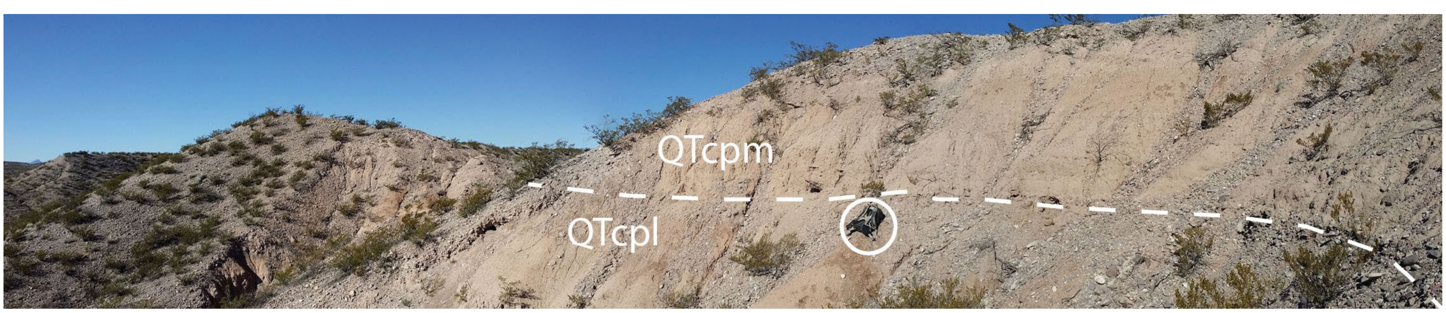

Figure 7. Contact (dashed white line) between middle (QTcpm) and lower (QTcpl) piedmont facies of the Camp Rice Formation. QTcpm is dominated by light-colored extra-channel sediment with occasional sheetflood or channel deposits. Note backpack (white circle) for scale. Section 33, T18S, R5W.

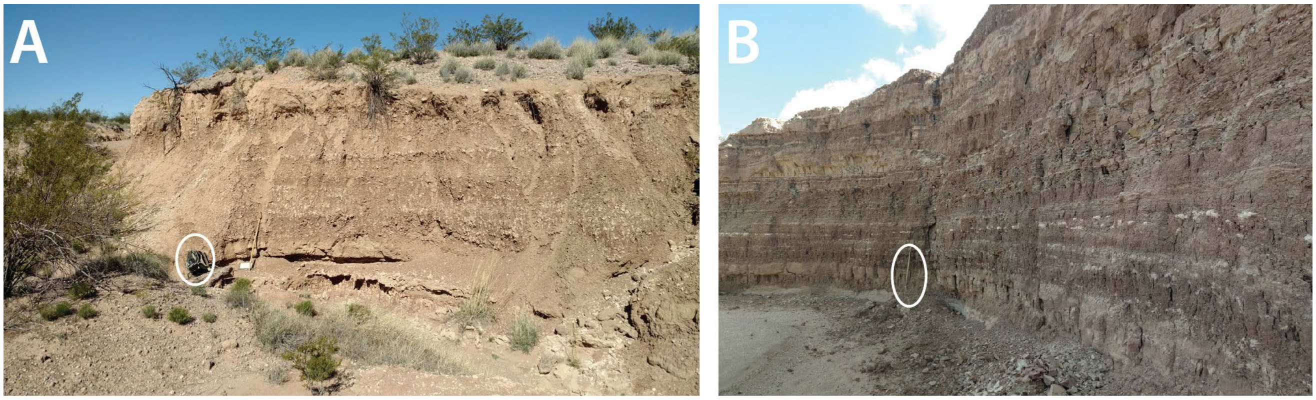

Figure 8. Transitional facies of the Camp Rice Formation (QTct). (A) Typical mud, sandy mud, and silt with stage II carbonate accumulation (nodules, tubules). Note backpack (white circle) for scale. Section 11, T19S, R5W. (B) Rare mottled shale beds in upper 15 m of unit. Fissile shale is interbedded with sandy mud and small lenses of silt-very fine sand. Walking stick (white oval) for scale is 1.5 m tall. Section 24, T19S, R5W.

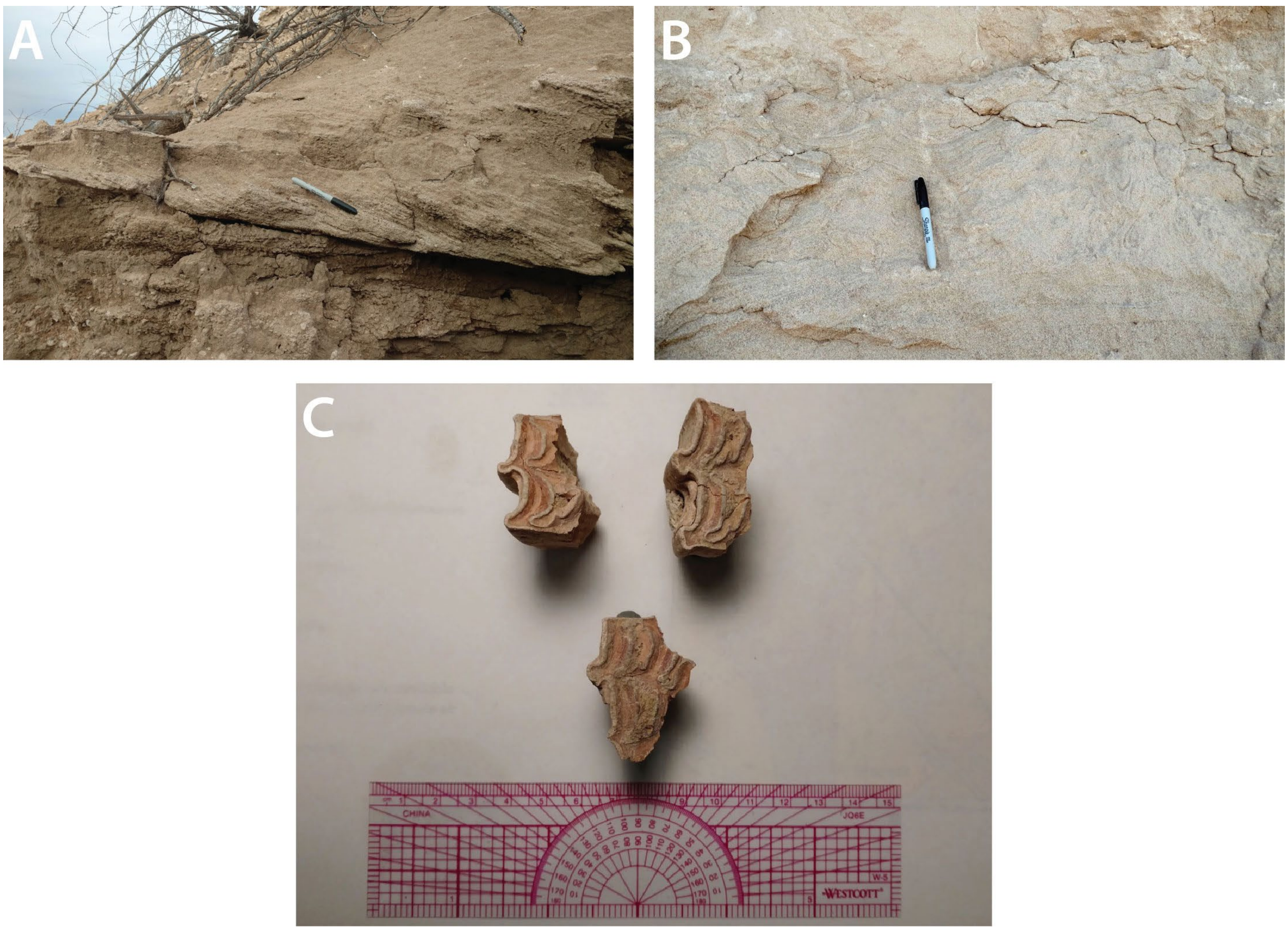

Figure 9. Upper axial-fluvial facies of the Camp Rice Formation (QTcf). Pen for scale in (A) and (B) is 14 cm long. (A) Planar cross-stratified axial sandstone interfingering with unit QTcpm. Note weak to moderate carbonate cementation in lower 15-20 cm of sandstone on impermeable mud below. Section 36, T18S, R5W. (B) Possible seismite in QTcf sand inferred from weak ball-and-flame structures above and to right of pen. Section 7, T19S, R4W. (C) *Equus scotti*(?) teeth recovered from a tongue of QTcf interfingering with transitional facies (QTct) mud ~20 m below La Mesa surface. Ruler is just over 15 cm long.

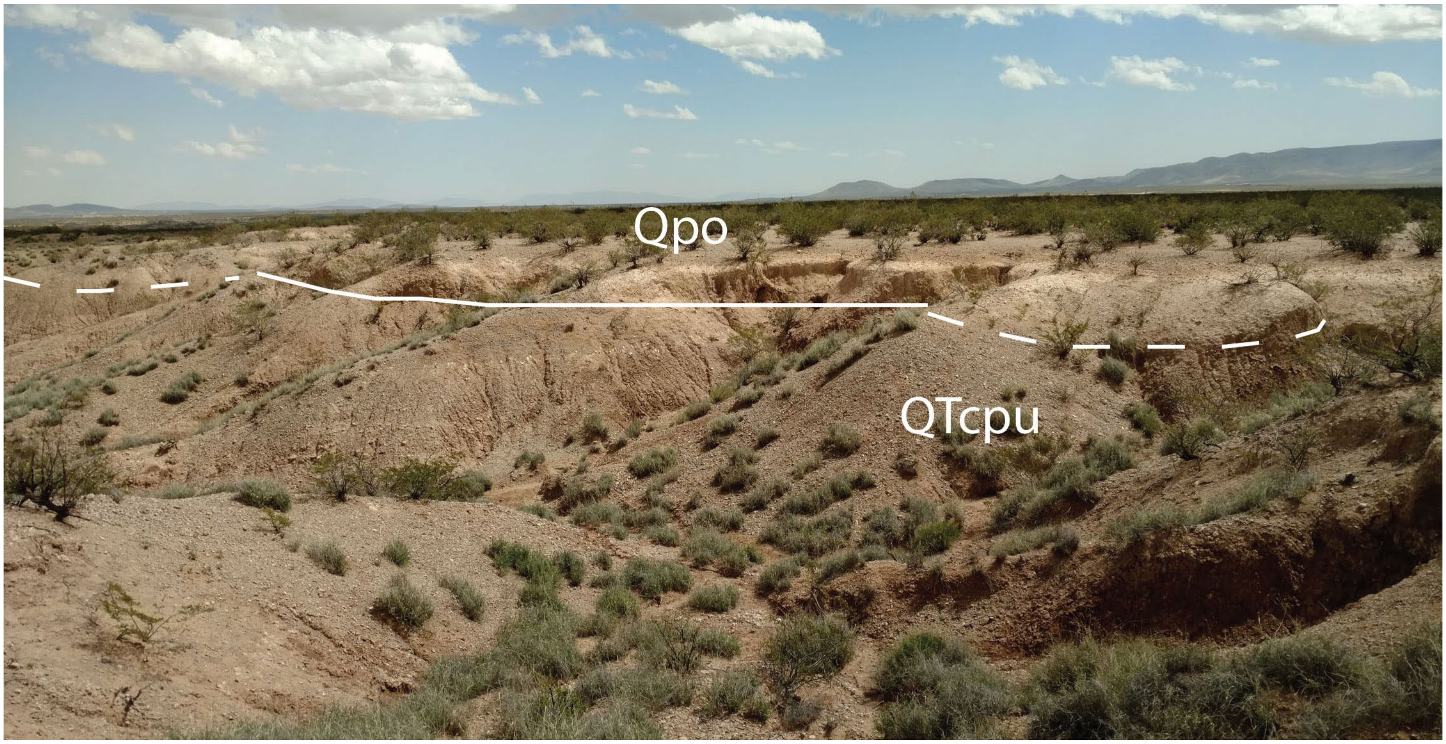

Figure 10. Uppermost 3-5 m of upper piedmont facies of the Camp Rice Formation (QTcpu) underlying contact with Qpo graded to La Mesa surface (solid, dashed white lines). QTcpu consists of reddish extra-channel mud and silt interbedded with volcanic-rich pebble channel-fills. Section 22, T19S, R5W.

matrix clay underlie La Mesa surface in the southern part of the quadrangle and are likely fluvial in origin whereas more poorly sorted gravels to the west may have been deposited by debris flows in proximal to medial alluvial fan settings. QTcpu may contain paleosols consisting of Btk horizons with stage II carbonate morphology (calcic nodules). QTcpu does not interfinger with underlying units and is 5-27 m thick.

Two minor units at the top of the Camp Rice Formation are associated with La Mesa surface. Reddish (5YR) beds of tabular clay containing rare pebbles (Qcl) are found in the southern part of the quadrangle and appear to grade westward to gray or brown (7.5YR) beds of piedmont gravels (Qcp). Qcl beds are no more than 3 m thick and in places form the parent material for a 1- to 2-m-thick petrocalcic soil featuring stage III+ to IV carbonate accumulation. Piedmont gravels may feature stage I+ to II calcic horizons at their surface and are less than 15 m thick.

Age of the Camp Rice Formation

Radiometric dating and magnetostratigraphic work by Mack and others (1993, 1996) on the Arroyo Cuervo and Hatch quadrangles has locally constrained the age of the Camp Rice Formation to ~3.5-0.8 Ma. More generally, the Palomas and Camp Rice Formations have been dated to ~5.0-0.8 Ma using fossil data (summarized by Morgan and Lucas, 2012), basalt and pumice radiometric ages (Bachman and Mehnert, 1978; Seager et al., 1984; Mack et al., 2009; Jochems, 2015; Koning et al., 2015, 2016), and magnetostratigraphic data (Repenning and May, 1986; Mack et al., 1993, 1998; Leeder et al., 1996). Neogene epochs, land mammal ages, and magnetic polarity chrons and subchrons referred to in the following discussion are shown in Figure 11.

Mack and others (1993) collected paleomagnetic samples from a section (Hatch Siphon) of the Camp Rice Formation beginning in the westernmost Hatch quadrangle and ending at La Mesa surface in the Arroyo Cuervo quadrangle. They identified an ~8 m section of Matuyama-age (2.58-0.78 Ma) floodplain deposits with stage III calcic paleosols underlain by ~60-65 m of interbedded axial-fluvial and floodplain deposits containing two reversed-polarity intervals interpreted as the Kaena (3.11-3.04 Ma) and Mammoth (3.33-3.20 Ma) subchrons. In particular, the former interval is confidently assigned to the Kaena subchron because it contains a pumice conglomerate layer with an $^{40}Ar/^{39}Ar$ age of ~3.1 Ma (Mack et al., 1996). This layer occurs ~30 m above the base of the section, which lies on mudstone of the Rincon Valley Formation that is only 3 m below the base of the interpreted Mammoth interval.

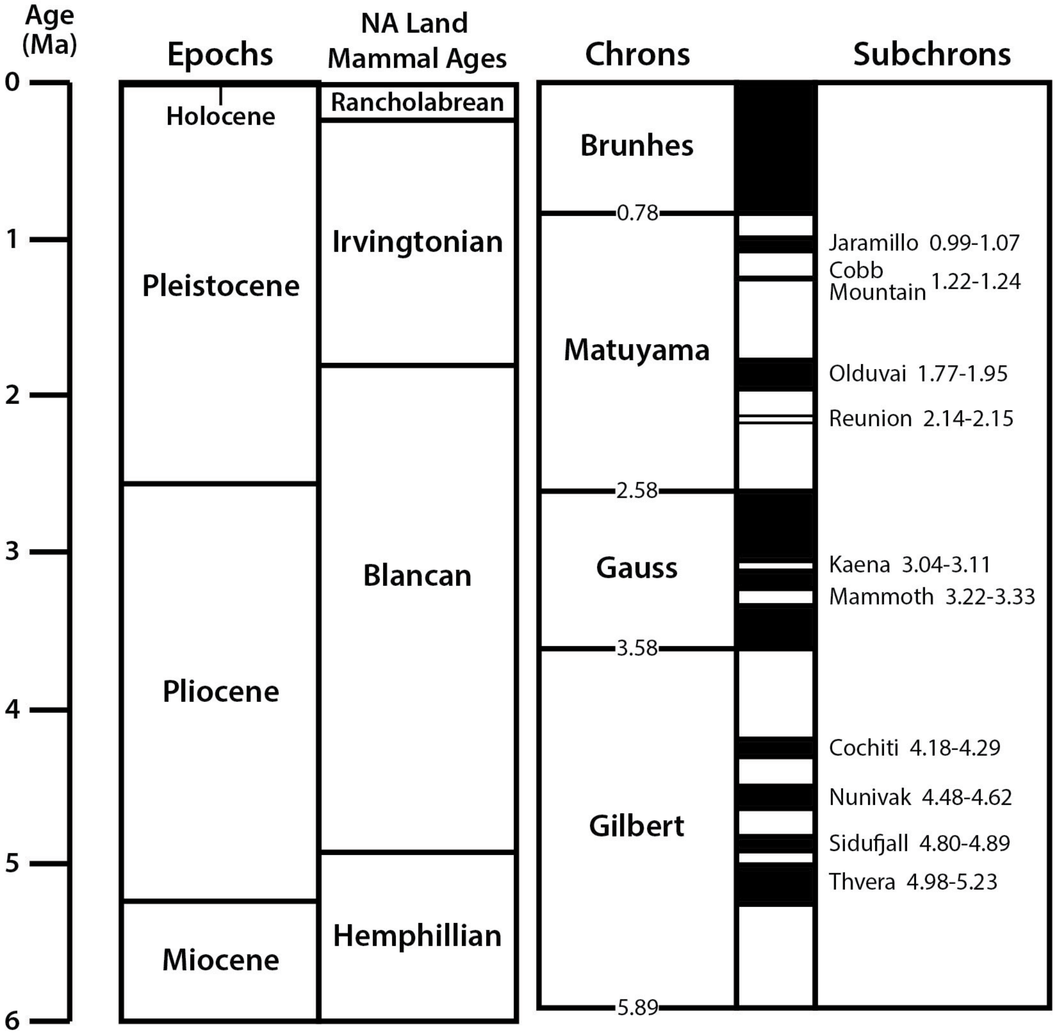

Figure 11. Neogene epochs, North American land mammal ages, and polarity reversal time scales. Polarity reversal time scale modified from Berggren and others (1995); black is normal magnetic polarity, white is reversed magnetic polarity.

The contact between lower axial-fluvial facies of the Camp Rice Formation and mudstone of the Rincon Valley Formation is well exposed and easily traced in the eastern half of the quadrangle. It is a fault-contact (Arroyo Cuervo fault) in the central part of the map area but otherwise depositional. Assuming an age of ~3.5-3.3 Ma based on the Hatch Siphon magnetostratigraphic section, the base of the Camp Rice Formation in the Arroyo Cuervo quadrangle is starkly diachronous with correlative deposits further north in the Truth or Consequences area (Koning et al., 2016). One hypothesis for this apparent diachroneity is that the ancestral Rio Grande was restricted to a narrow floodplain in the Hatch-Rincon basin during the 3.6-2.6 Ma Gauss chron (Mack et al., 2006), perhaps due to repeated down-dropping of the basin-floor between oppositely dipping faults. This speculative scenario requires that pre-3.6 Ma axial-fluvial and floodplain deposits of the Camp Rice Formation were eroded from the flanks of the graben.

Although correlative deposits in the Palomas basin have been dated to ~5-4.5 Ma (Seager et al., 1984; Jochems, 2015; Koning et al., 2015), the lower transitional and lower piedmont facies of the Camp Rice Formation in the quadrangle grade to and interbed with Tcf inferred to be Gauss-age based on the above discussion. Units QTcpm and QTct are laterally gradational and therefore generally time-equivalent. Several lines of evidence suggest that these units are approximately 3.1-2.6 Ma in age. First, correlation of the Hatch Siphon section to a stratigraphic section measured by Clemons (1979) suggests that the 3.1 Ma pumice bed could lie in the lower part of QTct, just above the upper contact of QTcpl (Fig. 12). Second, co-occurring fossils of the late Blancan horse *Equus simplicidens* and the large camel *Camelops* were recovered from units QTct and QTcpm, suggesting an age of no younger than 2.6 Ma (G. Morgan, pers. comm., 2017). This observation fits well with the age of the Hatch Siphon pumice as well as Blancan fossil localities elsewhere in the Palomas and

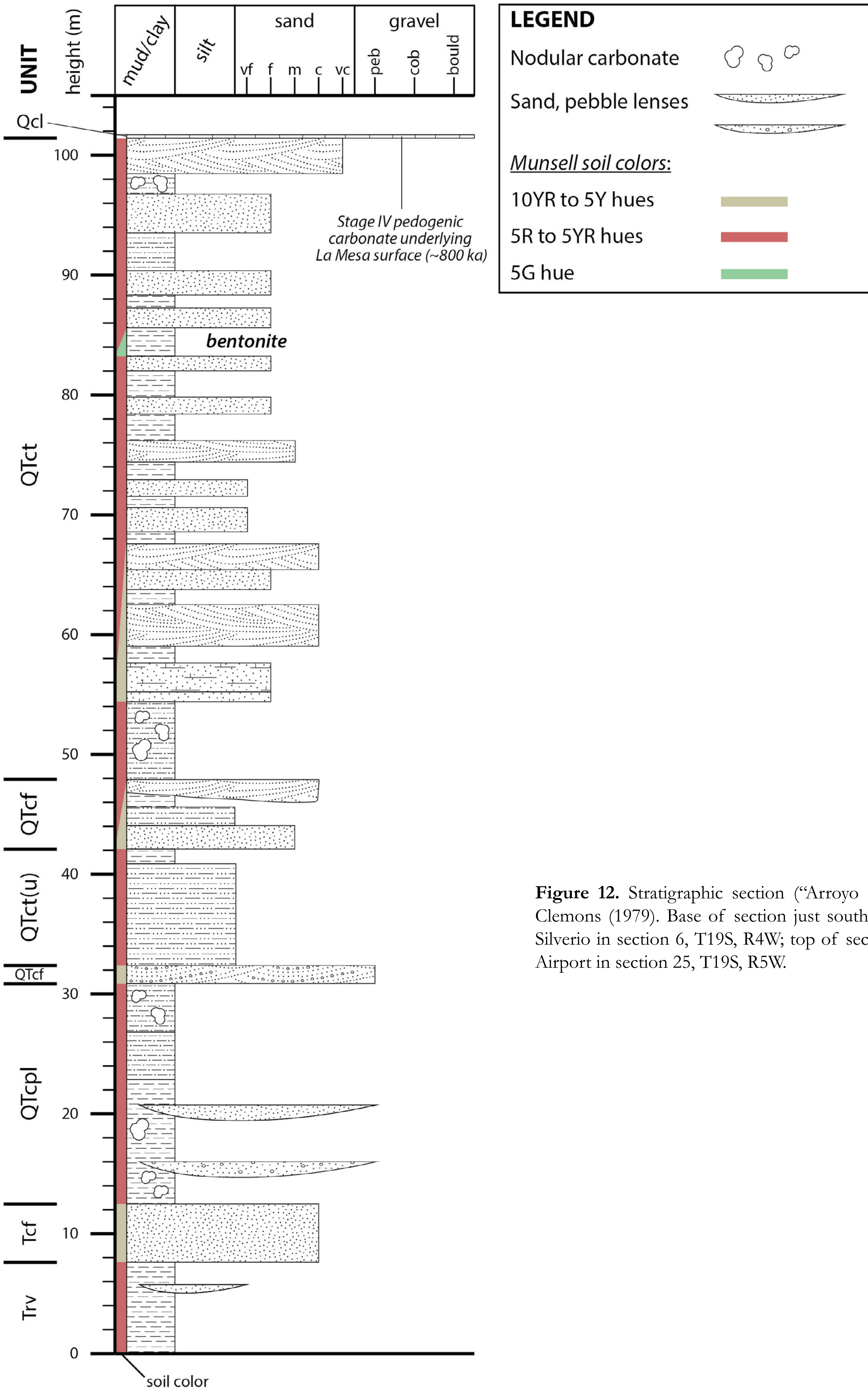

Figure 12. Stratigraphic section ("Arroyo Cuervo") measured by Clemons (1979). Base of section just south of La Capilla de Don Silverio in section 6, T19S, R4W; top of section west of old Hatch Airport in section 25, T19S, R5W.

Hatch-Rincon basins (Morgan et al., 2011; Morgan and Lucas, 2012).

In the Palomas basin, reddish channel-fill gravels and extra-channel silt and mud have been mapped as an upper piedmont facies of Plio-Pleistocene basin-fill (e.g., Jochems and Koning, 2015a). Unit QTcpu is lithologically similar to these deposits and probably similar in age as well. Correlative deposits in the Williamsburg quadrangle in the central Palomas basin were estimated to be ~2.6-1.8 Ma in age based on fossil evidence (G. Morgan, pers. comm., 2014; Jochems and Koning, 2015a). If indeed correlative, the top of QTcpu in the Arroyo Cuervo quadrangle must be significantly younger as constrained by the ~0.8 Ma La Mesa surface (Mack et al., 1993, 1998; Leeder et al., 1996). It should be noted that all piedmont facies of the Camp Rice Formation could be somewhat older near the western quadrangle boundary assuming that they prograded toward the ancestral Rio Grande from uplands to the west and southwest.

Beds of clay and gravel associated with La Mesa surface (Qcl, Qcp) likely belong to the latest early or perhaps earliest middle Pleistocene. Unit Qcp may be slightly older than unit Qcl because it appears to grade to an older (buried) QTcpu surface and is inset by piedmont (Qpo) graded to La Mesa in the southwest corner of the quadrangle. Stage IV petrocalcic horizons in unit Qcl suggest that La Mesa surface has been stable for hundreds of thousands of years (Gile et al., 1981).

QUATERNARY HISTORY (POST-CAMP RICE FORMATION)

Deposition of the Camp Rice Formation ceased ~0.8 Ma (Mack et al., 1993, 1998; Leeder et al., 1996), after which the Rio Grande and its tributaries began incising to eventually form the modern network of arroyos and stream valleys. Valley-margin deposits include inset stream terraces, whereas valley-floor deposits include low-lying terraces adjacent to modern stream courses.

Three terrace deposits of tributaries to the Rio Grande are found in the Arroyo Cuervo quadrangle; they are mostly concentrated along Arroyo Cuervo itself as well as an unnamed tributary in the central part of the map area. These deposits are typically thin (<6.5 m) strath terrace deposits composed of well graded pebbles through boulders of dominantly volcanic lithologies (<10% total Paleozoic carbonates and chert). The middle terrace deposit (Qtm) of Arroyo Cuervo exhibits finer texture at distal positions near the Rio Grande (Fig. 13), probably due to low slope along the paleo-longitudinal profile of Arroyo Cuervo as well as the prevalence of finer-grained beds of Tcf and Trv in that area. Tributary terraces are distinguished by landscape position (tread heights 3-33 m above modern grade), as well as clast varnishing and degree of soil development. For example, high terrace deposits (Qth) feature up to stage II calcic horizons and moderate varnish on up to 65% of clasts at its tread. Redder to strong brown colors (5-7.5YR), overall coarser texture, and abundant cross-stratified beds serve to distinguish terrace deposits from Camp Rice Formation gravels into which they are inset. Two broad erosional surfaces in the south half of the map area, the upper and lower La Capilla surfaces, appear to grade to Qth and Qtm, respectively.

Two Rio Grande terrace deposits are distinguished from those of its tributaries by clast content and morphology. These deposits contain up to 20% extra-basin clasts, particularly quartzite and greenish Cretaceous sedimentary lithologies. They are also grayer (10YR) in color than tributary terraces. The lower Rio Grande terrace (Qtrg1) has tread elevations of 15-21 m above modern grade and ranges from a strath to fill terrace up to 12 m thick. Based on these characteristics, it is likely correlative to the upper Pleistocene Picacho alluvium of Hawley (1965), Ruhe (1967), and Gile et al. (1981). The lower-middle Rio Grande terrace (Qtrg2) has tread elevations of 21-25 m above modern grade and is a fill deposit 15-18 m thick. It is tentatively correlated to the middle upper Pleistocene Tortugas alluvium based on its position as the next highest/oldest mainstem deposit above inferred Picacho alluvium, although its tread is lower than Tortugas surfaces in Selden Canyon (30-40 m above the Rio Grande floodplain; Gile et al., 1981). Both terraces have relatively dissected treads in the map area.

Two valley-floor deposits are commonly found in moderate to large drainages crossing the quadrangle: younger (Qay) and historical (Qah) alluvium, Qay being the more common of the two. It ranges in color from strong to yellowish brown (7.5-10YR) and consists of gravelly to silty sand with subordinate (up to 35%) pebble-cobble lenses and lags. Reddish colors (5YR) may predominate in the eastern part of the map area where younger alluvium consists largely of reworked Rincon Valley Formation mud and silt-sand. Treads of these deposits lie 2-3 m above modern grade. Charcoal collected from a Qay deposit in Arroyo Yeso yielded conventional radiocarbon ages of ~3.9 ^{14}C kyr BP or ~4.4-4.2 cal kyr BP

Figure 13. Alluvium of the middle tributary terrace (Qtm) of Arroyo Cuervo. Tributary terrace deposits are distinguished from Camp Rice Formation gravels by reddish or strong brown colors (5-7.5YR), common cross-stratification, and coarser bedload gravels. This deposit is an exception to the latter criteria because it contains mostly pebble gravels deposited at a distal position in the Arroyo Cuervo drainage. Walking stick for scale (lower right) is 1.5 m tall. Section 30, T18S, R4W.

(Fig. 14, Table 1). Metcalf (1969) reported a radiocarbon age of 9360±150 ^{14}C yr BP (~11.0-10.2 cal kyr BP) from correlative fan deposits just north of the quadrangle. This age is consistent with reported ages in the central Palomas basin (Jochems and Koning, 2015b). Although younger alluvium may be differentiated into 2 deposits elsewhere in the Palomas and Hatch-Rincon basins, it is treated as a single Holocene unit in this quadrangle.

Qah alluvium is brown (7.5YR) sand and pebble or pebble-cobble-boulder gravel in roughly equal proportions. These deposits are better stratified than Qay and underlie low-lying treads <1.5 m above modern grade. They are covered in many places by mixed eolian-alluvial sediment (Qea). Charcoal samples from correlative deposits in the Palomas basin returned radiocarbon ages of ~100-700 ^{14}C yr BP (Jochems and Koning, 2015b; Jochems and

Table 1—Summary radiocarbon geochronology for Arroyo Yeso samples.

Sample #	Lab #[a]	Deposit	Material Dated	UTM N[b]	UTM E[b]	Conventional Age (^{14}C yr BP$_{1950}$)[c]	2σ Calibrated Age Range (cal yr BP$_{1950}$)[d]	Median Age (cal yr BP$_{1950}$)[e]	δ^{13}C (‰)
16AC-763A	Beta-441927	Qay	charcoal	3623902	281604	3880 ± 30	4417-4235 (0.983) 4197-4185 (0.017)	4310 ± 120	-22.0
16AC-763B	Beta-441928	Qay	charcoal	3623902	281604	3860 ± 30	4411-4225 (0.882) 4204-4159 (0.118)	4290 ± 130	-23.1

[a]All samples dated by AMS analysis, Beta Analytic Inc., Miami, FL.

[b]Coordinates given in UTM Zone 13S, NAD83.

[c]Conservative error of ± 30 ^{14}C yr BP$_{1950}$ is given for all samples due to 1σ < 30 ^{14}C yr BP$_{1950}$ in each case.

[d]2σ calibrated age ranges calculated as relative probability using Calib 7.1 (Stuiver and Reimer 1993) and IntCal13 calibration curve of Reimer et al. (2013).

[e]Median age reported by averaging entire age range and rounding to nearest 10 yr. Error is difference between median and end values of range.

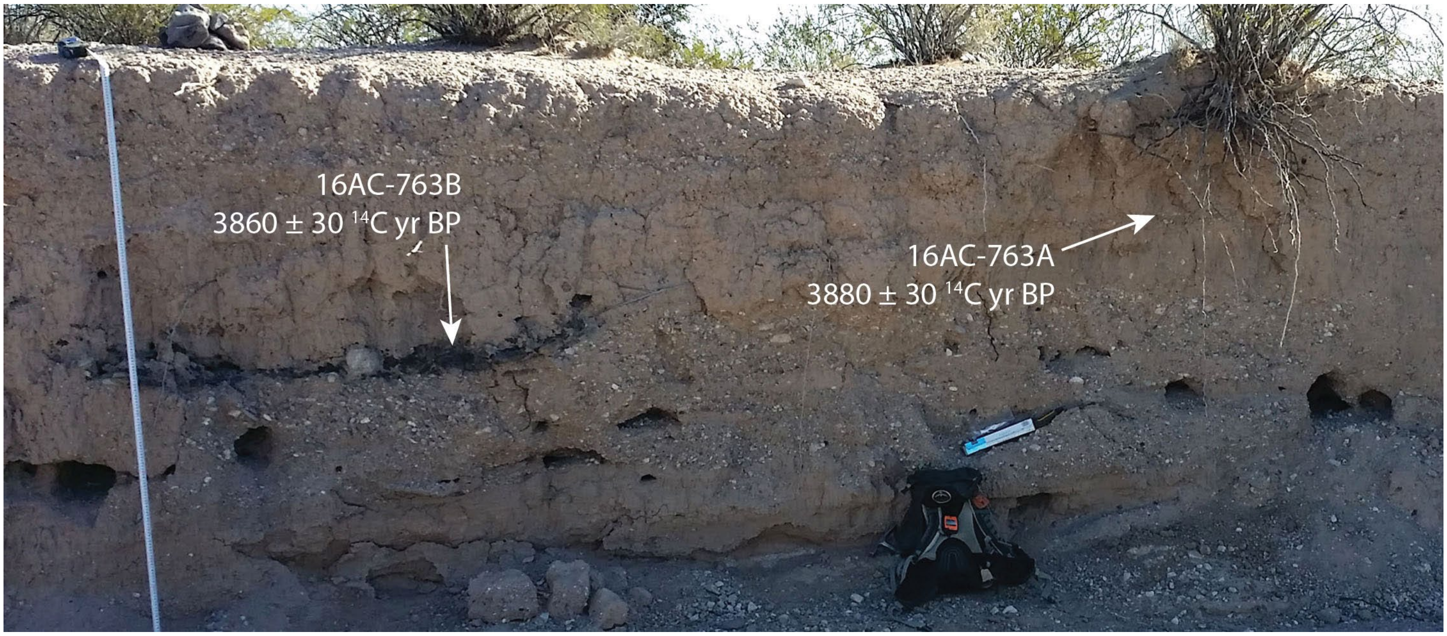

Figure 14. Younger alluvium (Qay) exposed in Arroyo Yeso. These deposits are characterized by brownish (10YR) colors, relatively few coarse channel fills, and occasional presence of stage I(+) calcic horizons. White arrows show locations of charcoal samples and associated radiocarbon ages. Tape in left of photo is 2 m long. Section 23, T18S, R5W.

Koning, 2017).

Traces of historical Rio Grande channels and oxbow lakes were mapped using 1937 aerial photography. These photos predate final construction of Caballo Dam (20 km upstream of quadrangle) by a year and show a somewhat more natural state of the river (Elephant Butte Dam, 63 km upstream, was completed in 1916). Mapping of old channels and floodplain features using air photos and satellite imagery suggests that the river maintained a historical channel of slightly larger width compared to the 1937 and modern channels (60-300, 30-270 m, and 30-85 m, respectively). However, sinuosity of the historical channel system was significantly higher than either of the 1937 or contemporary channels. Measured sinuosity ratios (stream length to valley axis length) are 2.0 (historical), 1.3 (1937), and 1.2 (modern). Thus, upstream dams have had the obvious effects of channel narrowing and straightening on the Rio Grande in the map area and Rincon Valley in general.

Other middle to late Quaternary deposits of note include several types of deposits mapped on high surfaces in the quadrangle. Eolian silt-sand, sheetwash, and colluvial deposits (Qesc) are commonly found underlying the upper and lower La Capilla geomorphic surfaces in the south-central part of the quadrangle (Fig. 15). Eolian sediment is commonly thicker on the eastern side of ridges, implying dominant westerly winds throughout the (late) Holocene.

Although generally constructional in the Palomas, Hatch-Rincon, and Mesilla basins (Gile et al., 1981; Lozinsky, 1986; McCraw and Love, 2012, and references therein), there is evidence that La Mesa surface may be erosional to some extent in the Arroyo Cuervo quadrangle and to the east (Hawley, 1965). For example, packages of coarse upper Palomas Formation observed to the north have no correlative in the map area despite the proximity of several uplifts (Good Sight Mountains, Sierra de las Uvas). Thin veneers of pebbly gravel underlying the somewhat irregular surface may be erosional lags. Deposits encountered on La Mesa surface and gradational surfaces extending south into Uvas Valley include fine-grained basin-floor loam, silt, and clay (Qbf) as well as clay and silt deposited in small playa lakes (Ql) (Seager et al., 1982). Locals note that depressions mapped as playas could be craters from practice bombs dropped by the US military during World II on a target range west of the old Hatch Airport (J. Gray, pers. comm., 2017).

Basin-fill (Qbf) deposits in the southernmost part of the quadrangle overlie lacustrine sediment associated with relict shoreline features of pluvial Lake Good Sight (Hawley, 1965). At its highstand of ~1372 m (Hawley, 1993), Lake Good Sight filled approximately 65 km^2 in the synclinal Uvas Valley and had a drainage basin of 590 km^2 (Allen, 2005). It likely formed then intermittently drained and filled beginning around the time of the last glacial maximum ~20 ka (Hawley et al., 1975). Dated records for larger pluvial lakes in southwestern New Mexico and

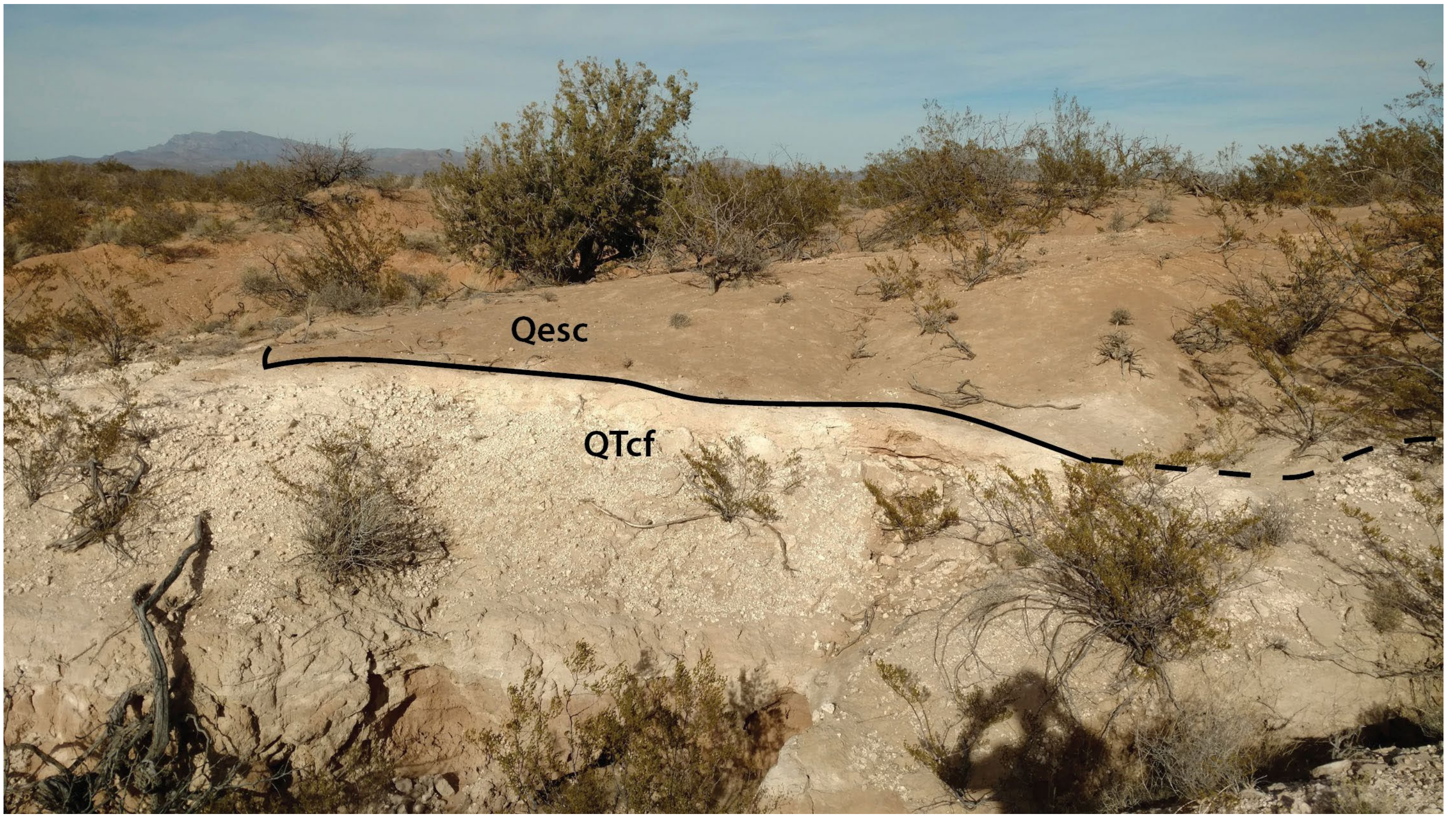

Figure 15. Undivided eolian silt-sand, sheetflood, and colluvial deposits (Qesc). This unit is commonly found mantling high, low-gradient surfaces including middle Pleistocene erosional surfaces (upper, lower La Capilla surface) in the southern part of the quadrangle. Whitish layer below contact on upper axial-fluvial facies (QTcf) is interpreted as a groundwater carbonate rather than a buried soil. Section 18, T19S, R4W.

northern Chihuahua show up to four highstand events since ~7-8 ka (Krider, 1998; Castiglia and Fawcett, 2006). No such record has yet been established for Lake Good Sight.

STRUCTURAL GEOLOGY

The Arroyo Cuervo fault is a south- to southwest-down fault that is the primary structure in the Arroyo Cuervo quadrangle. It extends at least 8 km from the northwestern corner of the quadrangle to a point near La Capilla de Don Silverio before its surface trace is lost. A 0.3 km trace of the fault is exposed in the southeast corner of section 5, T19S, R4W, where a dip of 73° was measured on a fault plane. A similarly oriented fault juxtaposes axial-fluvial facies of the Camp Rice Formation with Rincon Valley Formation in the southwestern corner of the Hatch quadrangle to the east (Seager et al., 1982; Seager, 1995). This is probably an extension of the Arroyo Cuervo fault, in which case its total length is at least 16 km.

The Arroyo Cuervo fault displaces middle piedmont facies (QTcpm) against lower piedmont gravels (QTcpl) in the western part of the map area, where its trace is marked by strong travertine-like calcite development (Fig. 16). U-series analysis of a sample from one exposure of the fault resulted in secular equilibrium (V. Polyak, pers. comm., 2016). Assuming that calcite precipitates along the fracture zone following a surface-rupturing earthquake (as described by Williams et al., 2017), the fault has not been active since at least the early Pleistocene or latest Pliocene. Near La Capilla, the fault places lower piedmont or axial-fluvial facies (Tcf) against Rincon Valley Formation. It also cuts transitional facies (QTct) near the eastern quadrangle boundary. The fault zone in these locations is typically expressed by well-cemented gravels or pebbly sand in the hanging wall, particularly in unit QTcpl. Exposures of the fault in the central and western parts of the map area are not sufficient to determine stratigraphic displacement, but it is probably on the order of several 10s of m. Displacement of unit QTcpm in the western part of the quadrangle is <10 m.

Gravity data suggests that the western tip of the Arroyo Cuervo fault may terminate against the northward projection of the west-down Good Sight fault (Fig. 17; Seager et al., 1982). Curiously, the hanging wall of the fault appears to coincide with a gravity high in the

Figure 16. Arroyo Cuervo fault trace, looking east. Strong development of travertine in fault zone and lack of fault scarps suggest recurrent movement during (but not after) deposition of the Camp Rice Formation. Stratigraphic displacement of units QTcpm and QTcpl is typically less than 10 m. Walking stick for scale (left) is 1.5 m tall. Section 28, T18S, R5W.

southeast part of the quadrangle (Daggett and Keller, 1982). Perhaps this high was associated with upland areas flanking the western margin of the Good Sight-Cedar Hills depression, in which case the Arroyo Cuervo fault would post-date this tectonic feature. This possibility cannot easily be field tested due to the lack of exposures predating the Rincon Valley Formation in the Arroyo Cuervo area. Another possibility is that the gravity high is centered on relatively shallow basement rock associated with the Rio Grande uplift (see below).

Rincon Valley and Camp Rice Formation strata in the quadrangle generally dip toward the northeast. One explanation for this pattern is Plio-Pleistocene movement along the southwest-down Derry fault and Arroyo Cuervo faults (Fig. 17; Seager and Mack, 2003). The northwesterly trend of these structures follows inferred trends of the Laramide Rio Grande uplift (Seager, 1983; Seager et al., 1986). Inversion of Laramide structures has been posited for a number of normal faults in the Caballo Mountains (Seager and Mack, 2003), and could explain the unusual trends of the aforementioned faults in the Hatch-Rincon basin.

HYDROGEOLOGY

Aquifers yielding water of adequate quantity and quality for domestic, municipal, and agricultural use are found in the Santa Fe Group and younger Quaternary valley fill units in the Palomas and Hatch-Rincon basins. The following discussion describes the potential of basin-fill and valley-floor units of the Arroyo Cuervo quadrangle for groundwater resources as well as implications for water quality.

Santa Fe Group units predating the Camp Rice Formation contain gravels of alluvial origin, particularly where they are found along the flanks of uplifts surrounding today's basins. However, the Rincon Valley Formation underlying local population centers and agricultural communities bears almost no groundwater or only insignificant amounts of poor quality water (Wilson et al., 1981), its permeability restricted by abundant clay and mudstone beds. Even where pre-Camp Rice Formation gravels are found, they are likely to be cemented by silica, calcite, or clay and therefore are expected to have greatly reduced intrinsic permeability. For example, fanglomerate facies of the Camp Rice Formation (Trvc) feature a matrix cemented almost entirely by clay where they are observed in the southwest part of the Arroyo Cuervo quadrangle. It is possible that cementation in such units decreases basinward (Koning et al., 2015), in which case they could form deep but viable aquifers in the center of the Hatch-Rincon basin.

The lower piedmont facies of the Camp Rice Formation (QTcpl) and its transitional base (QTcplt) contain gravelly channel-fills with varying degrees of cementation and relatively little clay (<15%) in their matrix. Although gravels are subordinate in each unit (cf. Koning et al., 2015; Jochems and Koning, 2017), they did at one time transmit groundwater as evidenced by strongly cemented, calcite-rich beds found above their contact with Rincon Valley Formation mudstone. Similar cementation is found where the lower piedmont facies is in fault contact with the Rincon Valley Formation (Fig. 18), as well as were moderately sorted, sandy to pebbly beds of the lower axial-fluvial facies (Tcf) lie on Miocene mudstones. Several small springs emit from the Camp Rice-Rincon

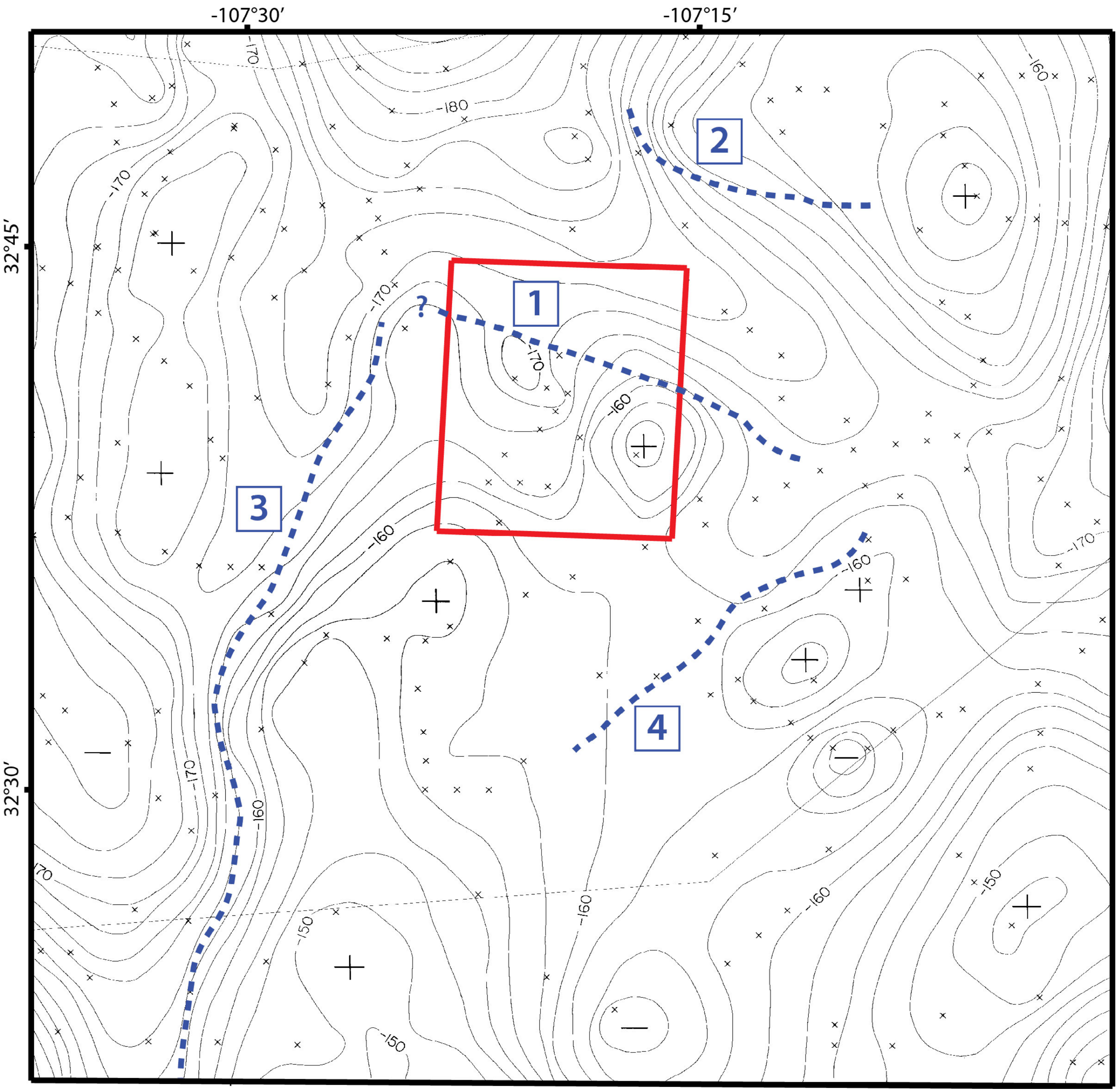

Figure 17. Complete Bouguer gravity anomaly map of western Hatch-Rincon basin and vicinity (modified from Daggett and Keller, 1982). The Arroyo Cuervo quadrangle is outlined in red. Faults (blue) numbered as follows: 1 = Arroyo Cuervo fault, 2 = Derry fault, 3 = Good Sight fault, and 4 = Sierra de las Uvas fault. Fault traces are interpretations of Seager and others (1982), with modification of Arroyo Cuervo fault from this study. Contours in mGals; x's denote locations of gravity measurements.

Valley contact in the quadrangle as well as in the Clark Spring Canyon 7.5-minute quadrangle to the northwest (Jochems and Koning, 2017). Thus, both depositional and fault contacts between lower Camp Rice Formation units and the Rincon Valley Formation represent significant hydrogeologic barriers. Although they contain well graded, uncemented, clast-supported gravels, units QTcpm and QTcpu lie above the zone of saturation in the Arroyo Cuervo quadrangle.

Late Pleistocene to Holocene valley-floor units have been shown to be high-quality, productive aquifers in the Palomas and Hatch-Rincon basins (Davie Jr. and Spiegel, 1967; Wilson et al., 1981). Well data from these areas suggest that gravels and sands in units Qah and Qay may be saturated as little as 1.5 m below the surface. These units act as hydraulic connections between the surface and units of the underlying Camp Rice and Palomas Formations in larger tributaries to the Rio Grande (Davie

Figure 18. Strongly cemented gravel/conglomerate beds of the lower piedmont facies of the Camp Rice Formation (QTcpl) near the Arroyo Cuervo fault. Such cementation commonly occurs where the unit is in fault or depositional contact with the Rincon Valley Formation, which acts as an aquiclude throughout the quadrangle. Note backpack and 1.5-m-tall walking stick (white oval) for scale. Section 35, T18S, R5W.

Jr. and Spiegel, 1967). However, historical alluvium in the Rio Grande floodplain (Qahrg) lies directly above clayey Rincon Valley Formation sediment acting as an aquiclude. This Holocene-aged floodplain material generally yields fresh to slightly saline water with ~500-1500 ppm total dissolved solids (TDS; Wilson et al., 1981). Younger alluvium (Qay) may have low permeability where it is predominantly sourced by the Rincon Valley Formation, as in the low-lying areas west of the Rio Grande in the east-central part of the map area. Any water locally present in unit Qay is likely of low quality due to abundant evaporites in the Rincon Valley Formation.

NON-METALLIC RESOURCES

A clay pit was mined from the 1930s to the early 1940s in the upper part of QTct along the Doña Ana-Sierra County line (section 19, T19S, R4W; section 24, T19S, R5W). This pit produced bentonite for drilling muds that was processed at Hatch (Patterson and Holmes, 1965). The montmorillonite clay exhibited strong oil-bleaching properties after clay treatment and could potentially yield 60 barrels of 15-centipoise viscosity per ton (Nutting, 1943, p. 151; Reynolds, 1952). Similar clays are observed in the Rincon Valley Formation as well as the upper piedmont facies of the Camp Rice Formation (QTcpu). No chemical analyses were made of clays found in units exposed on the Arroyo Cuervo quadrangle, but variable concentrations of mineral impurities (especially gypsum) are likely to affect their potential use and value.

Gravel and sand beds in the upper Santa Fe Group (e.g., Camp Rice Formation) and middle to late Pleistocene deposits have long been mined for aggregate (e.g., NM State Highway Department, 1964). In the map area, the lower piedmont facies of the Camp Rice Formation as well as terrace deposits are most likely to yield sufficient quantities of such material, but their viability as a source of aggregate is currently hindered by distance from paved highways.

ACKNOWLEDGMENTS

Mapping of the Arroyo Cuervo quadrangle was funded by the STATEMAP program, which is jointly supported by the U.S. Geological Survey and the New Mexico Bureau of Geology and Mineral Resources (NMBGMR). I thank Dr. J. Michael Timmons of NMBGMR for logistical support and coordination. Dr. Gary Morgan and Paul Sealey of the New Mexico Museum of Natural History and Science accompanied me to the quadrangle to collect fossils from the Camp Rice Formation. Dr. John W. Hawley kindly shared his reconnaissance mapping of the quadrangle and detailed knowledge of the local geology. Finally, I wish to express my extreme gratitude to James and Shannon Gray for their gracious hospitality and extensive knowledge of local roads and exposures.

REFERENCES

Allen, B.D., 2005, Ice age lakes in New Mexico, *in* Lucas, S.G., Morgan, G.S., and Zeigler, K.E., eds., New Mexico's Ice Ages: New Mexico Museum of Natural History and Science Bulletin 28, p. 107-114.

Bachman, G.O., and Mehnert, H.H., 1978, New K-Ar dates and the late Pliocene to Holocene geomorphic history of the Rio Grande region, New Mexico: Geological Society of America Bulletin, v. 89, p. 283–292.

Berggren, W.A., Helgen, F.J., Langerlis, C.G., Kent, D.V., Obradovich, J.D., Raffi, I., Raymo, M.E., and Shackleton, N.J., 1995, Late Neogene chronology—new perspectives in high-resolution stratigraphy: Geological Society of America Bulletin, v. 107, p. 1272–1287.

Birkeland, P.W., 1999, Soils and geomorphology: Oxford, UK, Oxford University Press, 448 p.

Birkeland, P.W., Machette, M.N., and Haller, K.M., 1991, Soils as a tool for applied Quaternary geology: Utah Geological and Mineral Survey Miscellaneous Publication 91–3, 63 p.

Castiglia, P.J., and Fawcett, P.J., 2006, Large Holocene lakes and climate change in the Chihuahuan Desert: Geology, v. 34, no. 2, p. 113-116, doi: 10.1130/G22036.1.

Chapin, C.E., and Cather, S.M., 1994, Tectonic setting of the axial basins of the northern and central Rio Grande rift, *in* Keller, G.R. and Cather, S.M. eds., Basins of the Rio Grande Rift: Structure, Stratigraphy, and Tectonic Setting: Geological Society of America Special Paper 29, v. 291, p. 5–25.

Clemons, R.E., 1979, Geology of Good Sight Mountains and Uvas Valley, southwest New Mexico: New Mexico Bureau of Mines and Mineral Resources Circular 169, 32 p.

Clemons, R.E., and Seager, W.R., 1973, Geology of Souse Springs quadrangle, New Mexico: New Mexico Bureau of Mines and Mineral Resources Bulletin 100, 31 p.

Compton, R.R., 1985, Geology in the field: New York, John Wiley & Sons, 398 p.

Daggett, P.H., and Keller, G.R., 1982, Complete Bouguer anomaly map of northwest part of Las Cruces 1° x 2° sheet, *in* Seager, W.R., Clemons, R.E., Hawley, J.W., and Kelley, R.E. eds., Geology of Northwest Part of Las Cruces 1° x 2° sheet: New Mexico Bureau of Mines and Mineral Resources Geologic Map 53, scale 1:125,000.

Davie Jr., W., and Spiegel, Z., 1967, Geology and water resources of Las Animas Creek and vicinity, Sierra County, New Mexico: New Mexico State Engineer Hydrographic Survey Report, 44 p.

Gile, L.H., Peterson, F.F., and Grossman, R.B., 1966, Morphological and genetic sequences of carbonate accumulation in desert soils: Soil Science, v. 101, p. 347–360.

Gile, L.H., Hawley, J.W., and Grossman, R.B., 1981, Soils and geomorphology in the Basin and Range area of southern New Mexico—guidebook to the Desert Project: New Mexico Bureau of Mines and Mineral Resources Memoir 39, 222 p.

Hawley, J.W., 1965, Geomorphic surfaces along the Rio Grande valley from El Paso, Texas, to Caballo Reservoir, New Mexico, *in* Fitzsimmons, J.P., and Lochman-Balk, C., eds., Southwestern New Mexico II: New Mexico Geological Society Guidebook 16, p. 188-198.

Hawley, J.W., comp., 1978, Guidebook to Rio Grande rift in New Mexico and Colorado: New Mexico Bureau of Mines and Mineral Resources Circular 163, 241 p.

Hawley, J.W., 1993, Geomorphic setting and late Quaternary history of pluvial-lake basins in the southern New Mexico region: New Mexico Bureau of Mines and Mineral Resources Open-File Report 391, 28 p.

Hawley, J.W., and Kottlowski, F.E., 1969, Quaternary geology of the south-central New Mexico border region, *in* Kottlowski, F.E. and LeMone, D.V. eds., Border Stratigraphy Symposium: New Mexico Bureau of Mines and Mineral Resources Circular 104, p. 89–115.

Hawley, J.W., Kottlowski, F.E., Seager, W.R., King, W.E., Strain, W.S., and LeMone, D.V., 1969, The Santa Fe Group in the south-central New Mexico border region, *in* Kottlowski, F.E., and LeMone, D.V., eds., Border Stratigraphy Symposium: New Mexico Bureau of Mines and Mineral Resources Circular 104, 52–76 p.

Hawley, J.W., Seager, W.R., and Corbitt, L., 1975, Exit road log B: Hatch to Deming via NM 26, *in* Seager, W.R., Clemons, R.E., and Callender, J.F., eds., Las Cruces Country: New Mexico Geology Society Guidebook 26, p. 56-60.

Ingram, R.L., 1954, Terminology for the thickness of stratification and parting units in sedimentary rocks: Geological Society of America Bulletin, v. 65, p. 937–938.

Jochems, A.P., 2015, Geologic map of the Williamsburg NW 7.5-minute quadrangle, Sierra County, New Mexico: New Mexico Bureau of Geology and Mineral Resources Open-File Geologic Map OF-GM 251, scale 1:24,000.

Jochems, A.P., and Koning, D.J., 2015a, Geologic map of the Williamsburg 7.5-minute quadrangle, Sierra County, New Mexico: New Mexico Bureau of Geology and Mineral Resources Open-File Geologic Map OF-GM 250, scale 1:24,000.

Jochems, A.P., and Koning, D.J., 2015b, Holocene stratigraphy and a preliminary geomorphic history for the Palomas basin, south-central New Mexico: New Mexico Geology, v. 37, p. 77–88.

Jochems, A.P., and Koning, D.J., 2017, Geologic map of the Clark Spring Canyon 7.5-minute quadrangle, Sierra County, New Mexico: New Mexico Bureau of Geology and Mineral Resources Open-File Geologic Map OF-GM 263, scale 1:24,000.

King, W.E., Hawley, J.W., Taylor, A.M., and Wilson, R.P., 1971, Geology and ground-water resources of central and western Doña Ana County, New Mexico: New Mexico Bureau of Mines and Mineral Resources Hydrologic Report 1, 64 p.

Koning, D.J., Jochems, A.P., and Cikoski, C.T., 2015, Geologic map of the Skute Stone Arroyo 7.5-minute quadrangle, Sierra County, New Mexico: New Mexico Bureau of Geology and Mineral Resources Open-File Geologic Map OF-GM 252, scale 1:24,000.

Koning, D.J., Jochems, A.P., Morgan, G.S., Lueth, V., and Peters, L., 2016, Stratigraphy, gravel provenance, and age of early Rio Grande deposits exposed 1-2 km northwest of downtown Truth or Consequences, New Mexico, *in* Frey, B.A., Karlstrom, K.E., Lucas, S.G., Williams, S., Zeigler, K., McLemore, V., and Ulmer-Scholle, D.S. eds., The Geology of the Belen Area: New Mexico Geological Society Guidebook 67, p. 459–478.

Krider, P.R., 1998, Paleoclimatic significance of late Quaternary lacustrine and alluvial stratigraphy, Animas Valley, New Mexico: Quaternary Research, v. 50, p. 283-289.

Leeder, M.R., Mack, G.H., and Salyards, S.L., 1996, Axial-transverse fluvial interactions in half-graben—Plio-Pleistocene Palomas Basin, southern Rio Grande rift, New Mexico, USA: Basin Research, v. 12, p. 225–241.

Lozinsky, R.P., 1986, Geology and late Cenozoic history of the Elephant Butte area, Sierra County, New Mexico: New Mexico Bureau of Mines and Mineral Resources Circular 187, 40 p.

Mack, G.H., and Seager, W.R., 1990, Tectonic control on facies distribution of the Camp Rice and Palomas Formations (Pliocene-Pleistocene) in the southern Rio Grande rift: Geological Society of America Bulletin, v. 102, p. 45–53, doi:10.1130/0016-7606(1990)102<0045:TCOFDO>2.3.CO;2.

Mack, G.H., and Seager, W.R., 1995, Transfer zones in the southern Rio Grande rift: Journal of the Geological Society [London], v. 152, p. 551–560.

Mack, G.H., Salyards, S.L., and James, W.C., 1993, Magnetostratigraphy of the Plio-Pleistocene Camp Rice and Palomas Formations in the Rio Grande rift of southern New Mexico: American Journal of Science, v. 293, p. 49–77.

Mack, G.H., Seager, W.R., and Kieling, J., 1994a, Late Oligocene and Miocene faulting and sedimentation, and evolution of the southern Rio Grande rift, New Mexico: Sedimentary Geology, v. 92, p. 79–96.

Mack, G.H., Nightengale, A.L., Seager, W.R., and Clemons, R.E., 1994b, The Oligocene Goodsight-Cedar Hills half graben near Las Cruces and its implications to the evolution of the Mogollon-Datil volcanic field and to the southern Rio Grande rift, *in* Chamberlin, R.M., Kues, B.S., Cather, S.M., Barker, J.M., and McIntosh, W.C., eds., Mogollon Slope, West-Central New Mexico and East-Central Arizona:

New Mexico Geological Society Guidebook 45, p. 135–142.

Mack, G.H., James, W.C., and Salyards, S.L., 1994c, Late Pliocene and early Pleistocene sedimentation as influenced by intrabasinal faulting, southern Rio Grande rift, *in* Keller, G.R. and Cather, S.M., eds., Basins of the Rio Grande Rift: Structure, Stratigraphy, and Tectonic Setting: Geological Society of America Special Paper 291, p. 257–264.

Mack, G.H., McIntosh, W.C., Leeder, M.R., and Monger, H.C., 1996, Plio-Pleistocene pumice floods in the ancestral Rio Grande, southern Rio Grande rift, USA: Sedimentary Geology, v. 103, p. 1–8.

Mack, G.H., Salyards, S.L., McIntosh, W.C., and Leeder, M.R., 1998, Reversal magnetostratigraphy and radioisotopic geochronology of the Plio-Pleistocene Camp Rice and Palomas Formations, southern Rio Grande rift, *in* Mack, G.H., Austin, G.S., and Barker, J.M. eds., Las Cruces Country II: New Mexico Geological Society Guidebook 49, p. 229–236.

Mack, G.H., Seager, W.R., Leeder, M.R., Perez-Arlucea, M., and Salyards, S.L., 2006, Pliocene and Quaternary history of the Rio Grande, the axial river of the southern Rio Grande rift, New Mexico, USA: Earth-Science Reviews, v. 79, p. 141–162.

Mack, G.H., Dunbar, N., and Foster, R., 2009, New sites of 3.1-Ma Pumice beds in axial-fluvial strata of the Camp Rice and Palomas Formations, southern Rio Grande rift: New Mexico Geology, v. 31, p. 31–37.

McCraw, D.J., and Love, D.W., 2012, An overview and delineation of the Cuchillo geomorphic surface, Engle and Palomas Basins, New Mexico, *in* Lucas, S.G., McLemore, V.T., Lueth, V.W., Spielmann, J.A., and Krainer, K., eds., Geology of the Warm Springs Region: New Mexico Geological Society Guidebook 63, p. 491–498.

Metcalf, A.L., 1969, Quaternary surfaces, sediments, and mollusks: southern Mesilla Valley New Mexico, *in* Córdoba, D.A., Wengerd, S.A., and Shomaker, J., eds., Guidebook of the Border Region: New Mexico Geological Society Guidebook 20, p. 158–164.

Morgan, G.S., and Lucas, S.G., 2012, Cenozoic vertebrates from Sierra County, southwestern New Mexico, *in* Lucas, S.G., McLemore, V.T., Lueth, V.W., Spielmann, J.A., and Krainer, K., eds., Geology of the Warm Springs Region: New Mexico Geological Society Guidebook 63, p. 525–540.

Morgan, G.S., Sealey, P.L., and Lucas, S.G., 2011, Pliocene and early Pleistocene (Blancan) vertebrates from the Palomas Formation in the vicinity of Elephant Butte Lake and Caballo Lake, Sierra County, southwestern New Mexico, *in* Sullivan, R.M., Lucas, S.G., and Spielmann, J.A., eds., Fossil Record 3: New Mexico Museum of Natural History and Science Bulletin 53, p. 664–736.

Munsell Color, 2009, Munsell soil color book: Grand Rapids, MI, X-Rite.

New Mexico Bureau of Geology and Mineral Resources, 2003, Geologic map of New Mexico: New Mexico Bureau of Geology and Mineral Resources, scale 1:500,000.

New Mexico State Highway Department, 1964, Aggregate resources and soils study, New Mexico Interstate Route 25, New Mexico State Highway Department, pagination varies.

Nutting, P.G., 1943, Absorbent clays, their distribution, properties, production and uses: U.S. Geological Survey Bulletin 928-C, p. 127-221.

Patterson, S.H., and Holmes, R.W., 1965, Clays, in Mineral and Water Resources of New Mexico: New Mexico Bureau of Mines and Mineral Resources Bulletin 87, p. 312-322.

Reimer, P.J., Bard, E., Bayliss, A., Beck, J.W., Blackwell, P.G., Bronk Ramsey, C., Buck, C.E., Cheng, H., Edwards, R.L., Friedrich, M., and others, 2013, IntCal13 and Marine13 radiocarbon age calibration curves 0-50,000 years cal BP: Radiocarbon, v. 55, p. 1869–1887.

Repenning, C.A., and May, S.R., 1986, New evidence for the age of lower part of the Palomas Formation, *in* Clemons, R.E., King, W.E., Mack, G.H., and Zidek, J., eds., Truth or Consequences Region: New Mexico Geological Society Guidebook 37, p. 257–260.

Reynolds, D.H., 1952, Bentonite—occurrence, properties, utilization: New Mexico Miner, v. 14, no. 3, p. 9, 24-25.

Ruhe, R.V., 1967, Geomorphic surfaces and surficial deposits in southern New Mexico: New Mexico Bureau of Mines and Mineral Resources Memoir 18, 66 p.

Seager, W.R., 1995, Geologic map of the Hatch 7.5-minute quadrangle, Doña Ana County, New Mexico [released 2010]: New Mexico Bureau of Geology and Mineral Resources Open-File Geologic Map OF-GM 213, scale 1:24,000.

Seager, W.R., and Mack, G.H., 1991, Geology of Garfield quadrangle, Sierra and Doña Ana Counties, New Mexico: New Mexico Bureau of Mines and Mineral Resources Bulletin 128, 24 p.

Seager, W.R., and Mack, G.H., 1998, Geology of the McLeod Tank quadrangle, Sierra County, New Mexico: New Mexico Bureau of Mines and Mineral Resources Geologic Map 77, scale 1:24,000.

Seager, W.R., and Mack, G.H., 2003, Geology of the Caballo Mountains, New Mexico: New Mexico Bureau of Geology and Mineral Resources Memoir 49, 144 p.

Seager, W.R., Hawley, J.W., and Clemons, R.E., 1971, Geology of San Diego Mountain area, Doña Ana County, New Mexico: New Mexico Bureau of Mines and Mineral Resources Bulletin 97, 38 p.

Seager, W.R., Clemons, R.E., Hawley, J.W., and Kelley, R.E., 1982, Geology of northwest part of Las Cruces 1° x 2° sheet, New Mexico: New Mexico Bureau of Mines and Mineral Resources Geologic Map 53, scale 1:125,000.

Seager, W.R., Shafiqullah, M., Hawley, J.W., and Marvin, R.F., 1984, New K-Ar dates from basalts and the evolution of the southern Rio Grande rift: Geological Society of America Bulletin, v. 95, p. 87–99.

Seager, W.R., Mack, G.H., Raimonde, M.S., and Ryan, R.G., 1986, Laramide basement-cored uplift and basins in south-central New Mexico, *in* Clemons, R.E., King, W.E., and Mack, G.H., eds., Truth or Consequences Region: New Mexico Geological Society Guidebook 37, p. 123–130.

Seager, W.R., Hawley, J.W., Kottlowski, F.E., and Kelley, S.A., 1987, Geology of east half of Las Cruces and northeast El Paso 1° x 2° sheets, New Mexico: New Mexico Bureau of Mines and Mineral Resources Geologic Map 57, scale 1:125,000, scale 3 sheets.

Soil Survey Staff, 1999, Soil taxonomy: U.S. Department of Agriculture, US. Department of Agriculture Handbook 436, 869 p.

Strain, W.S., 1966, Blancan mammalian fauna and Pleistocene formation, Hudspeth County, Texas: Texas Memorial Museum Bulletin 10, 55 p.

Stuiver, M., and Reimer, P.J., 1993, Extended ^{14}C data base and revised CALIB radiocarbon calibration program: Radiocarbon, v. 35, p. 215–230.

Udden, J.A., 1914, Mechanical composition of clastic sediments: Geological Society of America Bulletin, v. 25, p. 655–744.

USDA, 2008, Natural Agricultural Imagery Program (NAIP) factsheet: U.S. Department of Agriculture, U.S. Department of Agriculture, 2 p.

Wentworth, C.K., 1922, A scale of grade and class terms for clastic sediments: Journal of Geology, v. 30, p. 377–392.

Western Regional Climate Center, 2016, Hatch, New Mexico NCDC 1981-2010 monthly normals: <<http://www.wrcc.dri.edu/cgi-bin/cliMAIN.pl?nm3855>>. Last accessed November 28, 2016.

Williams, R.T., Goodwin, L.B., Sharp, W.D., and Mozley, P.S., 2017, Reading a 400,000-year record of earthquake frequency for an intraplate fault: Proceedings of the National Academy of Sciences, v. 114, p. 4893–4898, doi: 10.1073/pnas.1617945114.

Wilson, C.A., White, R.R., Orr, B.R., and Roybal, R.G., 1981, Water resources of the Rincon and Mesilla Valleys and adjacent areas, New Mexico: New Mexico State Engineer Technical Report 43, 514 p.

APPENDIX A

Detailed descriptions of lithologic units on the
Arroyo Cuervo 7.5-minute quadrangle

QUATERNARY

Eolian and hillslope units

Qea Eolian and alluvial sand, undivided (Holocene) – Light brown (7.5YR 6/3-4) to light yellowish brown (10YR 6/4) silt-sand in thickly laminated to medium (0.8-25 cm), tabular to lenticular beds. Loose, very weakly calcareous, and horizontal-planar laminated to planar cross-stratified (foresets up to 15 cm thick). Sand is moderately well sorted, subangular to rounded, fU grains composed of 65-70% quartz, 15-20% lithics (volcanic, chert, mafic), and 15-20% feldspar with little or no interstitial clay. Approximately 35% of beds contain stringers of fine pebbles consisting of moderately sorted, subrounded to rounded calcite nodules, volcanics, quartzite, and granite. No soil or clast varnish observed at surface. Surface is commonly rippled. Deposit forms coppice dunes and occasional blow-outs less than 50 cm deep. >1.2 m thick.

Qesc Eolian sand, slopewash, and hillslope colluvium, undivided (Holocene to upper Pleistocene) – Yellowish red (5YR 5/6-8), clayey to pebbly silt-sand and pebble gravel deposited by eolian and hillslope processes. Loose, weakly calcareous, and massive to ripple or planar cross-stratified. Sand is quartzose and consists of vfL-fU grains. Contains 5-10% exotic pebbles such as quartzite and granite. Cumulic soil development indicated by stronger chroma and vague blocky peds is common in the upper 0.5-1.0 m of the deposit, which may form coppice dunes and blow-outs. Commonly mantles Camp Rice Formation or middle Pleistocene terraces in the central and southern parts of the quadrangle. 1.2-2 m thick.

Closed-basin units

Ql Playa deposits (Holocene) – Loose clay and silt deposited in small playas. Likely under 5 m thick [description from Seager et al., 1982].

Qbf Basin-floor deposits (Holocene to uppermost Pleistocene) – Loose, undissected loam, silt, or clay that may be slightly gravelly in places. No more than 15 m thick [description from Seager et al., 1982].

Valley-floor units

daf Disturbed or artificial fill (modern) – Sand and gravel that has been moved by humans to form berms and dams, or has been reworked/remobilized for construction of infrastructure or buildings.

Qaa Active alluvium of the Rio Grande (modern) – Sandy pebble-cobble gravel in the axial channel of the Rio Grande, commonly in longitudinal or transverse bars. Loose. Clasts consist of poorly to moderately sorted, subrounded to rounded pebbles and cobbles. Boulders may be present, transported from local tributaries to the active channel during larger flood events. Clast lithologies are diverse, reflecting bedrock exposed throughout the Rio Grande catchment. Sand is moderately to very well sorted, subrounded to rounded, fine- to coarse-grained, and quartzose. Total thickness unknown but likely 1-3 m.

Qam Modern alluvium (modern to ~80 years old) – Gray (7.5-10YR 5/1) to brown (7.5YR 5/2) pebbly sand and sandy pebble-cobble and pebble-cobble-boulder gravel in modern channels, troughs, and bars. Loose, non-calcareous, and cross-stratified. Gravel is imbricated, poorly sorted, subangular to well rounded (mostly subrounded to rounded), and consists of pebbles (55-90%), cobbles (10-40%), and boulders (5-15%) of >80% volcanic lithologies with minor Paleozoic carbonates and chert. Sand consists of fU-cL grains composed of 60-65% lithics (volcanics>chert>carbonate), 25-30% quartz, and 5-15% feldspar; no clay present. Occasionally, channel margins feature light brown (7.5YR 6/3), thin (<3-4 cm) veneers of mud (65-70% silt, 30-35% clay). Maximum thickness approximately 3 m.

Qamrg Modern alluvium of the Rio Grande (modern to ~80 years old) – Similar to Qam but with overall grayer colors (10YR hue). Deposit identified from active channel observed in 1937 aerial photographs. Clast lithologies are diverse, reflecting bedrock exposed throughout Rio Grande catchment. Total thickness unknown but likely 1-3 m.

Qamh Modern and historical alluvium, undivided (modern to ~600 years old) – Modern alluvium (Qam) and subordinate historical alluvium (Qah). See detailed descriptions of each individual unit.

Qah Historical alluvium (~80 to ~600 years old) – Brown (7.5YR 4-5/3-4) sand and sandy pebble and pebble-cobble-boulder gravel in tabular to lenticular beds. Loose and commonly trough cross-stratified. Gravel is clast-supported, imbricated, very poorly to poorly sorted, subrounded to well rounded and consists of pebbles (60-100%), cobbles (0-30%), and boulders (0-10%) of ~80% felsic to intermediate volcanics and ~20% Paleozoic carbonate and chert. Matrix consists of very poorly sorted, subangular to rounded, very fine to medium sand composed of 60-70% lithics (volcanic), 20-30% quartz, and 10-20% feldspar with minor to subordinate clay flakes. Deposit is inset into younger alluvium (Qay). Tread heights <1.5 m above modern grade. <2-2.5 m thick.

Qahrg Historical alluvium of the Rio Grande (~80 to ~600 years old) – Similar to Qah but with overall grayer colors (10YR hue). Deposit identified outside of active channel observed in 1937 aerial photographs. Clast lithologies are diverse, reflecting bedrock exposed throughout Rio Grande catchment. Low-relief (typically <1 m) furrows and berms on the surface of this deposit represent banks, scroll bars, and oxbow lakes of the historical Rio Grande. Maximum tread heights 2.3-2.5 m above modern grade. Well data suggest a typical thickness of 4-5 m.

Qahm Historical and modern alluvium, undivided (modern to ~600 years old) – Historical alluvium (Qah) and subordinate modern alluvium (Qam). See detailed descriptions of each individual unit.

Qahy Historical and younger alluvium, undivided (~80 years old to lower Holocene) – Historical alluvium (Qah) and subordinate younger alluvium (Qay). See detailed descriptions of each individual unit.

Qary Recent (historical + modern) and younger alluvium, undivided (modern to lower Holocene) – Recent alluvium (Qah and Qam, undivided) and subordinate younger alluvium (Qay). See detailed descriptions of each individual unit.

Qay Younger alluvium (middle to lower Holocene) – Yellowish brown (10YR 5/4) to strong brown, brown, or light brown (7.5YR 4-5/3-6; 6/3-4), gravelly to silty sand in thin to thick (6-80 cm), tabular beds. Loose, moderately to strongly calcareous, internally massive to weakly planar cross-stratified (foresets up to 10 cm thick), and vaguely normally graded. Sand consists of moderately to moderately well sorted, subangular to rounded, silty vfL-fL (15% fU-cU) grains composed of 55-75% lithics (volcanic), 15-25% quartz, and 10-25% feldspar with 0-5% clay chips. Sandy beds contain 10% scattered fine to medium pebbles and rare charcoal fragments. Deposit contains rare to subordinate (1-35%) pebble to cobble gravel lags and lenses up to 75 cm thick. Gravel consists of moderately to strongly calcareous, clast-supported, trough cross-stratified to well imbricated, fine to very coarse pebbles and fine to medium cobbles. Clasts are poorly to moderately sorted, subrounded to rounded, and consist of ~2/3 felsites and ~1/3 intermediate volcanics with 3-5% Paleozoic carbonate and chert. Gravel matrix consists of poorly sorted, subangular to rounded, fL-cU sand grains of similar composition to sandy beds but with 10% tannish to reddish free-grain argillans. Deposit features buried soils including 15-20 cm thick cumulic (Bw) horizons, ~30 cm thick Bt horizons with prismatic peds and ped argillans, and 45-60 cm thick Btk horizons with ped argillans and stage I+ carbonate morphology (carbonate masses). Deposit is capped by a 20-25 cm thick A horizon that is eroded in places. Strongly bioturbated by fine to coarse roots. Radiocarbon samples from an exposure in section 23, T18S, R5W returned conventional ages of 3880±30 and 3860±30 ^{14}C yr BP. Correlative fan deposits (Qfay) exposed in the southernmost Garfield 7.5-minute quadrangle returned a conventional radiocarbon age of 9360±150 ^{14}C yr BP (Metcalf, 1969). Deposit is inset into older terraces (Qtg) and inset by historical alluvium (Qah). Includes sediment correlative to both Leasburg and Fillmore alluvium described by Gile et al. (1981). Tread height 2.1-2.8 m above modern grade. >2-3 m thick.

Qayrg Younger alluvium of the Rio Grande (middle to lower Holocene) – Similar to Qay but with both redder and grayer colors (5YR, 10YR hues). Clast sizes may be bimodal between pea-sized pebbles and boulders. Clast lithologies are diverse, reflecting bedrock exposed throughout Rio Grande catchment. Includes sediment correlative to both Leasburg and Fillmore alluvium described by Gile et al. (1981). Tread heights 3.5-7 m above modern grade. Well data suggest a maximum thickness of 19-25 m.

Qaym Younger and modern alluvium, undivided (modern to lower Holocene) – Younger alluvium (Qay) and subordinate modern alluvium (Qam). See detailed descriptions of each individual unit.

Qayh Younger and historical alluvium, undivided (~80 years old to lower Holocene) – Younger alluvium (Qay) and subordinate historical alluvium (Qah). See detailed descriptions of each individual unit.

Qayr Younger and recent (historical + modern) alluvium, undivided (modern to lower Holocene) – Younger alluvium (Qay) and subordinate recent alluvium (Qah and Qam, undivided). See detailed descriptions of each individual unit.

Alluvial fan and piedmont units

Qfamh Modern and historical fan alluvium, undivided (modern to ~600 years old) – Modern fan alluvium (Qfam) and subordinate historical fan alluvium (Qfah). Modern fan alluvium is typically sandy pebble-cobble gravel graded to modern stream courses; see description for Qfah.

Qfah Historical fan alluvium (~80 to ~600 years old) – Loose deposits of gravel graded to low-lying terraces formed on historical alluvium (Qah). 1.5-3 m thick.

Qfahm Historical and modern fan alluvium, undivided (modern to ~600 years old) – Historical fan alluvium (Qfah) and subordinate modern fan alluvium (Qfam). Modern fan alluvium is typically sandy pebble-cobble gravel graded to modern stream courses; see description for Qfah.

Qfahy Historical and younger fan alluvium, undivided (~80 years old to lower Holocene) – Historical fan alluvium (Qfah) and subordinate younger fan alluvium (Qfay). See detailed descriptions of each individual unit.

Qfary Recent (historical + modern) and younger fan alluvium, undivided (modern to lower Holocene) – Recent fan alluvium (Qfah and Qfam, undivided) and subordinate younger fan alluvium (Qfay). See detailed descriptions of each individual unit.

Qfay Younger fan alluvium (middle to lower Holocene) – Dark brown (10YR 3/3) clayey silt in massive to medium (20-30 cm), mostly tabular beds. Loose, weakly to moderately calcareous, and internally massive. Silt contains 10-15% vfU-fU sand grains and up to 5% scattered fine to coarse pebbles. Subordinate (25-35%) beds consist of brown to dark brown or dark yellowish brown (10YR 4/3 to 3/3-4), loose, moderately calcareous, mostly clast-supported, medium- to thick-bedded (12 to over 50 cm), broadly lenticular, imbricated, very poorly sorted, subangular to rounded pebble-cobble-boulder gravel. Clasts consist of pebbles (50-100%), cobbles (0-25%), and boulders (0-30%) up to 40 cm in diameter of volcanic lithologies reworked from QTc. Gravel matrix consists of very poorly to poorly sorted, subangular to subrounded, silt-cL sand composed of 70-75% lithics (volcanic), 15-20% quartz, and 10-15% feldspar with up to 35% brownish clay bridges. Deposit may feature a stage I+ soil below the surface (carbonate nodules, filaments, and masses); elsewhere, this soil has been erosionally stripped. Heavily bioturbated by medium to very coarse roots and burrows. A deposit exposed in the southernmost part of the Garfield 7.5-minute quadrangle returned a conventional radiocarbon age of 9360±150 ^{14}C yr BP (Metcalf, 1969). Deposit is graded to low-lying terraces formed on younger alluvium (Qay). 1.8 to >4 m thick.

Qfaym Younger and modern fan alluvium, undivided (modern to lower Holocene) – Younger fan alluvium (Qfay) and subordinate modern fan alluvium (Qfam). Modern fan alluvium is typically sandy pebble-cobble gravel graded to modern stream courses; see detailed description for Qfay.

Qfayr Younger and recent (historical + modern) fan alluvium, undivided (modern to lower Holocene) – Younger fan alluvium (Qfay) and subordinate recent fan alluvium (Qfah and Qfam, undivided). See detailed descriptions of each individual unit.

Qpo Piedmont alluvium (upper to middle Pleistocene?) – Pebble gravel and sandy pebble gravel that is weakly consolidated to cemented in upper part by soil carbonate or clay. Gravel may be matrix- or clast-supported and consists of poorly sorted, subangular to rounded clasts. Stage II to IV carbonate morphology (carbonate nodules, laminar carbonate) is common in upper 1 m. Underlies fan and terrace deposits and erosion-surface veneers graded to closed-basin floors. 1.2-8 m thick [description modified from Seager et al., 1982].

Terrace units

Terrace deposits of the Rio Grande

Qtrg Rio Grande terrace deposits, undivided (upper to middle Pleistocene) – Loose deposits of sandy gravel and pebbly sand lenses with common extra-basin clasts. Locally subdivided into 2 deposits:

Qtrg1 Lowest Rio Grande terrace deposit (upper Pleistocene) – Light brownish gray (10YR 6/2) to brown or strong brown (7.5YR 5/4 or 4/6), sandy pebble and pebble-cobble gravel and subordinate pebbly sand in thin to very thick (6-120 cm), tabular to lenticular or wedge-shaped beds. Loose, weakly calcareous, and well imbricated to vaguely cross-stratified to (rarely) massive. Gravel beds comprise 65-95% of deposit and consist of poorly sorted, rounded to well rounded pebbles (75-90%) and cobbles (10-25%) of volcanic lithologies (40-55%), Paleozoic sedimentary lithologies and chert (15-25%), quartzite (10-15%), granite (5-10%), and Cretaceous sedimentary lithologies (3-5%). Gravel matrix consists of poorly to moderately sorted, subangular to well rounded (mostly rounded), vfU-mL sand composed of 65-70% quartz, 15-20% feldspar, and 10-20% lithics (volcanic>chert + granite). Matrix sand contains 10-20% outsized coarse sand grains to granules. Sandy beds comprise 5-35% of deposit and consist of moderately sorted, subangular to rounded, silt to fU sand composed of 50-60% quartz, 25-30% feldspar, and 15-20% lithics, and may contain stringers and small lenses of fine to medium pebble gravel. Deposit may be slightly to moderately bioturbated by fine to medium roots and medium to very coarse burrows. Stage II calcic horizons are common with 70-80% of clasts covered by carbonate coats or rinds. Deposit is likely correlative to the Picacho alluvium of Hawley (1965), Ruhe (1967), Hawley and Kottlowski (1969), Metcalf (1969), and Gile et al. (1981). Tread height 15-21 m above modern grade. 1-12 m thick.

Qtrg2 Lower-middle Rio Grande terrace deposit (upper to middle Pleistocene) – Dark yellowish brown (moist; 10YR 4/4) to pale brown (dry; 10YR 6/3), sandy pebble-cobble gravel and sand in thick (35-90 cm), broadly lenticular beds. Loose, weakly calcareous, and well imbricated to vaguely cross-stratified (foresets up to 40 cm thick). Gravel beds comprise 65-80% of deposit and consist of poorly to moderately sorted, rounded to well rounded pebbles (55-65%) and cobbles (35-45%) of intermediate volcanics (45-60%), felsites (30-40%), Paleozoic sedimentary lithologies (5-15%), granite and amphibolite (5-10%), quartzite (3-5%), and miscellaneous lithologies (trace to 2%). Gravel matrix consists of very poorly to poorly sorted, subrounded to well rounded, fU-vcL sand (10-20% vcU sand to granules) composed of 65-70% quartz, 15-20% feldspar, and 10-20% lithics (volcanics, chert) with no clay. Sand lenses constitute 20-35% of deposit and are planar cross-stratified. Surface of deposit may be erosionally stripped; elsewhere, clasts at surface feature 15-20% weak varnish. Deposit may be correlative to the Tortugas alluvium of Hawley (1965), Ruhe (1967), Hawley and Kottlowski (1969), Metcalf (1969), and Gile et al. (1981). Tread height 21-25 m above modern grade. 15-18 m thick.

Terrace deposits of Rio Grande tributaries

Qtg Terrace deposits of Rio Grande tributaries, undivided (upper to middle Pleistocene) – Loose to weakly consolidated deposits of sandy gravel and pebbly sand found along Rio Grande tributaries in the central, southern, and western parts of the quadrangle. Locally subdivided into 3 deposits:

Qtl Lower tributary terrace deposit (upper Pleistocene) – Dark reddish brown to light reddish brown (5YR 3-6/3), sandy pebble-cobble gravel in thin to thick (7-85 cm), tabular to broadly lenticular beds. Loose to weakly consolidated, weakly calcareous, and well imbricated to vaguely trough cross-stratified or massive. Gravel is poorly to moderately sorted, subrounded to well rounded, and consists of pebbles (70-95%) and cobbles (5-30%) of felsites (55-60%), intermediate volcanics including diorite and dacite (35-40%), and Paleozoic carbonates, chert, and basalt (5-10% total). Matrix consists of poorly sorted, subangular to rounded, fL-cU sand (up to 2% vcL-vcU grains) composed of 60-70% lithics (volcanic>chert), 20-30% quartz, and 5-10% feldspar with 5-10% reddish clay chips and free-grain argillans. Well sorted pebbly beds comprise 50-60% of deposit. Poorly sorted pebble-cobble gravel beds that are occasionally matrix-supported comprise 40-50% of deposit. Packages of A and Bt horizons may be up to 55 cm thick on slopes of deposit. Weak varnish observed on 5-15% of clasts at surface. Strath forms up to 30 cm of scour on underlying units. Tread height 3-6 m above modern grade. 5.1-5.5 m thick.

Qtm Middle tributary terrace deposit (upper to middle Pleistocene) – Reddish brown to brown (5-7.5YR 4/3-4), sandy pebble-cobble gravel in medium to thick (15-100 cm), tabular to broadly lenticular beds. Loose, weakly to strongly calcareous, and well imbricated to vaguely trough or planar cross-stratified (foresets 15-20 cm thick). Gravel is clast-supported, very poorly to poorly sorted, subrounded to well rounded, and consists of pebbles (60-90%), cobbles (5-30%), and boulders (0-

10%) up to 60 cm in diameter of subequal proportions of felsites and intermediate volcanics with subordinate amounts of chert (up to 5%) and Paleozoic carbonates (up to 4%). Matrix consists of poorly sorted, subangular to rounded, fL-vcL sand comprised of 45-75% lithics (volcanic>>chert), 10-40% quartz, and 5-20% feldspar with 10-15% reddish free-grain argillans. Deposit contains minor (5-10%) thin lenses of brown (7.5YR 5/3), loose, weakly calcareous, internally massive to horizontal-planar laminated, moderately sorted, subangular to rounded, pebbly (fine to medium, <10%), fU-cL sand comprised of 65-75% lithics (volcanic>>chert), 20-25% quartz, and 10-15% feldspar. Deposit features stage I+ carbonate morphology (clast coatings) in upper 1-1.5 m as well as occasional manganese oxide staining of clasts, particularly just above its basal strath. Weak to moderate varnish observed on 10-30% of clasts at surface. Tread height 8-21 m above modern grade. 3-6.4 m thick.

Qth Higher tributary terrace deposit (middle Pleistocene) – Yellowish red (moist; 5YR 4/6) to reddish brown or brown (dry; 5-7.5YR 5/3), sandy pebble-cobble gravel in very thin to thick (3-60 cm), mostly lenticular beds. Loose, non- to very weakly calcareous, and well imbricated to trough or planar cross-stratified (foresets 3-15 cm thick) with rare lateral accretion sets. Gravel is clast-supported, poorly to moderately sorted, subrounded to rounded, and consists of pebbles (75-95%), cobbles (5-25%), and small boulders (<2%) of volcanics (85-95%) and Paleozoic carbonates and chert/jasperoid (5-10%). Matrix consists of poorly to moderately well sorted, subangular to rounded, fU-cL sand (5-10% cU-vcU) comprised of 45-55% lithics (volcanic>>chert), 40-45% quartz, and 10-15% feldspar with 5-8% reddish free-grain argillans. Subordinate (15-25%) beds consist of ripple laminated to massive sand similar to gravel matrix. Moderate varnish observed on 55-65% of clasts at surface. Stage I+ to II carbonate morphology (coated clasts, tubules) observed in upper 1.2-1.4 m of deposit. Rarely, thin (less than 6 cm) sandy beds in body of deposit feature pervasive iron oxide staining. Tread height 17-33 m above modern grade. No more than 5 m thick in most places.

QUATERNARY-TERTIARY

Basin-fill units

QTc Camp Rice Formation (lower Pleistocene to lower Pliocene) – Gravel, sand, silt, and clay deposited by coalesced fan complexes and the ancestral Rio Grande in the Palomas and Hatch-Rincon basins. Fossil data (summarized by Morgan and Lucas, 2012), basalt radiometric ages (Bachman and Mehnert, 1978; Seager et al., 1984; Jochems, 2015; Koning et al., 2015, 2016), and magnetostratigraphic data (Repenning and May, 1986; Mack et al., 1993, 1998; Leeder et al., 1996), indicate an age range of ~5.0-0.8 Ma for the Camp Rice Formation and the correlative Palomas Formation to the north. Where not significantly eroded, the surface soil may be marked by a petrocalcic horizon that is 1-2 m thick and generally exhibits stage IV carbonate morphology. Total thickness of 25-77 m in quadrangle. Includes 10 subunits:

Qcp Camp Rice Formation facies associated with piedmont slopes graded to La Mesa surface – Pinkish gray to light brown (7.5YR 6/2-3), sandy pebble-cobble-boulder gravel that is poorly exposed. Clasts include pebbles (60-70%), cobbles (25-30%), and boulders (5-15%) of intermediate volcanic lithologies derived from the Good Sight Mountains with occasional (5-10%) rhyolite containing sparse quartz and sanidine phenocrysts. Unit contains subordinate sandy silt. Stage I+ to II calcic horizons at surface are indicated by numerous (50-80%) clasts with thin calcite coats. Surface appears to grade below that on QTcpu to north. <15 m thick (Seager et al., 1982).

Qcl Camp Rice Formation sediments associated with La Mesa surface – Yellowish red to light reddish brown (5YR 5/6 to 6/4), sandy clay in thick (35-80 cm), tabular beds. Loose to weakly consolidated, strongly calcareous, and internally massive. Contains 8-12% subangular to rounded, mL-vcL sand grains composed of >70% lithics (volcanic) and no more than 30% quartz + feldspar. Unit is capped by a 30-cm-thick petrocalcic soil featuring stage III+ to IV carbonate morphology. 1-3 m thick.

QTcpu Upper piedmont facies of the Camp Rice Formation – Reddish brown to light reddish brown (5YR 5-6/4), sandy pebble-cobble gravel in medium to thick (20-55 cm) beds. Loose and weakly calcareous. Gravel is clast-supported, imbricated, poorly sorted, subangular to rounded (mostly subrounded to rounded), and consists of pebbles (80-90%) and cobbles (10-20%) comprised of volcanics (85-95%) and Paleozoic carbonate and chert (up to 10%). Gravel matrix consists of poorly sorted, subangular to rounded, silty mL-vcL sand comprised of 60-75% lithics (volcanic), 20-30% quartz, and 5-20% feldspar with common dark reddish brown free-grain argillans. To the east, the unit more commonly features buried soils and becomes dominated by finer grained beds, including: (1) reddish brown (5YR 4/3-4), moderately calcareous mud in medium (30 cm), internally massive beds; and (2) reddish brown (5YR 4/4), weakly calcareous, moderately well sorted to well sorted, silty vfL-fL sand (10-15% fU-cL) of similar composition to gravel matrix but lacking clay. Sand is massive and contains up to 3% scattered subrounded, fine pebbles of volcanic lithologies. Paleosols are typically Btk horizons with stage II carbonate morphology (calcic nodules). Overall distribution of gravel to sand + mud in unit is 60-70% to 30-40%, respectively. 5-27 m thick.

QTctu Upper transitional facies of the Camp Rice Formation – Similar to the transitional facies (QTct) of the Camp Rice Formation. This unit is found above a tongue of axial-fluvial facies (QTcf) that is traceable over 2-3 km in section 7, T19S, R4W. It contains a higher percentage (up to 35-40%) of sandy and sandy pebble beds than does QTct. 3-6 m thick.

QTct Transitional facies of the Camp Rice Formation – Slightly sandy mud, silt, and sand in medium to thick (20-80 cm), tabular beds (rare lenses). Loose and non- to moderately calcareous or carbonate-cemented. Sandy mud is the most common lithology (50-65% of unit) and consists of yellowish red to strong brown (5-7.5YR 4/6), internally massive mud that contains disseminated gypsum as veinlets and blades, particularly in the upper 10-15 m of the unit. The next most common lithology (30-45% of unit) is light brown (7.5YR 6/3-4), internally massive, well sorted silt with 5-10% very fine sand grains. Approximately 25-30% of the unit consists of strong brown (7.5YR 4-5/6), internally massive to thickly horizontal-planar laminated to ripple cross-stratified, moderately to moderately well sorted, subangular to rounded, vfL-mL sand comprised of 55-65% quartz, 20-25% lithics (dark mafic minerals, volcanics, chert), and 10-25% feldspar with no more than 3-5% clay. All three lithologies (mud, silt, and sand) may feature rare calcic paleosols that are likely hydromorphic as indicated by a lack of well-developed Bt horizons. Very rarely, unit contains lenses of light yellowish brown (2.5Y 6/4) to pale olive (5Y 6/4), loose, moderately calcareous, thickly laminated to thick-bedded (0.5-50 cm), internally massive to horizontal-planar laminated to (rarely) ripple cross-laminated, well sorted, subrounded to well rounded, silty fU-mU sand comprised of 75-80% frosted quartz, 10-15% lithics (volcanic, amphibolite, chert), and 5-10% feldspar with no clay. This sand contains 3-5% scattered, subrounded to well rounded, fine to medium pebbles of volcanics, chert, quartzite, and granite. It has yielded fossils of camel (*Camelops*), peccary (*Platygonus*), desert tortoise (*Gopherus*), and mud turtle (*Kinosternon*) (G. Morgan, pers. comm., 2017). Another rare lithology found in the upper ~15 m of the unit includes mottled reddish brown to light reddish brown (5YR 5-6/3-4) to light brownish gray (2.5Y 6/2), fissile shale with reduced zones concentrated around small (<0.8 cm) clusters of organic material and 0.3-0.5 cm partings/laminations of very fine sand. Unit is laterally gradational with QTcf to east and QTcpm to west. Overall, unit is up to 65 m thick, though thin intervals of 2-7 m may be bound by QTcf tongues.

QTcf Upper axial-fluvial facies of the Camp Rice Formation – Tongues of light brownish gray to pale brown (10YR 6/2-3) sand and pebbly sand in very thin to medium (2-30 cm), stacked, mostly lenticular beds. Loose to weakly calcite-cemented and planar cross-stratified (foresets up to 10 cm thick) to occasionally massive. Sand consists of poorly to moderately sorted, subangular to well rounded, mL-cL grains of 45-50% quartz, 30-35% lithics (volcanics, granite, quartzite), and 10-20% feldspar; no clay observed. Contains subrounded to well rounded granules and fine to coarse pebbles of volcanics (50-55%), granite (15-20%), Paleozoic sedimentary lithologies (~10%), and lesser amounts of chert, quartzite, and basalt. Subordinate (<20%) beds include yellowish red (5YR 4-5/6), loose, weakly calcareous, massive mud with occasional calcic or manganese oxide masses. Carbonate rhizoliths up to 2 cm in diameter are commonly found in float but calcic soil horizons are not observed. Vertebrate fossils are common in this unit, including the Blancan horses *Equus simplicidens* and *E. scotti*(?) as well as the small camel *Hemiauchenia* (G. Morgan, pers. comm., 2017). Forms scoured contacts on transitional (QTct) and middle piedmont facies (QTcpm). One relatively thick (18 m) tongue in the southeastern part of the quadrangle exhibits a laterally gradational contact with QTct. 0-18 m thick.

QTcpm Middle piedmont facies of the Camp Rice Formation – Silty clay, sandy silt, and sandy gravel in thin to very thick (7-110 cm), tabular to lenticular beds. Loose to moderately consolidated and non- to moderately calcareous. Gravel constitutes 30-45% of unit by volume and is clast-supported, imbricated to weakly horizontally laminated (where sandy), poorly sorted, subrounded to rounded, and consists of mostly pebbles with <10 to 45% cobbles of felsites (45-55%), intermediate volcanics including diorite and dacite (20-30%), and Paleozoic carbonates, chert/jasperoid, and basalt (total 15-35%). Gravel matrix consists of dark grayish brown to grayish brown (10YR 4-5/2), poorly to moderately sorted, subangular to rounded, fL-cL sand composed of 75-80% lithics (volcanic>>chert), 10-15% quartz, and 5-15% feldspar grains with trace clay particles. Silt and clay beds are strong to light brown (7.5YR 4/6 to 6/3) and internally massive. Silt beds may contain 5-10% grains of subangular to subrounded, mU-cU sand composed of >85% lithic (volcanic) grains as well as 10-12% clay and 3-5% angular to subrounded, fine to medium pebbles. Sandy beds are somewhat common in the central part of the quadrangle and consist of brown to pinkish gray (7.5YR 4/3 to 6-7/2), weakly consolidated, moderately calcareous, thin-bedded (6-10 cm), lenticular, internally massive to vaguely trough cross-stratified, moderately sorted, rounded, fL-mU grains of 55-65% lithics (mostly volcanic), 10-20% quartz, and 10-15% feldspar; no clay observed. Buried soils observed in unit include stage I to II calcic (Btk) horizons with carbonate masses and filaments in finer-grained beds to stage IV horizons (K) with laminar carbonate in gravels; better developed soils occur in the western part of the quadrangle. Unit conformably overlies the lower piedmont facies (QTcpl) and is laterally gradational with the transitional facies (QTct). 9 to 31 m thick.

QTcpl Lower piedmont facies of the Camp Rice Formation – Sandy to clayey silt, pebble gravel/conglomerate, and sandy pebble-cobble-boulder gravel/conglomerate in thin to thick (5-70 cm), tabular to broadly lenticular beds. Loose to well consolidated and weakly to moderately calcareous. Silt beds constitute 50-60% of unit by volume and are yellowish red to light reddish brown (5YR 5/6 to 6/4), blocky weathering/massive, and contain 5-8% poorly sorted, subrounded granules to fine pebbles of mostly volcanic lithologies. Silt beds also have rare (3-5%) 10- to 20-cm-thick lenses of clast-supported pebble-cobble gravel. Gravel/conglomerate constitutes 40-50% of unit by volume and is clast- to matrix-supported, imbricated to vaguely trough cross-stratified, very poorly to moderately sorted, subangular to rounded, and consists of pebbles (70-90%), cobbles (10-30%), and boulders (10-15%) of felsites (35-60%), intermediate volcanics (20-60%), and lesser proportions of Paleozoic carbonate and chert. However, in the northeast corner of the quadrangle (section 16, T18S, R4W), clasts are dominated by Paleozoic sedimentary lithologies derived from fault blocks to the north (e.g., Nakaye Mountain). Gravel matrix consists of reddish brown to yellowish red (5YR 4/3-6) to brown or light brown (7.5YR 5-6/3-4), very poorly sorted, angular to subrounded, vfU-cU sand composed of 70-80% lithics (volcanic), 10-20% quartz, and 5-15% feldspar with 0-15% reddish clay chips and free-grain argillans. Occasionally, unit features ledges of pinkish white (7.5YR 8/2), moderately consolidated, thin- to medium-bedded (8-20 cm), tabular, massive calcrete containing 15-20% scattered, angular to subrounded, mostly lithic (>60%), vfU-vcL sand grains. Such beds are commonly found in central and eastern parts of quadrangle. Stage I to II calcic (Bk) horizons observed in upper 15-35 cm of many beds. Cumulic (Bw) horizons observed elsewhere are up to 45 cm thick. Unit shares mostly conformable contacts with QTcplt below and QTcpm above; in places, unit lies on Trv with angular unconformity. 7-45 m thick.

QTcplt Lower transitional piedmont facies of the Camp Rice Formation – Silt, sand, and pebble gravel/conglomerate that are generally reddish to reddish brown in color. Gravel/conglomerate beds are subordinate, lack clay in matrix, and consist of mostly pebbles comprised of felsites (40-45%), intermediate volcanics (35-40%), and Paleozoic carbonate and chert (15-20%). Silt and fine sand beds contain 5-15% pebbles of similar lithologies. May contain stage II calcic horizons with carbonate nodules in places. Conformably underlies QTcpl; disconformably underlain by Tcf or Trv. 0-15 m thick.

Tcf Lower axial-fluvial facies of the Camp Rice Formation – Dark yellowish brown to yellowish brown (moist; 10YR 4-5/4) to pale brown (dry; 10YR 6/3) sand and subordinate pebble gravel in thin to medium (5-30 cm), mostly lenticular beds. Loose, non-calcareous, and internally massive to planar cross-stratified (foresets up to 20 cm thick). Sand is poorly to moderately sorted, rounded to well rounded, fU-cL grains composed of 70-80% quartz, 10-15% feldspar, and 10-15% lithics (dark mafic minerals, volcanics) with no clay. Contains mud rip-ups up to 40-45 cm in diameter. Fine to coarse pebble gravel constitutes 10-15% of unit by volume and is clast-supported, imbricated, poorly sorted, and subrounded to rounded; clasts include abundant granite. The matrix of gravel lenses is similar to the sand described above. These lenses are occasionally bound by layers of carbonate nodules up to 5 cm thick. Fossilized wood specimens including the family Cupressaceae (S. Manchester, pers. comm., 2017) are common in unit; vertebrate fossil fragments are also observed. Overlies disconformity or slight angular unconformity with Trv. 4-15 m thick.

TERTIARY

Santa Fe Group basin-fill units predating the Camp Rice Formation

Trv Rincon Valley Formation (upper Miocene) – Dark reddish brown to red (2.5-5YR 3/4 to 4/6) mudstone and clayey silt with minor silty sandstone in thin to very thick (4-110 cm), tabular beds. Mudstone is internally massive and commonly contains gypsum in the form of prismatic crystals, shards, and amalgamated masses. Gypsum also occurs in tabular horizons up to 10 cm thick as well as secondary coatings on fractures. Silty sandstone is light reddish brown to light brown (5-7.5YR 6/3-4), massive to ripple cross-laminated, and very fine-grained (10-15% fL-mL grains). Thin laminations of red mud occur in sandstone beds, which may also contain up to 5% outsized granules of volcanic lithologies. Underlies disconformity or slight angular unconformity with QTcpl, QTcplt, or Tcf. >430 m thick based on projection from Hatch quadrangle to east (Seager, 1995).

Trvc Fanglomerate facies of the Rincon Valley Formation (upper Miocene) – Light reddish brown (2.5-5YR 6/3-4) to reddish yellow (5YR 6/6) pebble-cobble-boulder conglomerate and subordinate sandstone in thin to thick (8-85 cm), tabular to occasionally lenticular beds. Indurated/moderately to strongly clay-cemented, non-calcareous, and reverse graded. Clasts are moderately imbricated, very poorly to poorly sorted, subrounded to rounded, and consist of pebbles (50-95%), cobbles (5-40%), and boulders (0-10%) dominated by intermediate volcanic lithologies (80-85%). Where not replaced by clay, matrix consists of poorly to moderately sorted, subrounded to rounded, fU-cU (mostly mL-cL) sand comprised of 70-80% lithics (volcanic), 10-20% quartz, and 10-15% feldspar. Subordinate (5-15%) beds consist of very weakly calcareous, weakly to moderately consolidated, internally massive to trough cross-stratified, poorly sorted, subrounded to rounded, pebbly (fine to medium), fU-cU sandstone. Sand and pebble compositions in sandstone are similar to those in conglomerate but with 40-50% reddish clay bridges. Unit also contains rare (<5%) beds of matrix-supported pebble-cobble gravel. Total thickness unknown but greater than 9 m.

UNITS IN CROSS SECTION ONLY

Thr Hayner Ranch Formation (middle to lower Miocene) – Dark gray to tan conglomerate, conglomeritic sandstone, and mudstone with clasts of Uvas basaltic andesite and Bell Top ash-flow tuff. Unit is either conformably or unconformably overlain by Trv in different areas. At least 427 m thick [description from Seager, 1995].

APPENDIX B

Maximum clast sizes measured for select units on the
Arroyo Cuervo 7.5-minute quadrangle

Maximum clast size measurements were made of the 10 largest clasts in an area of approximately 75-100 m^2. The longest (a) and intermediate (b) axes of each clast were measured. Clast lithologies were usually noted as well. All UTM coordinates are given in NAD 83, zone 13S.

TABLE B.1 MAXIMUM CLAST SIZE MEASUREMENTS AT WAYPOINT 170222_2-7				
		a axis (cm)	b axis (cm)	clast-type
Northing	3618242	51	38.5	
Easting	284016	31.5	23	
Unit	Qam	35	32.5	
Mean (a axis)	37	36	26	
Median (a axis)	37	37	22	
Mean (b axis)	27	39	21	
Median (b axis)	24.5	48	35.5	
n	10	22.5	22	
		33.5	22	
		40	31	

TABLE B.2 MAXIMUM CLAST SIZE MEASUREMENTS AT WAYPOINT 170223_3-1				
		a axis (cm)	b axis (cm)	clast-type
Northing	3621167	43	34	breccia
Easting	279629	29	23.5	undivided tuff
Unit	Qam	32	24	crystal-poor intermediate volcanic
Mean (a axis)	30	26.5	18.5	Kneeling Nun tuff
Median (a axis)	29	27.5	17.5	undivided tuff
Mean (b axis)	21	29	20.5	basalt or crystal-poor intermediate volcanic
Median (b axis)	20.5	25	16.5	Kneeling Nun tuff
n	10	35	17	basalt
		28	20.5	chert breccia
		26.5	21	crystal-poor intermediate volcanic

TABLE B.3 MAXIMUM CLAST SIZE MEASUREMENTS AT WAYPOINT 170119_17				
		a axis (cm)	b axis (cm)	clast-type
Northing*	3619779	5	3	granite
Easting*	283523	5	2.5	crystal-rich intermediate volcanic
Unit	QTcf	5.5	3	granite
Mean (a axis)	5	4	3	Paleozoic carbonate
Median (a axis)	5	4.5	2	crystal-rich intermediate volcanic
Mean (b axis)	3	5	2.5	basalt
Median (b axis)	3	6.5	3	crystal-poor intermediate volcanic
n	10	6	4	crystal-poor intermediate volcanic
		4.5	2.5	crystal-rich intermediate volcanic
		6.5	5	crystal-poor intermediate volcanic

*Approximate location (±10 m).

TABLE B.4 MAXIMUM CLAST SIZE MEASUREMENTS AT WAYPOINT 170223_3-2c				
		a axis (cm)	b axis (cm)	clast-type
Northing	3619921	20.5	13	undivided tuff
Easting	277596	14	9.5	chert/jasperoid
Unit	QTcpu	21	7	crystal-poor intermediate volcanic
Mean (a axis)	17	21	15.5	crystal-poor felsite
Median (a axis)	16	20	12	crystal-poor felsite
Mean (b axis)	11	14	14.5	undivided tuff
Median (b axis)	11.25	15	10.5	Kneeling Nun tuff
n	10	17.5	10	crystal-poor felsite
		14	8	crystal-rich intermediate volcanic
		15	14.5	volcanic breccia

TABLE B.5 MAXIMUM CLAST SIZE MEASUREMENTS AT WAYPOINT 170323_2-1d				
		a axis (cm)	b axis (cm)	clast-type
Northing	3616501	12	8	crystal-poor felsite
Easting	282201	13.5	10	Kneeling Nun tuff
Unit	QTct	14	13.5	undivided intrusive
Mean (a axis)	13	12.5	11	undivided tuff
Median (a axis)	13	12	7.5	crystal-rich intermediate volcanic
Mean (b axis)	9	12.5	9	crystal-poor intermediate volcanic
Median (b axis)	9	10.5	7	crystal-poor intermediate volcanic
n	10	14	12	groundwater carbonate
		13	5.5	crystal-rich intermediate volcanic
		12	5	Kneeling Nun tuff

TABLE B.6 MAXIMUM CLAST SIZE MEASUREMENTS AT WAYPOINT 170119_9				
		a axis (cm)	b axis (cm)	clast-type
Northing	3619854	10.5	7	crystal-poor intermediate volcanic
Easting	283465	6	4	Kneeling Nun tuff
Unit	QTcpm	5	3.5	undivided tuff
Mean (a axis)	6	6	3.5	crystal-rich intermediate volcanic
Median (a axis)	6	5	3.5	crystal-rich intermediate volcanic
Mean (b axis)	4	7	4.5	crystal-poor felsite
Median (b axis)	4	7.5	5	crystal-poor intermediate volcanic
n	10	5	4	crystal-rich intermediate volcanic
		4	4	crystal-poor intermediate volcanic
		4	4	volcanic breccia

TABLE B.7 MAXIMUM CLAST SIZE MEASUREMENTS AT WAYPOINT 170119_4				
		a axis (cm)	b axis (cm)	clast-type
Northing	3620249	15.5	8	Paleozoic carbonate
Easting	283415	15	12	intrusive
Unit	QTcpl	15	10	crystal-poor felsite
Mean (a axis)	19	13.5	8.5	crystal-rich intermediate volcanic
Median (a axis)	18	13.5	8.5	Paleozoic carbonate
Mean (b axis)	12	20	19	basalt
Median (b axis)	11	20	9.5	crystal-poor felsite
n	10	28	13	Kneeling Nun tuff
		24	14.5	crystal-poor intermediate volcanic
		21	20.5	undivided tuff (lithic tuff)

TABLE B.8 MAXIMUM CLAST SIZE MEASUREMENTS AT WAYPOINT 170413_2-1				
		a axis (cm)	b axis (cm)	
Northing	3620396	16	6	Permian Abo Formation
Easting	287320	15.5	6	Permian Abo Formation
Unit	Tcf	17	10	Permian Abo Formation
Mean (a axis)	15	13.5	10.5	Paleozoic carbonate
Median (a axis)	16	12	8	Paleozoic carbonate
Mean (b axis)	9	16.5	14.5	basalt
Median (b axis)	9.5	13	9.5	basalt
n	10	22.5	9.5	chert/jasperoid
		15.5	12	crystal-rich intermediate volcanic
		10	7	granite

TABLE B.9 MAXIMUM CLAST SIZE MEASUREMENTS AT WAYPOINT 170322_1-2a				
		a axis (cm)	b axis (cm)	clast-type
Northing	3615618	44	34	undivided tuff
Easting	277913	41	19.5	undivided intrusive
Unit	Trvc	32.5	23.5	undivided intermediate volcanic
Mean (a axis)	35	30	29.5	lithic tuff
Median (a axis)	33	34.5	24	rhyolite
Mean (b axis)	26	32.5	29	crystal-poor intermediate volcanic
Median (b axis)	25	27	21.5	undivided intermediate volcanic
n	10	47	32	rhyolite
		28	26.5	rhyolite
		33	22	undivided intermediate volcanic

APPENDIX C

Paleocurrent data from the Arroyo Cuervo 7.5-minute quadrangle

Paleocurrent measurements are from clast imbrication, cross-stratification exposed in three dimensions, or channel axis trends measured using a Brunton pocket transit. Azimuthal mean and median values are provided. For paleocurrent measurements with individual values from the NW and NE (±SE) quadrants, values in the NW quadrant are subtracted from 360°. For measurements with individual values from the SW, NW, and NE quadrants, values in the NE quadrant are added to 360°, and final mean and median values are then converted back to a value from 0-360°.

TABLE C.1 IMBRICATION PALEOCURRENT MEASUREMENTS AT WAYPOINT 161207_1-5b						
		Flow direction measurements				
Northing	3620901	100	92	63	60	114
Easting	288058	100	61	63	100	114
Unit	Qtr1	100	61	75	100	85
Mean	84	88	61	75	100	85
Median	85	88	61	73	121	85
n	50	92	99	60	121	104
		92	99	60	69	104
		92	99	60	69	72
		92	81	60	69	72
		92	81	60	114	72

TABLE C.2 3D CROSS-STRATIFICATION PALEOCURRENT MEASUREMENTS AT WAYPOINT 161013_3-3d		
		Flow direction measurements
Northing	3618767	101
Easting	286384	89
Unit	QTcf	74
Mean	93	125
Median	90	91
n	10	83
		99
		64
		119
		84

TABLE C.3 3D CROSS-STRATIFICATION PALEOCURRENT MEASUREMENTS AT WAYPOINT 170119_15		
		Flow direction measurements
Northing	3619790	141
Easting	283532	125
Unit	QTcf	154
Mean	141	148
Median	142	143
n	10	151
		136
		125
		129
		159

TABLE C.4 IMBRICATION PALEOCURRENT MEASUREMENTS AT WAYPOINT 170202_1-2g			
		Flow direction measurements	
Northing	3616628	90	
Easting	285253	90	
Unit	QTcf	88	
Mean	99	90	
Median	94	110	
n	10	110	
		113	
		113	
		86	
		98	

TABLE C.5 CHANNEL AXES PALEOCURRENT MEASUREMENTS AT WAYPOINT 170202_1-3j			
		Flow direction measurements	
Northing	3616426	200	
Easting	285264	196	
Unit	QTcf		
Mean	198		
Median	198		
n	2		

TABLE C.6 3D CROSS-STRATIFICATION PALEOCURRENT MEASUREMENTS AT WAYPOINT 170323_2-2a			
		Flow direction measurements	
Northing	3616033	170	130
Easting	281632	128	175
Unit	QTcf	156	
Mean	153	153	
Median	155	131	
n	12	165	
		119	
		135	
		193	
		178	

TABLE C.7 CHANNEL AXES PALEOCURRENT MEASUREMENTS AT WAYPOINT 170412_1-5h		
		Flow direction measurements
Northing	3614609	164
Easting	283560	170
Unit	QTcf	
Mean	167	
Median	167	
n	2	

TABLE C.8 3D CROSS-STRATIFICATION PALEOCURRENT MEASUREMENTS AT WAYPOINT 170413_2-3b		
		Flow direction measurements
Northing	3617088	145
Easting	287035	170
Unit	QTcf	209
Mean	167	197
Median	159	158
n	10	155
		159
		157
		144
		172

TABLE C.9 IMBRICATION PALEOCURRENT MEASUREMENTS AT WAYPOINT 161102_3b						
		Flow direction measurements				
Northing	3616502	88	54	74	45	86
Easting	282183	76	54	74	45	86
Unit	QTct	76	89	74	53	86
Mean	54	76	89	60	53	86
Median	54	76	89	60	53	24
n	49	310	53	60	86	24
		310	53	60	86	24
		310	27	60	28	14
		47	34	60	47	14
		47	34	45	47	

TABLE C.10 IMBRICATION PALEOCURRENT MEASUREMENTS AT WAYPOINT 170322_1-4g					
		Flow direction measurements			
Northing	3615448	170	71	107	146
Easting	280142	170	119	149	94
Unit	QTct	170	119	149	94
Mean	121	170	143	84	94
Median	130	149	143	84	
n	34	108	130	84	
		108	130	84	
		71	130	146	
		71	130	146	
		71	130	146	

TABLE C.11 IMBRICATION PALEOCURRENT MEASUREMENTS AT WAYPOINT 170222_2-3j						
		Flow direction measurements				
Northing	3616535	26	15	259	20	264
Easting	278042	26	55	259	20	264
Unit	QTcpu	26	55	259	34	263
Mean	333	26	55	259	247	263
Median	358	26	55	284	6	263
n	49	21	31	284	6	358
		21	312	284	255	358
		1	295	286	255	14
		15	295	286	255	47
		15	295	20	264	

TABLE C.12 IMBRICATION PALEOCURRENT MEASUREMENTS AT WAYPOINT 170222_2-5a						
		Flow direction measurements				
Northing	3617663	94	45	63	99	55
Easting	277476	94	22	38	31	55
Unit	QTcpu	94	22	38	31	55
Mean	52	33	22	38	31	35
Median	45	33	22	38	45	35
n	48	55	69	38	45	14
		32	69	109	45	44
		32	63	109	45	44
		45	63	99	63	
		45	63	99	70	

TABLE C.13 IMBRICATION PALEOCURRENT MEASUREMENTS AT WAYPOINT 170322_1-3i							
		Flow direction measurements					
Northing	3615862	121	75	120	72	84	135
Easting	278740	121	85	120	72	84	135
Unit	QTcpu	121	85	120	72	110	
Mean	107	92	85	108	73	110	
Median	109	68	106	108	73	110	
n	52	68	106	149	73	113	
		157	134	149	94	128	
		157	120	149	102	128	
		157	120	72	102	128	
		91	120	72	102	135	

TABLE C.14 IMBRICATION PALEOCURRENT MEASUREMENTS AT WAYPOINT 170322_1-4e							
		Flow direction measurements					
Northing	3615189	107	35	3	49	63	93
Easting	279658	107	353	59	49	102	93
Unit	QTcpu	107	353	59	100	102	
Mean	50	107	353	59	100	102	
Median	49	35	339	59	100	51	
n	52	35	339	62	100	51	
		35	21	62	83	51	
		35	21	49	26	22	
		35	3	49	26	22	
		35	3	49	26	22	

TABLE C.15 IMBRICATION PALEOCURRENT MEASUREMENTS AT WAYPOINT 170323_2-3e				
		Flow direction measurements		
Northing	3614218	80	92	74
Easting	280988	80	92	95
Unit	QTcpu	80	54	95
Mean	86	80	54	95
Median	80	117	111	52
n	29	117	111	52
		117	111	52
		117	74	70
		117	74	70
		92	74	

TABLE C.16 IMBRICATION PALEOCURRENT MEASUREMENTS AT WAYPOINT 170412_1-3a				
		Flow direction measurements		
Northing	3613218	84	127	100
Easting	284012	84	63	100
Unit	QTcpu	84	63	
Mean	94	106	63	
Median	101	106	106	
n	22	38	106	
		104	72	
		127	72	
		127	102	
		127	102	

TABLE C.17 IMBRICATION PALEOCURRENT MEASUREMENTS AT WAYPOINT 150812_1-2c								
		Flow direction measurements						
Northing	3625502	97	70	140	75	56	52	75
Easting	279141	87	51	140	75	134	85	90
Unit	QTcpm	44	60	71	93	63	76	101
Mean	76	44	60	100	59	63	110	98
Median	73	35	60	100	106	30	77	98
n	70	93	120	60	106	30	110	104
		58	92	60	61	69	110	95
		55	45	75	74	92	105	65
		55	46	121	81	37	70	65
		70	46	122	56	52	50	39

TABLE C.18 IMBRICATION PALEOCURRENT MEASUREMENTS AT WAYPOINT 150812_1-3		
		Flow direction measurements
Northing	3625336	70
Easting	277978	70
Unit	QTcpm	70
Mean	99	86
Median	81	171
n	10	156
		151
		81
		81
		81

TABLE C.19 IMBRICATION PALEOCURRENT MEASUREMENTS AT WAYPOINT 150812A_1-4b					
		Flow direction measurements			
Northing	3624847	121	21	194	
Easting	277713	71	21	205	
Unit	QTcpm	90	21	205	
Mean	106	90	104	31	
Median	104	92	104	31	
n	27	38	231	133	
		38	236	169	
		113	140		
		55	153		
		156	153		

TABLE C.20 IMBRICATION PALEOCURRENT MEASUREMENTS AT WAYPOINT 150812B_1-4b					
		Flow direction measurements			
Northing	3624847	23	35	125	67
Easting	277713	23	35	156	67
Unit	QTcpm	100	45	96	48
Mean	67	100	56	96	
Median	56	64	56	96	
n	33	65	76	47	
		35	71	47	
		53	122	46	
		45	44	101	
		44	125	50	

TABLE C.21 IMBRICATION PALEOCURRENT MEASUREMENTS AT WAYPOINT 150812A_1-4c			
		Flow direction measurements	
Northing	3624692	73	38
Easting	278131	15	38
Unit	QTcpm	70	38
Mean	57	70	81
Median	61	70	81
n	15	68	
		55	
		61	
		61	
		35	

TABLE C.22 IMBRICATION PALEOCURRENT MEASUREMENTS AT WAYPOINT 150812B_1-4c					
		Flow direction measurements			
Northing	3624692	40	32	91	
Easting	278131	40	32	79	
Unit	QTcpm	66	89	56	
Mean	71	48	70	70	
Median	70	64	70	70	
n	28	84	70	70	
		84	70	102	
		61	113	102	
		61	126		
		32	91		

TABLE C.23 IMBRICATION PALEOCURRENT MEASUREMENTS AT WAYPOINT 150812C_1-4c					
		Flow direction measurements			
Northing	3624692	45	67	121	74
Easting	278131	31	105	61	
Unit	QTcpm	31	105	61	
Mean	61	118	26	6	
Median	61	43	40	79	
n	31	39	85	81	
		60	11	11	
		60	11	11	
		85	93	88	
		51	121	74	

TABLE C.24 IMBRICATION PALEOCURRENT MEASUREMENTS AT WAYPOINT 150923_2-1e			
		Flow direction measurements	
Northing	3624152	351	353
Easting	279662	351	96
Unit	QTcpm	59	96
Mean	58	59	70
Median	70	35	83
n	15	75	
		75	
		99	
		73	
		38	

TABLE C.25 IMBRICATION PALEOCURRENT MEASUREMENTS AT WAYPOINT 151216_1-1c						
		Flow direction measurements				
Northing	3621200	31	7	31	340	51
Easting	278285	31	1	71	11	85
Unit	QTcpm	71	1	71	11	54
Mean	46	71	8	75	70	70
Median	51	71	59	79	120	69
n	49	58	51	69	36	113
		10	25	69	36	67
		10	25	57	36	20
		344	1	83	80	20
		30	35	61	80	

TABLE C.26 IMBRICATION PALEOCURRENT MEASUREMENTS AT WAYPOINT 151216_1-3d						
		Flow direction measurements				
Northing	3620395	81	76	125	122	94
Easting	279206	81	74	118	122	100
Unit	QTcpm	57	74	118	122	106
Mean	105	57	99	120	30	153
Median	112	50	51	134	87	174
n	50	50	51	120	119	174
		50	69	120	81	174
		117	79	27	144	159
		85	175	137	144	159
		85	179	137	70	121

TABLE C.27 IMBRICATION PALEOCURRENT MEASUREMENTS AT WAYPOINT 151217_2-2e				
		Flow direction measurements		
Northing	3619824	139	170	115
Easting	279954	150	128	176
Unit	QTcpm	150	144	176
Mean	139	88	149	166
Median	143	129	179	141
n	25	129	95	
		134	154	
		68	154	
		68	124	
		143	170	

TABLE C.28 IMBRICATION PALEOCURRENT MEASUREMENTS AT WAYPOINT 170222_2-4a				
		Flow direction measurements		
Northing	3616914	33	104	15
Easting	277870	33	104	29
Unit	QTcpm	33	59	29
Mean	34	33	59	27
Median	31	33	59	27
n	26	4	48	27
		4	48	
		5	48	
		5	15	
		26	15	

TABLE C.29 IMBRICATION PALEOCURRENT MEASUREMENTS AT WAYPOINT 150729_2f				
		Flow direction measurements		
Northing	3624930	125	220	211
Easting	281089	83	220	115
Unit	QTcpl	200	220	94
Mean	133	210	144	94
Median	130	210	144	36
n	29	150	99	166
		121	110	130
		101	110	130
		101	45	130
		144	45	

TABLE C.30 IMBRICATION PALEOCURRENT MEASUREMENTS AT WAYPOINT 150729_2g				
		Flow direction measurements		
Northing	3624921	44	97	46
Easting	281085	44	97	46
Unit	QTcpl	44	123	98
Mean	94	119	73	106
Median	97	71	198	106
n	26	21	120	106
		89	120	
		89	179	
		97	146	
		97	110	

TABLE C.31 IMBRICATION PALEOCURRENT MEASUREMENTS AT WAYPOINT 150729A_3				
		Flow direction measurements		
Northing	3625120	95	96	91
Easting	279960	50	124	42
Unit	QTcpl	104	47	42
Mean	83	104	90	121
Median	91	33	91	88
n	25	33	15	
		66	110	
		66	121	
		139	76	
		96	115	

TABLE C.32 IMBRICATION PALEOCURRENT MEASUREMENTS AT WAYPOINT 150729B_3				
		Flow direction measurements		
Northing	3625120	46	21	142
Easting	279960	51	70	28
Unit	QTcpl	130	75	28
Mean	100	130	46	160
Median	111	178	139	160
n	26	55	139	160
		55	139	
		92	139	
		53	141	
		53	142	

TABLE C.33 IMBRICATION PALEOCURRENT MEASUREMENTS AT WAYPOINT 150813A_2-1c					
		Flow direction measurements			
Northing	3623328	84	78	142	111
Easting	281583	84	78	123	74
Unit	QTcpl	84	78	82	
Mean	96	84	64	65	
Median	84	84	152	71	
n	32	124	81	71	
		124	114	88	
		124	112	116	
		75	96	116	
		80	120	111	

TABLE C.34 IMBRICATION PALEOCURRENT MEASUREMENTS AT WAYPOINT 150813B_2-1c					
		Flow direction measurements			
Northing	3623328	159	165	119	211
Easting	281583	159	165	119	211
Unit	QTcpl	159	79	119	170
Mean	134	140	120	116	190
Median	120	160	120	116	201
n	39	160	120	200	110
		66	105	156	117
		163	58	96	107
		90	110	96	107
		130	110	140	

TABLE C.35 IMBRICATION PALEOCURRENT MEASUREMENTS AT WAYPOINT 150813_2-2e					
		Flow direction measurements			
Northing	3623899	45	71	25	59
Easting	281400	31	80	25	56
Unit	QTcpl	31	7	144	
Mean	55	15	30	144	
Median	48	38	30	144	
n	32	78	31	41	
		20	48	60	
		23	48	139	
		72	88	111	
		72	25	52	

TABLE C.36 IMBRICATION PALEOCURRENT MEASUREMENTS AT WAYPOINT 150823_2-2e				
		Flow direction measurements		
Northing	3623899	139	92	72
Easting	281400	139	92	119
Unit	QTcpl	37	94	105
Mean	84	37	94	91
Median	90	51	340	74
n	29	60	97	74
		65	97	108
		89	97	90
		89	81	90
		56	81	

TABLE C.37 IMBRICATION PALEOCURRENT MEASUREMENTS AT WAYPOINT 150922_1-2f				
		Flow direction measurements		
Northing	3624454	74	15	61
Easting	282188	81	61	75
Unit	QTcpl	10	61	75
Mean	65	46	41	90
Median	70	70	41	70
n	25	70	69	
		73	69	
		73	60	
		73	84	
		73	84	

TABLE C.38 IMBRICATION PALEOCURRENT MEASUREMENTS AT WAYPOINT 150923A_2-2a				
		Flow direction measurements		
Northing	3622912	85	49	10
Easting	282919	85	49	89
Unit	QTcpl	109	2	63
Mean	50	51	2	
Median	52	46	71	
n	23	52	52	
		52	52	
		61	52	
		1	31	
		49	31	

TABLE C.39 IMBRICATION PALEOCURRENT MEASUREMENTS AT WAYPOINT 150923B_2-2a					
		Flow direction measurements			
Northing	3622912	350	69	95	91
Easting	282919	74	64	31	
Unit	QTcpl	74	64	61	
Mean	73	99	64	82	
Median	74	81	64	82	
n	31	81	101	80	
		81	101	61	
		27	101	61	
		94	56	110	
		88	60	60	

TABLE C.40 IMBRICATION PALEOCURRENT MEASUREMENTS AT WAYPOINT 151028A_1-1				
		Flow direction measurements		
Northing	3621595	96	111	81
Easting	278045	96	111	116
Unit	QTcpl	75	54	116
Mean	88	99	62	80
Median	92	90	95	80
n	25	90	95	
		90	103	
		40	92	
		97	79	
		54	92	

TABLE C.41 IMBRICATION PALEOCURRENT MEASUREMENTS AT WAYPOINT 151028B_1-1				
		Flow direction measurements		
Northing	3621595	84	88	112
Easting	278045	78	88	112
Unit	QTcpl	130	70	96
Mean	104	130	70	111
Median	111	130	134	111
n	26	103	114	111
		103	119	
		80	119	
		80	119	
		119	100	

TABLE C.42 IMBRICATION PALEOCURRENT MEASUREMENTS AT WAYPOINT 151028_1-3							
		Flow direction measurements					
Northing	3621269	114	160	133	149	145	176
Easting	278950	121	160	179	192	145	152
Unit	QTcpl	100	114	194	153	195	152
Mean	138	100	114	149	153	210	121
Median	136	145	128	149	149	126	121
n	60	119	124	125	149	113	113
		166	124	125	137	183	122
		151	89	125	125	183	90
		146	89	153	125	134	90
		137	118	182	140	134	90

TABLE C.43 IMBRICATION PALEOCURRENT MEASUREMENTS AT WAYPOINT 151029_2-1b					
		Flow direction measurements			
Northing	3621849	94	120	93	115
Easting	280023	94	91	104	81
Unit	QTcpl	104	91	126	153
Mean	110	104	97	126	90
Median	109	131	133	111	109
n	37	131	135	111	109
		93	79	111	96
		142	91	131	
		142	91	131	
		120	93	115	

TABLE C.44 IMBRICATION PALEOCURRENT MEASUREMENTS AT WAYPOINT 151029_2-1f				
		Flow direction measurements		
Northing	3621609	116	114	134
Easting	280691	99	108	106
Unit	QTcpl	140	108	106
Mean	121	140	175	105
Median	115	130	175	113
n	30	136	121	113
		136	134	105
		127	134	94
		96	107	94
		96	153	123

TABLE C.45 IMBRICATION PALEOCURRENT MEASUREMENTS AT WAYPOINT 151216_1-1a						
		Flow direction measurements				
Northing	3621214	42	84	245	56	21
Easting	278410	42	84	67	55	69
Unit	QTcpl	66	41	67	115	69
Mean	65	70	41	27	54	81
Median	68	76	41	76	54	69
n	50	25	47	76	64	64
		89	76	79	37	64
		89	83	145	86	76
		62	70	75	99	76
		62	35	56	99	12

TABLE C.46 IMBRICATION PALEOCURRENT MEASUREMENTS AT WAYPOINT 151216_1-1h						
		Flow direction measurements				
Northing	3620789	119	84	112	81	78
Easting	277684	119	126	112	81	78
Unit	QTcpl	129	119	55	81	78
Mean	100	127	110	55	81	81
Median	102	91	110	55	129	56
n	49	91	130	128	126	111
		91	120	104	126	111
		91	120	102	143	116
		95	72	88	91	115
		84	72	116	78	

TABLE C.47 IMBRICATION PALEOCURRENT MEASUREMENTS AT WAYPOINT 151217_2-1b						
		Flow direction measurements				
Northing	3620317	131	56	83	132	104
Easting	281418	133	56	158	86	104
Unit	QTcpl	133	50	71	100	64
Mean	99	133	52	71	105	64
Median	102	65	115	100	140	77
n	50	92	111	112	140	129
		85	83	71	140	129
		121	70	71	75	86
		121	70	105	75	110
		148	67	109	121	110

TABLE C.48 IMBRICATION PALEOCURRENT MEASUREMENTS AT WAYPOINT 151217_2-1c						
		Flow direction measurements				
Northing	3620450	43	114	99	68	73
Easting	281675	59	95	108	68	73
Unit	QTcpl	74	60	70	124	73
Mean	92	74	71	128	124	89
Median	96	114	71	128	40	101
n	50	84	75	63	111	99
		91	75	105	111	86
		114	97	105	114	128
		114	97	105	114	128
		114	85	45	71	128

TABLE C.49 CHANNEL AXIS PALEOCURRENT MEASUREMENTS AT WAYPOINT 151217_2-1d		
		Flow direction measurements
Northing	3620089	40
Easting	281654	15
Unit	QTcpl	15
Mean	35	20
Median	30	65
n	6	55

TABLE C.50 IMBRICATION PALEOCURRENT MEASUREMENTS AT WAYPOINT 151217_2-3						
		Flow direction measurements				
Northing	3620717	99	123	100	91	91
Easting	280177	99	123	139	91	95
Unit	QTcpl	111	134	114	91	90
Mean	115	111	133	114	91	95
Median	113	111	159	114	150	95
n	50	111	159	125	131	95
		148	70	110	131	125
		148	70	103	131	125
		148	119	105	100	127
		74	119	129	100	163

TABLE C.51 IMBRICATION PALEOCURRENT MEASUREMENTS AT WAYPOINT 160218_2-1e								
		Flow direction measurements						
Northing	3621968	186	130	130	154	179	125	182
Easting	282426	186	130	120	190	179	160	
Unit	QTcpl	186	130	171	159	119	160	
Mean	164	170	130	155	200	119	160	
Median	169	169	168	155	181	205	160	
n	61	169	168	131	181	205	160	
		169	168	205	170	140	191	
		169	186	173	170	140	169	
		170	149	174	186	140	201	
		130	149	174	179	125	210	

TABLE C.52 IMBRICATION PALEOCURRENT MEASUREMENTS AT WAYPOINT 160218_2-2f						
		Flow direction measurements				
Northing	3620161	156	136	130	106	140
Easting	282171	170	120	141	106	122
Unit	QTcpl	170	120	129	155	122
Mean	142	153	120	129	137	142
Median	140	128	120	129	120	164
n	49	136	129	179	151	172
		140	163	179	195	172
		114	134	164	195	179
		84	90	181	140	169
		100	130	159	140	

TABLE C.53 IMBRICATION PALEOCURRENT MEASUREMENTS AT WAYPOINT 160218_2-4b							
		Flow direction measurements					
Northing	3619733	100	65	71	130	106	16
Easting	282873	110	65	85	130	106	
Unit	QTcpl	65	80	85	37	74	
Mean	83	65	124	121	104	134	
Median	80	65	112	121	49	154	
n	51	6	135	136	47	110	
		5	135	10	79	95	
		30	135	66	44	130	
		30	135	80	75	115	
		46	24	59	40	65	

TABLE C.54 IMBRICATION PALEOCURRENT MEASUREMENTS AT WAYPOINT 160316_1-3c							
		Flow direction measurements					
Northing	3619991	120	109	74	60	81	51
Easting	283690	117	109	74	65	85	51
Unit	QTcpl	117	93	75	65	65	51
Mean	82	75	93	73	65	106	
Median	75	75	111	60	65	60	
n	53	100	114	60	86	89	
		100	114	60	117	89	
		94	114	53	70	56	
		115	84	53	70	56	
		99	84	53	70	111	

TABLE C.55 IMBRICATION PALEOCURRENT MEASUREMENTS AT WAYPOINT 160316_1-4c							
		Flow direction measurements					
Northing	3619689	67	89	85	34	80	90
Easting	284034	79	89	85	34	103	104
Unit	QTcpl	75	111	102	90	126	104
Mean	86	72	113	102	100	126	104
Median	87	72	82	78	100	42	
n	54	95	82	100	96	42	
		95	82	80	69	42	
		121	101	80	69	42	
		97	85	99	69	119	
		97	85	34	80	119	

TABLE C.56 IMBRICATION PALEOCURRENT MEASUREMENTS AT WAYPOINT 161011_1-1m					
		Flow direction measurements			
Northing	3618532	78	25	32	55
Easting	285563	100	66	40	104
Unit	QTcpl	100	76	40	106
Mean	63	44	58	56	52
Median	58	109	58	34	35
n	37	109	58	34	35
		73	58	96	73
		73	61	43	
		100	105	43	
		25	19	55	

TABLE C.57 IMBRICATION PALEOCURRENT MEASUREMENTS AT WAYPOINT 161102A_1b							
		Flow direction measurements					
Northing	3618020	111	144	139	131	118	155
Easting	281675	111	144	139	131	118	155
Unit	QTcpl	165	127	120	156	144	155
Mean	144	169	127	159	156	144	155
Median	143	155	127	159	156	180	
n	54	186	152	141	159	180	
		134	152	141	159	180	
		134	132	141	175	120	
		120	132	108	175	120	
		120	139	108	175	120	

TABLE C.58 IMBRICATION PALEOCURRENT MEASUREMENTS AT WAYPOINT 161102B_1b						
		Flow direction measurements				
Northing	3618020	139	126	138	109	139
Easting	281675	139	146	113	151	159
Unit	QTcpl	109	127	113	162	120
Mean	131	109	127	143	162	126
Median	127	109	127	156	162	109
n	46	109	127	201	162	109
		115	141	150	100	
		115	141	150	100	
		134	119	150	100	
		126	119	150	100	

TABLE C.59 IMBRICATION PALEOCURRENT MEASUREMENTS AT WAYPOINT 161208_2-1l				
		Flow direction measurements		
Northing	3618199	160	146	158
Easting	283004	170	146	158
Unit	QTcpl	170	167	173
Mean	138	137	47	
Median	146	137	47	
n	23	137	71	
		137	71	
		128	71	
		128	161	
		189	161	

TABLE C.60 IMBRICATION PALEOCURRENT MEASUREMENTS AT WAYPOINT 161208_2-1m							
		Flow direction measurements					
Northing	3617970	128	116	160	159	151	148
Easting	283455	128	116	160	159	151	
Unit	QTcpl	95	132	175	159	151	
Mean	139	95	132	175	178	160	
Median	140	95	132	175	178	155	
n	51	92	125	175	121	155	
		92	125	173	121	155	
		113	131	173	145	140	
		113	131	173	74	140	
		116	131	159	74	148	

TABLE C.61 IMBRICATION PALEOCURRENT MEASUREMENTS AT WAYPOINT 170119_7						
		Flow direction measurements				
Northing	3620029	105	56	91	70	38
Easting	283539	105	104	108	57	38
Unit	QTcpl	47	45	86	20	85
Mean	64	47	89	86	20	78
Median	63	38	89	39	82	78
n	50	38	89	39	82	56
		38	109	69	25	56
		61	88	65	25	70
		61	88	31	38	70
		56	88	31	38	70

TABLE C.62 IMBRICATION PALEOCURRENT MEASUREMENTS AT WAYPOINT 170221_1-2					
		Flow direction measurements			
Northing	3617920	83	45	78	76
Easting	280645	83	109	78	76
Unit	QTcpl	76	60	111	76
Mean	83	76	60	111	
Median	78	76	60	111	
n	33	78	108	111	
		78	108	111	
		68	108	111	
		68	58	90	
		45	58	90	

TABLE C.63 IMBRICATION PALEOCURRENT MEASUREMENTS AT WAYPOINT 170221_1-2f				
		Flow direction measurements		
Northing	3618155	73	67	83
Easting	279967	73	67	83
Unit	QTcpl	81	55	
Mean	72	128	55	
Median	69	128	55	
n	22	62	55	
		62	70	
		62	70	
		67	70	
		67	70	

TABLE C.64 IMBRICATION PALEOCURRENT MEASUREMENTS AT WAYPOINT 170222_2-2c								
		Flow direction measurements						
Northing	3617901	86	73	89	62	83	82	76
Easting	279256	86	73	89	111	83	80	
Unit	QTcpl	86	73	147	111	83	80	
Mean	86	86	73	147	111	92	57	
Median	83	86	75	147	111	92	57	
n	61	65	75	123	77	66	57	
		65	89	123	77	66	57	
		65	89	123	83	85	90	
		65	89	123	83	85	86	
		65	89	62	83	85	76	

TABLE C.65 IMBRICATION PALEOCURRENT MEASUREMENTS AT WAYPOINT 170223_3-2d						
		Flow direction measurements				
Northing	3619986	41	86	83	84	11
Easting	277957	41	86	83	84	11
Unit	QTcpm	41	36	83	70	11
Mean	57	41	94	54	70	11
Median	67	53	94	67	33	11
n	50	53	68	67	33	51
		86	68	67	33	51
		86	83	67	33	51
		86	83	84	33	8
		86	83	84	11	8

TABLE C.66 IMBRICATION PALEOCURRENT MEASUREMENTS AT WAYPOINT 150729A_2c				
		Flow direction measurements		
Northing	3625129	86	130	116
Easting	281634	122	59	116
Unit	QTcplt	86	59	
Mean	102	55	96	
Median	105	134	96	
n	22	134	81	
		110	42	
		100	56	
		129	146	
		130	146	

TABLE C.67 IMBRICATION PALEOCURRENT MEASUREMENTS AT WAYPOINT 150729B_2c				
		Flow direction measurements		
Northing	3625129	96	78	95
Easting	281634	92	78	100
Unit	QTcplt	71	78	100
Mean	92	72	91	111
Median	92	85	46	95
n	26	85	46	129
		101	116	
		76	134	
		82	164	
		82	98	

TABLE C.68 IMBRICATION PALEOCURRENT MEASUREMENTS AT WAYPOINT 150922A_1-3d						
		Flow direction measurements				
Northing	3623687	35	65	45	122	61
Easting	282811	104	65	45	91	61
Unit	QTcplt	59	65	44	91	59
Mean	63	31	91	44	91	51
Median	61	92	36	42	59	24
n	50	92	69	42	76	40
		42	77	42	44	44
		61	77	108	75	44
		61	77	64	75	81
		74	45	64	35	105

TABLE C.69 IMBRICATION PALEOCURRENT MEASUREMENTS AT WAYPOINT 150922B_1-3d							
		Flow direction measurements					
Northing	3623687	71	29	140	106	99	105
Easting	282811	61	29	52	106	71	
Unit	QTcplt	91	77	52	133	71	
Mean	84	15	335	52	114	108	
Median	85	25	335	85	114	70	
n	51	103	335	85	114	85	
		103	108	122	113	85	
		103	84	73	110	104	
		96	84	115	41	98	
		29	140	106	51	145	

TABLE C.70 IMBRICATION PALEOCURRENT MEASUREMENTS AT WAYPOINT 150729A_1				
		Flow direction measurements		
Northing	3625459	94	89	
Easting	282559	71	116	
Unit	Tcf	71	116	
Mean	87	32	107	
Median	89	32	134	
n	19	65	134	
		65	98	
		121	81	
		89	54	
		86		

TABLE C.71 IMBRICATION PALEOCURRENT MEASUREMENTS AT WAYPOINT 150729B_1				
		Flow direction measurements		
Northing	3625459	89	116	90
Easting	282559	89	115	90
Unit	Tcf	110	115	
Mean	96	110	71	
Median	91	110	135	
n	22	101	56	
		91	91	
		91	91	
		82	85	
		116	61	

TABLE C.72 IMBRICATION PALEOCURRENT MEASUREMENTS AT WAYPOINT 150729_1c					
		Flow direction measurements			
Northing	3622562	101	130	136	86
Easting	282712	108	71	134	110
Unit	Tcf	171	133	133	154
Mean	130	141	104	133	
Median	133	141	104	167	
n	33	120	139	138	
		128	139	100	
		128	99	133	
		136	159	166	
		136	136	166	

TABLE C.73 IMBRICATION PALEOCURRENT MEASUREMENTS AT WAYPOINT 150923_2-4a						
		Flow direction measurements				
Northing	3622922	139	135	144	230	143
Easting	283859	139	191	144	196	143
Unit	Tcf	139	191	236	196	196
Mean	166	126	199	128	180	203
Median	165	130	199	128	180	178
n	45	130	165	128	138	
		127	156	175	207	
		113	156	175	160	
		113	175	230	201	
		135	175	230	201	

TABLE C.74 IMBRICATION PALEOCURRENT MEASUREMENTS AT WAYPOINT 150923_3-1i				
		Flow direction measurements		
Northing	3625030	223	168	205
Easting	284185	223	151	169
Unit	Tcf	186	175	169
Mean	183	180	175	185
Median	179	185	169	184
n	30	185	169	201
		187	169	201
		184	178	201
		176	178	175
		195	161	175

TABLE C.75 IMBRICATION PALEOCURRENT MEASUREMENTS AT WAYPOINT 150924_3-3g			
		Flow direction measurements	
Northing	3623807	110	186
Easting	284255	160	204
Unit	Tcf	144	161
Mean	162	181	161
Median	163	178	161
n	20	166	159
		166	165
		65	161
		90	181
		205	181

TABLE C.76 IMBRICATION PALEOCURRENT MEASUREMENTS AT WAYPOINT 160217_1-2a								
		Flow direction measurements						
Northing	3621941	149	95	61	49	114	76	106
Easting	283915	149	51	56	121	81	101	120
Unit	Tcf	149	51	56	101	56	106	89
Mean	105	231	51	56	116	106	175	
Median	106	114	53	81	116	109	175	
n	63	114	108	116	100	109	175	
		140	140	116	100	129	90	
		91	140	116	100	149	101	
		201	140	75	100	95	75	
		95	179	49	114	76	95	

TABLE C.77 IMBRICATION PALEOCURRENT MEASUREMENTS AT WAYPOINT 160218_2-1				
		Flow direction measurements		
Northing	3621824	130	26	102
Easting	282268	69	40	102
Unit	Tcf	69	33	102
Mean	87	84	119	68
Median	90	106	119	68
n	29	117	116	74
		117	90	122
		86	59	122
		116	45	130
		14	30	

TABLE C.78 IMBRICATION PALEOCURRENT MEASUREMENTS AT WAYPOINT 160317_2-4g						
		Flow direction measurements				
Northing	3624023	125	127	105	176	182
Easting	285563	125	127	105	176	182
Unit	Tcf	125	139	122	176	111
Mean	140	150	124	122	176	111
Median	130	165	124	122	176	115
n	50	165	124	139	190	120
		140	124	139	141	120
		109	189	171	141	91
		109	189	95	121	133
		109	189	186	182	133

TABLE C.79 IMBRICATION PALEOCURRENT MEASUREMENTS AT WAYPOINT 161011_1-3b					
		Flow direction measurements			
Northing	3619442	111	189	174	130
Easting	285555	129	185	174	140
Unit	Tcf	129	150	168	140
Mean	159	71	201	168	140
Median	164	176	192	168	140
n	36	171	192	158	180
		109	192	158	
		195	174	160	
		139	174	160	
		139	174	130	

TABLE C.80 IMBRICATION PALEOCURRENT MEASUREMENTS AT WAYPOINT 161013_3-1c				
		Flow direction measurements		
Northing	3620300	354	30	18
Easting	287392	354	30	18
Unit	Tcf	354	10	45
Mean	3	350	34	339
Median	18	308	27	348
n	29	310	311	19
		310	311	19
		25	311	21
		25	18	21
		25	18	

TABLE C.81 IMBRICATION PALEOCURRENT MEASUREMENTS AT WAYPOINT 170203_2-1				
		Flow direction measurements		
Northing	3618348	295	58	285
Easting	288599	295	58	44
Unit	Tcf	295	40	44
Mean	7	295	29	
Median	32	32	29	
n	23	32	51	
		32	51	
		38	285	
		38	285	
		13	285	

TABLE C.82 IMBRICATION PALEOCURRENT MEASUREMENTS AT WAYPOINT 170203_2-2			
		Flow direction measurements	
Northing	3618337	52	105
Easting	288511	54	98
Unit	Tcf	54	120
Mean	94	97	129
Median	97	97	129
n	19	97	73
		97	73
		92	106
		105	106
		105	

TABLE C.83 IMBRICATION PALEOCURRENT MEASUREMENTS AT WAYPOINT 170413_2-1a						
		Flow direction measurements				
Northing	3620394	117	87	151	104	137
Easting	287312	155	87	151	74	137
Unit	Tcf	155	102	151	74	137
Mean	103	119	102	151	84	77
Median	96	119	72	151	84	77
n	47	94	72	96	84	77
		94	72	96	84	77
		94	100	96	82	
		94	100	104	82	
		87	100	104	89	

TABLE C.84 IMBRICATION PALEOCURRENT MEASUREMENTS AT WAYPOINT 170322A_1-2a					
		Flow direction measurements			
Northing	3615618	126	137	133	155
Easting	277913	126	137	133	155
Unit	Trvc	126	137	134	155
Mean	131	126	137	134	134
Median	134	126	76	150	134
n	37	151	76	150	123
		151	76	150	123
		151	133	150	
		147	133	74	
		147	133	74	

TABLE C.85 IMBRICATION PALEOCURRENT MEASUREMENTS AT WAYPOINT 170322B_1-2a					
		Flow direction measurements			
Northing	3615618	128	148	160	134
Easting	277913	128	137	160	134
Unit	Trvc	128	137	160	134
Mean	149	164	137	167	163
Median	148	164	137	167	163
n	38	164	136	167	169
		164	136	167	169
		150	136	132	169
		150	136	134	
		148	136	134	

APPENDIX D

Clast counts for select units on the
Arroyo Cuervo 7.5-minute quadrangle

Clast counts were conducted by random selection of clasts of at least 0.5 cm diameter from approximately 50-200 cm^2 areas of outcrops. Clast lithology categories are modified from Table 2 of Koning and others (2016).

TABLE D.1 CLAST-COUNT DATA FOR UNIT Qam (WAYPOINT 170222_2-7)		
Date	02/22/17	*n = 100*
UTM Location	3618242N, 284016E	
	n	% total
Total felsic volcanics	14	14%
Crystal-poor felsic volcanics	10	10%
Crystal-rich felsic volcanics	4	4%
Tuffs, undivided	6	6%
Kneeling Nun tuff	7	7%
Vicks Peak tuff		0%
Total intermediate volcanics	54	54%
Crystal-poor intermediate volcanics	33	33%
Crystal-rich intermediate volcanics	21	21%
Paleozoic carbonates		0%
Abo Formation		0%
Sandstone+siltstone, undivided	4	4%
Chert and jasperoid	4	4%
Vein quartz	1	1%
Granite		0%
Quartzite		0%
Basalt	2	2%
Other	8	8%
Comments	Other = 8% calcic nodules or groundwater calcite	

TABLE D.2 CLAST-COUNT DATA FOR UNIT Qam (170223_3-1)		
Date	02/23/17	*n = 101*
UTM Location	3621167N, 279629E	
	n	% total
Total felsic volcanics	8	8%
Crystal-poor felsic volcanics	6	6%
Crystal-rich felsic volcanics	2	2%
Tuffs, undivided	9	9%
Kneeling Nun tuff	10	10%
Vicks Peak tuff		0%
Total intermediate volcanics	56	55%
Crystal-poor intermediate volcanics	31	31%
Crystal-rich intermediate volcanics	25	25%
Paleozoic carbonates	7	7%
Abo Formation		0%
Sandstone+siltstone, undivided	1	1%
Chert and jasperoid	4	4%
Vein quartz		0%
Granite		0%
Quartzite		0%
Basalt	2	2%
Other	4	4%
Comments	Other = 2% volcanic breccia, 2% intermediate intrusive	

TABLE D.3 CLAST-COUNT DATA FOR UNIT Qtr1 (WAYPOINT 160317_2-4a)		
Date	03/17/16	*n = 103*
UTM Location	3623637N, 286051E	
	n	% total
Total felsic volcanics	25	24%
Crystal-poor felsic volcanics	16	16%
Crystal-rich felsic volcanics	9	9%
Tuffs, undivided		0%
Kneeling Nun tuff	3	3%
Vicks Peak tuff		0%
Total intermediate volcanics	24	23%
Crystal-poor intermediate volcanics	13	13%
Crystal-rich intermediate volcanics	11	11%
Paleozoic carbonates	14	14%
Abo Formation	1	1%
Sandstone+siltstone, undivided*	8	8%
Chert and jasperoid	5	5%
Vein quartz	1	1%
Granite	4	4%
Quartzite	14	14%
Basalt	2	2%
Other	2	2%
Comments	Other = 1% meta-sandstone, 1% volcanic breccia	

*One sandstone clast identified as Bliss Formation.

TABLE D.4 CLAST-COUNT DATA FOR UNIT Qtr1 (WAYPOINT 161207_1-5b)		
Date	12/07/16	*n = 101*
UTM Location	3620901N, 288058E	
	n	% total
Total felsic volcanics	23	22%
Crystal-poor felsic volcanics	13	13%
Crystal-rich felsic volcanics	10	10%
Tuffs, undivided	1	1%
Kneeling Nun tuff	4	4%
Vicks Peak tuff	6	6%
Total intermediate volcanics	18	17%
Crystal-poor intermediate volcanics	5	5%
Crystal-rich intermediate volcanics	13	13%
Paleozoic carbonates	8	8%
Abo Formation	3	3%
Sandstone+siltstone, undivided*	9	9%
Chert and jasperoid	9	9%
Vein quartz		0%
Granite	6	6%
Quartzite	13	13%
Basalt		0%
Other	3	3%
Comments	Other = 2% meta-sandstone, 1% petrified wood	

*One sandstone clast identified as Bliss Formation.

TABLE D.5 CLAST-COUNT DATA FOR UNIT Qtm (WAYPOINT 160217_1-3a)		
Date	02/17/16	*n = 103*
UTM Location	3621650N, 283915E	
	n	% total
Total felsic volcanics	26	25%
Crystal-poor felsic volcanics	19	18%
Crystal-rich felsic volcanics	7	7%
Tuffs, undivided	7	7%
Kneeling Nun tuff	11	11%
Vicks Peak tuff		0%
Total intermediate volcanics	46	45%
Crystal-poor intermediate volcanics	26	25%
Crystal-rich intermediate volcanics	20	19%
Paleozoic carbonates	4	4%
Abo Formation	1	1%
Sandstone+siltstone, undivided*		0%
Chert and jasperoid	5	5%
Vein quartz		0%
Granite		0%
Quartzite		0%
Basalt	1	1%
Other	2	2%
Comments	Other = 1% meta-sandstone, 1% unknown lithology	

*One sandstone clast identified as Bliss Formation.

TABLE D.6 CLAST-COUNT DATA FOR UNIT QTcf (WAYPOINT 170119_17)		
Date	01/19/17	*n = 105*
UTM Location	3619779N, 283523E*	
	n	% total
Total felsic volcanics	12	11%
Crystal-poor felsic volcanics	10	10%
Crystal-rich felsic volcanics	2	2%
Tuffs, undivided	8	8%
Kneeling Nun/Hells Mesa tuff	8	8%
Vicks Peak tuff	2	2%
Total intermediate volcanics	24	23%
Crystal-poor intermediate volcanics	17	16%
Crystal-rich intermediate volcanics	7	7%
Paleozoic carbonates	6	6%
Abo Formation	4	4%
Sandstone+siltstone, undivided	8	8%
Chert and jasperoid	4	4%
Vein quartz	2	2%
Granite	17	16%
Quartzite	3	3%
Basalt	3	3%
Other	4	4%
Comments	Other = 2% undivided intrusive, 1% volcanic breccia	

*Approximate location (±10 m).

TABLE D.7 CLAST-COUNT DATA FOR UNIT QTcpu (WAYPOINT 170223_3-2c)		
Date	02/23/17	*n = 101*
UTM Location	3619921N, 277596E	
	n	% total
Total felsic volcanics	24	24%
Crystal-poor felsic volcanics	18	18%
Crystal-rich felsic volcanics	6	6%
Tuffs, undivided	15	15%
Kneeling Nun tuff	9	9%
Vicks Peak tuff		0%
Total intermediate volcanics	31	31%
Crystal-poor intermediate volcanics	15	15%
Crystal-rich intermediate volcanics	16	16%
Paleozoic carbonates	6	6%
Abo Formation		0%
Sandstone+siltstone, undivided	1	1%
Chert and jasperoid	9	9%
Vein quartz		0%
Granite		0%
Quartzite		0%
Basalt	2	2%
Other	4	4%
Comments	Other = 2% undivided intrusive, 1% volcanic breccia, 1% unknown lithology	

TABLE D.8 CLAST-COUNT DATA FOR UNIT QTct (WAYPOINT 170323_2-1d)		
Date	03/23/17	*n = 100*
UTM Location	3616501N, 282201E	
	n	% total
Total felsic volcanics	9	9%
Crystal-poor felsic volcanics	6	6%
Crystal-rich felsic volcanics	3	3%
Tuffs, undivided	4	4%
Kneeling Nun/Hells Mesa tuff	15	15%
Vicks Peak tuff		0%
Total intermediate volcanics	48	48%
Crystal-poor intermediate volcanics	22	22%
Crystal-rich intermediate volcanics	26	26%
Paleozoic carbonates		0%
Abo Formation		0%
Sandstone+siltstone, undivided*	3	3%
Chert and jasperoid	3	3%
Vein quartz		0%
Granite		0%
Quartzite		0%
Basalt	1	1%
Other	17	17%
Comments	Other = 13% ground-water carbonate, 2% undivided intrusive, 1% volcaniclastic sand-stone, 1% volcanic breccia	

*Locally-derived Camp Rice axial-fluvial sandstone.

TABLE D.9 CLAST-COUNT DATA FOR UNIT QTcpm (WAYPOINT 150812_1-4d)		
Date	08/12/15	*n = 50*
UTM Location	3624894N, 278228E	
	n	% total
Total felsic volcanics	4	8%
Crystal-poor felsic volcanics	4	8%
Crystal-rich felsic volcanics		0%
Tuffs, undivided	9	18%
Kneeling Nun tuff	8	16%
Vicks Peak tuff	1	2%
Total intermediate volcanics	18	36%
Crystal-poor intermediate volcanics	9	18%
Crystal-rich intermediate volcanics	9	18%
Paleozoic carbonates	3	6%
Abo Formation	2	4%
Sandstone+siltstone, undivided		0%
Chert and jasperoid	2	4%
Vein quartz		0%
Granite		0%
Quartzite		0%
Basalt	1	2%
Other	2	4%
Comments	Other = 4% volcaniclastic of unrecorded grain size	

TABLE D.10 CLAST-COUNT DATA FOR UNIT QTcpm (WAYPOINT 151216_1-1c)		
Date	12/16/15	*n = 50*
UTM Location	3621200N, 278285E	
	n	% total
Total felsic volcanics	4	8%
Crystal-poor felsic volcanics	4	8%
Crystal-rich felsic volcanics		0%
Tuffs, undivided	14	28%
Kneeling Nun tuff	7	14%
Vicks Peak tuff		0%
Total intermediate volcanics	12	24%
Crystal-poor intermediate volcanics	7	14%
Crystal-rich intermediate volcanics	5	10%
Paleozoic carbonates	2	4%
Abo Formation		0%
Sandstone+siltstone, undivided		0%
Chert and jasperoid*	8	16%
Vein quartz	1	2%
Granite		0%
Quartzite		0%
Basalt	2	4%
Other		0%
Comments		

*2 chert clasts consisted of brecciated chert.

TABLE D.11 CLAST-COUNT DATA FOR UNIT QTcpm (WAYPOINT 170119_9)		
Date	01/19/17	*n = 100*
UTM Location	3619854N, 283465E	
	n	% total
Total felsic volcanics	15	15%
Crystal-poor felsic volcanics	10	10%
Crystal-rich felsic volcanics	5	5%
Tuffs, undivided	4	4%
Kneeling Nun tuff	18	18%
Vicks Peak tuff		0%
Total intermediate volcanics	49	49%
Crystal-poor intermediate volcanics	26	26%
Crystal-rich intermediate volcanics	23	23%
Paleozoic carbonates	6	6%
Abo Formation		0%
Sandstone+siltstone, undivided		0%
Chert and jasperoid	3	3%
Vein quartz		0%
Granite		0%
Quartzite		0%
Basalt		0%
Other	5	5%
Comments	Other = 3% undivided intrusive, 2% volcanic breccia	

TABLE D.12 CLAST-COUNT DATA FOR UNIT QTcpl (WAYPOINT 150729_2f)		
Date	07/29/15	*n = 50*
UTM Location	3624930N, 281089E	
	n	% total
Total felsic volcanics	1	2%
Crystal-poor felsic volcanics	1	2%
Crystal-rich felsic volcanics		0%
Tuffs, undivided	12	24%
Kneeling Nun tuff	6	12%
Vicks Peak tuff		0%
Total intermediate volcanics	18	36%
Crystal-poor intermediate volcanics	14	28%
Crystal-rich intermediate volcanics	4	8%
Paleozoic carbonates	4	8%
Abo Formation		0%
Sandstone+siltstone, undivided	2	4%
Chert and jasperoid	4	8%
Vein quartz		0%
Granite		0%
Quartzite		0%
Basalt	2	4%
Other	1	2%
Comments	Other = 2% yellow mudstone	

TABLE D.13 CLAST-COUNT DATA FOR UNIT QTcpl (WAYPOINT 151028_1-1)		
Date	10/28/15	*n = 49*
UTM Location	3621595N, 278045E	
	n	% total
Total felsic volcanics	5	10%
Crystal-poor felsic volcanics	5	10%
Crystal-rich felsic volcanics		0%
Tuffs, undivided	21	43%
Kneeling Nun tuff	2	4%
Vicks Peak tuff		0%
Total intermediate volcanics	11	22%
Crystal-poor intermediate volcanics	6	12%
Crystal-rich intermediate volcanics	5	10%
Paleozoic carbonates	5	10%
Abo Formation		0%
Sandstone+siltstone, undivided		0%
Chert and jasperoid	1	2%
Vein quartz	1	2%
Granite		0%
Quartzite		0%
Basalt	1	2%
Other	2	4%
Comments	Other = 4% tuffaceous breccia	

TABLE D.14 CLAST-COUNT DATA FOR UNIT QTcpl (WAYPOINT 160218_2-1e)		
Date	02/18/16	*n = 98*
UTM Location	3621968N, 282426E	
	n	% total
Total felsic volcanics	24	24%
Crystal-poor felsic volcanics	16	16%
Crystal-rich felsic volcanics*	8	8%
Tuffs, undivided	2	2%
Kneeling Nun tuff	13	13%
Vicks Peak tuff		0%
Total intermediate volcanics	39	40%
Crystal-poor intermediate volcanics	25	26%
Crystal-rich intermediate volcanics	14	14%
Paleozoic carbonates	5	5%
Abo Formation		0%
Sandstone+siltstone, undivided		0%
Chert and jasperoid	9	9%
Vein quartz		0%
Granite		0%
Quartzite		0%
Basalt	1	1%
Other	5	5%
Comments	Other = 5% undivided intrusive	

*May include undiv. crystalline tuffs (not specified in field).

TABLE D.15 CLAST-COUNT DATA FOR UNIT QTcpl (WAYPOINT 170119_4)		
Date	01/19/17	*n = 99*
UTM Location	3620249N, 283415E	
	n	% total
Total felsic volcanics	18	18%
Crystal-poor felsic volcanics	16	16%
Crystal-rich felsic volcanics	2	2%
Tuffs, undivided	7	7%
Kneeling Nun tuff	13	13%
Vicks Peak tuff		0%
Total intermediate volcanics	43	43%
Crystal-poor intermediate volcanics	32	32%
Crystal-rich intermediate volcanics	11	11%
Paleozoic carbonates	7	7%
Abo Formation		0%
Sandstone+siltstone, undivided		0%
Chert and jasperoid	8	8%
Vein quartz		0%
Granite		0%
Quartzite		0%
Basalt	1	1%
Other	2	2%
Comments	Other = 2% intrusive	

TABLE D.16 CLAST-COUNT DATA FOR UNIT QTcplt (WAYPOINT 150729_2c)		
Date	07/29/15	*n = 45*
UTM Location	3625129N, 281643E	
	n	% total
Total felsic volcanics	2	4%
Crystal-poor felsic volcanics	2	4%
Crystal-rich felsic volcanics		0%
Tuffs, undivided	16	36%
Kneeling Nun tuff	1	2%
Vicks Peak tuff		0%
Total intermediate volcanics	17	38%
Crystal-poor intermediate volcanics	9	20%
Crystal-rich intermediate volcanics	8	18%
Paleozoic carbonates	2	4%
Abo Formation		0%
Sandstone+siltstone, undivided		0%
Chert and jasperoid	5	11%
Vein quartz	1	2%
Granite		0%
Quartzite		0%
Basalt		0%
Other	1	2%
Comments	Other = 2% mud rip-up	

TABLE D.17 CLAST-COUNT DATA FOR UNIT Tcf (WAYPOINT 150924_3-1b)		
Date	09/24/15	*n = 48*
UTM Location	3625119N, 283279E	
	n	% total
Total felsic volcanics	7	15%
Crystal-poor felsic volcanics	7	15%
Crystal-rich felsic volcanics		0%
Tuffs, undivided	19	40%
Kneeling Nun/Hells Mesa tuff	4	8%
Vicks Peak tuff		0%
Total intermediate volcanics	1	2%
Crystal-poor intermediate volcanics	1	2%
Crystal-rich intermediate volcanics		0%
Paleozoic carbonates	6	13%
Abo Formation	3	6%
Sandstone+siltstone, undivided	1	2%
Chert and jasperoid	2	4%
Vein quartz		0%
Granite	3	6%
Quartzite		0%
Basalt		0%
Other	2	4%
Comments	Other = 2% amphibolite, 2% fine volcaniclastic sandstone	

TABLE D.18 CLAST-COUNT DATA FOR UNIT Trvc (WAYPOINT 170322_1-2a)		
Date	03/22/17	*n = 101*
UTM Location	3615618N, 277913E	
	n	% total
Total felsic volcanics	8	8%
Crystal-poor felsic volcanics	5	5%
Crystal-rich felsic volcanics	3	3%
Tuffs, undivided	3	3%
Kneeling Nun/Hells Mesa tuff		0%
Vicks Peak tuff		0%
Total intermediate volcanics	83	82%
Crystal-poor intermediate volcanics	55	54%
Crystal-rich intermediate volcanics	28	28%
Paleozoic carbonates		0%
Abo Formation		0%
Sandstone+siltstone, undivided	1	1%
Chert and jasperoid		0%
Vein quartz		0%
Granite		0%
Quartzite		0%
Basalt	1	1%
Other	5	5%
Comments	Other = 3% undivided intrusive, 2% volcani-clastic sandstone	

APPENDIX E

Radiocarbon dating analyses from samples collected on the
Arroyo Cuervo 7.5-minute quadrangle

Samples 16AC-763A and 16AC-763B were collected from Arroyo Yeso in section 23, T18S, R5W on March 16, 2016.

Beta Analytic Inc.
DR. M.A. TAMERS and MR. D.G. HOOD
4985 S.W. 74 COURT
MIAMI, FLORIDA, USA 33155
PH: 305-667-5167 **FAX:** 305-663-0964
beta@radiocarbon.com

REPORT OF RADIOCARBON DATING ANALYSES

Mr. Andrew Jochems — Report Date: 7/29/2016

New Mexico Bureau of Geology & Mineral Resources — Material Received: 7/20/2016

Sample Data	Measured Radiocarbon Age	Isotopes Results o/oo	Conventional Radiocarbon Age(*)
Beta - 441927	3830 +/- 30 BP	d13C= -22.0	3880 +/- 30 BP

SAMPLE: 16AC-763A
ANALYSIS: AMS-Standard delivery
MATERIAL/PRETREATMENT: (charred material): acid/alkali/acid
2 SIGMA CALIBRATION : Cal BC 2465 to 2280 (Cal BP 4415 to 4230) and Cal BC 2245 to 2230 (Cal BP 4195 to 4180)
Cal BC 2245 to 2230 (Cal BP 4195 to 4180)

Sample Data	Measured Radiocarbon Age	Isotopes Results o/oo	Conventional Radiocarbon Age(*)
Beta - 441928	3830 +/- 30 BP	d13C= -23.1	3860 +/- 30 BP

SAMPLE: 16AC-763B
ANALYSIS: AMS-Standard delivery
MATERIAL/PRETREATMENT: (charred material): acid/alkali/acid
2 SIGMA CALIBRATION : Cal BC 2460 to 2270 (Cal BP 4410 to 4220) and Cal BC 2260 to 2205 (Cal BP 4210 to 4155)
Cal BC 2260 to 2205 (Cal BP 4210 to 4155)

Sample Data	Measured Radiocarbon Age	Isotopes Results o/oo	Conventional Radiocarbon Age(*)
Beta - 441929	420 +/- 30 BP	d13C= -27.1	390 +/- 30 BP

SAMPLE: CS-25-Qah
ANALYSIS: AMS-Standard delivery
MATERIAL/PRETREATMENT: (charred material): acid/alkali/acid
2 SIGMA CALIBRATION : Cal AD 1440 to 1520 (Cal BP 510 to 430) and Cal AD 1575 to 1630 (Cal BP 375 to 320)
Cal AD 1575 to 1630 (Cal BP 375 to 320)

Sample Data	Measured Radiocarbon Age	Isotopes Results o/oo	Conventional Radiocarbon Age(*)
Beta - 441930	350 +/- 30 BP	d13C= -26.5	330 +/- 30 BP

SAMPLE: CS-25-QayA
ANALYSIS: AMS-Standard delivery
MATERIAL/PRETREATMENT: (charred material): acid/alkali/acid
2 SIGMA CALIBRATION : Cal AD 1465 to 1645 (Cal BP 485 to 305)

Results are ISO-17025 accredited. AMS measurements were made on one of 4 in-house NEC SSAMS accelerator mass spectrometers.The reported age is the "Conventional Radiocarbon Age", corrected for isotopic fraction using the d13C. Age is reported as RCYBP (radiocarbon years before present, abbreviated as BP, "present" = AD 1950). By international convention, the modern reference standard was 95% the 14C signature of NBS SRM-4990C (oxalic acid) and calculated using the Libby 14C half life (5568 years). Quoted error on the BP date is 1 sigma (1 relative standard deviation with 68% probability) of counting error (only) on the combined measurements of sample, background and modern reference standards. Total error at Beta (counting + laboratory) is known to be well within +/- 2 sigma. d13C values are reported in parts per thousand (per mil) relative to PDB-1 measured on a Thermo Delta Plus IRMS. Typical d13C error is +/- 0.3 o/oo. Percent modern carbon (pMC) and Delta 14C (D14C) are not absolute. They equate to the Conventional Radiocarbon Age. Calendar calibrated results were calculated the material appropriate 2013 database (INTCAL13, MARINE13 or SHCAL13). See graph report for references.

CALIBRATION OF RADIOCARBON AGE TO CALENDAR YEARS

(Variables: C13/C12 = -22 o/oo : lab. mult = 1)

Laboratory number	**Beta-441927 : 16AC-763A**
Conventional radiocarbon age	**3880 ± 30 BP**
Calibrated Result (95% Probability)	**Cal BC 2465 to 2280 (Cal BP 4415 to 4230)** **Cal BC 2245 to 2230 (Cal BP 4195 to 4180)**
Intercept of radiocarbon age with calibration curve	Cal BC 2395 (Cal BP 4345) Cal BC 2385 (Cal BP 4335) Cal BC 2345 (Cal BP 4295)
Calibrated Result (68% Probability)	Cal BC 2460 to 2295 (Cal BP 4410 to 4245)

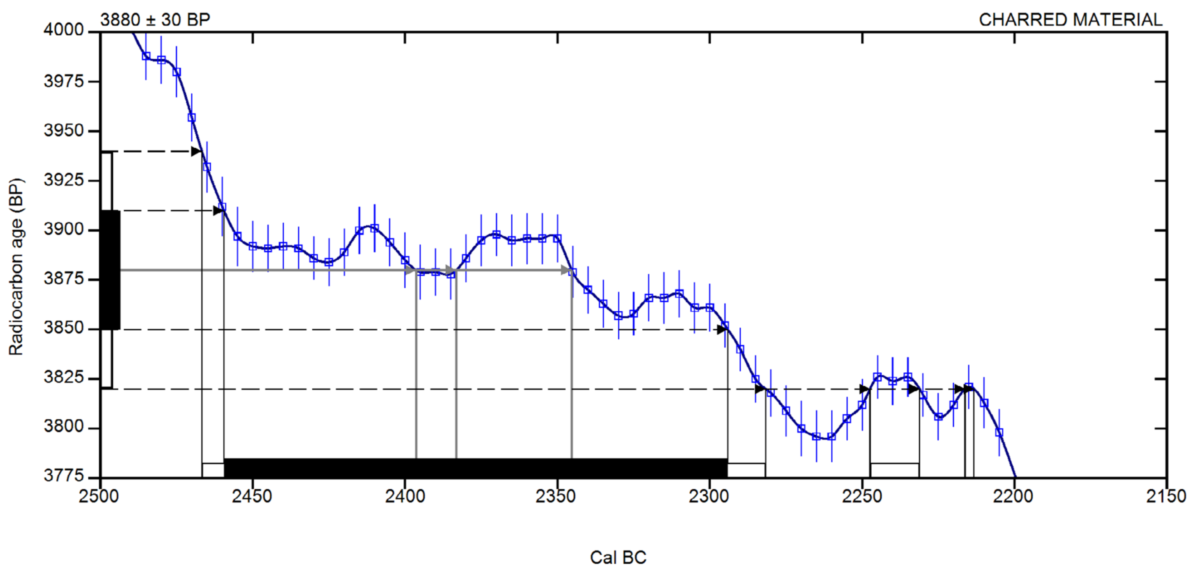

Database used
INTCAL13

References

Mathematics used for calibration scenario
A Simplified Approach to Calibrating C14 Dates, Talma, A. S., Vogel, J. C., 1993, Radiocarbon 35(2):317-322
References to INTCAL13 database
Reimer PJ et al. IntCal13 and Marine13 radiocarbon age calibration curves 0–50,000 years cal BP. Radiocarbon 55(4):1869–1887., 2013.

Beta Analytic Radiocarbon Dating Laboratory
4985 S.W. 74th Court, Miami, Florida 33155 • Tel: (305)667-5167 • Fax: (305)663-0964 • Email: beta@radiocarbon.com

CALIBRATION OF RADIOCARBON AGE TO CALENDAR YEARS

(Variables: C13/C12 = -23.1 o/oo : lab. mult = 1)

Laboratory number	**Beta-441928 : 16AC-763B**
Conventional radiocarbon age	**3860 ± 30 BP**
Calibrated Result (95% Probability)	**Cal BC 2460 to 2270 (Cal BP 4410 to 4220)** **Cal BC 2260 to 2205 (Cal BP 4210 to 4155)**
Intercept of radiocarbon age with calibration curve	Cal BC 2335 (Cal BP 4285) Cal BC 2325 (Cal BP 4275) Cal BC 2300 (Cal BP 4250)
Calibrated Result (68% Probability)	Cal BC 2435 to 2420 (Cal BP 4385 to 4370) Cal BC 2405 to 2380 (Cal BP 4355 to 4330) Cal BC 2350 to 2285 (Cal BP 4300 to 4235)

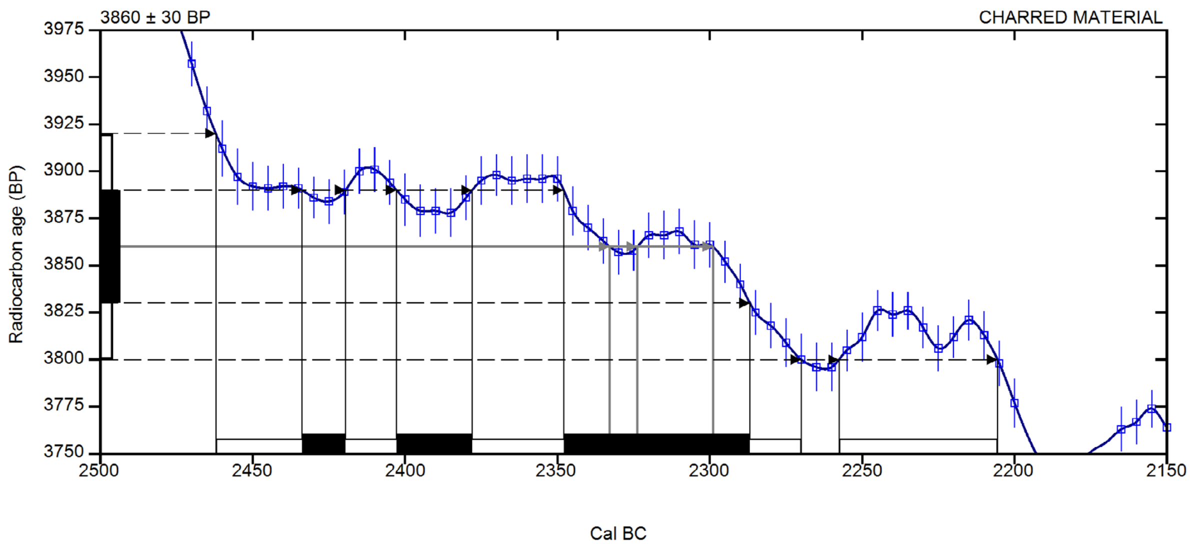

Database used

INTCAL13

References

Mathematics used for calibration scenario

A Simplified Approach to Calibrating C14 Dates, Talma, A. S., Vogel, J. C., 1993, Radiocarbon 35(2):317-322

References to INTCAL13 database

Reimer PJ et al. IntCal13 and Marine13 radiocarbon age calibration curves 0–50,000 years cal BP. Radiocarbon 55(4):1869–1887., 2013.